The Geological Society of America
Field Guide 77

Triassic–Jurassic great lakes of the Hartford Rift Basin—Exemplars of the deep-water, stratified-lake paradigm and why Walther's "Law" does not apply

Paul E. Olsen
Department of Earth and Environmental Sciences, Lamont-Doherty Earth Observatory of Columbia University, 61 Route 9W, Palisades, New York 10964, USA

Nicholas G. McDonald
Olde Geologist Books, 55 Asher Avenue, Pawcatuck, Connecticut 06379, USA

Sean T. Kinney
Department of Earth and Planetary Sciences, Rutgers University, Piscataway, New Jersey 08854, USA

ABSTRACT

Fossil fishes reported in 1816 from Connecticut were among the earliest Mesozoic vertebrates described from North America, predating publications on dinosaur footprints by two decades. Their environmental and taphonomic context continues to yield new insights but still remains contentious. Nearly all articulated fish occur in gray to black microlaminated mudrock composed of millimeter-scale couplets tracible over basin-scale distances. This facies preserves exquisite lacustrine fossils, constituting Konservat-Lagerstätten comparable to the strata producing the famous Chinese feathered dinosaurs. Debates on this facies center on two paradigmatic concepts: the "deep-water, stratified-lake model" and Walther's "Law." On this field trip, we use outcrops, cores, slabbed sections, and fossils to explore several linked sedimentological and taphonomic questions, including: (1) Were these lakes perennial and chemically stratified, with an anoxic hypolimnion? (2) Are microlaminated sediments with whole fish lateral equivalents of shallow lake sequences, as Walther's Law would predict? (3) Are the couplets true varves? (4) Did the stratified lakes routinely attain 50 m or more in depth? (5) Did high-stand lakes in the Connecticut Valley extend into other basins, making them among Earth's largest lakes? (6) What is the potential for finding extraordinary fossils such as feathered dinosaurs in the Connecticut Valley? Because of their historical and geological context, these Lagerstätten constitute some of the most illustrative research and teaching resources in North America.

Olsen, P.E., McDonald, N.G., and Kinney, S.T., 2026, Triassic–Jurassic great lakes of the Hartford Rift Basin—Exemplars of the deep-water, stratified-lake paradigm and why Walther's "Law" does not apply, *in* Wintsch, R.P., Drzewiecki, P.A., and Hobbs, K.M., eds., Investigating Paleoenvironments and Provenance in Sedimentary and Metasedimentary Basins: New York, New Mexico, and Connecticut: Geological Society of America Field Guide 77, p. 19–65, https://doi.org/10.1130/2026.0077(02).

INTRODUCTION

The remains of well-preserved fishes are among the most familiar fossils from latest Triassic and Early Jurassic rift Hartford Rift Basin strata (Figs. 1 and 2). Among the earliest mention of fossil vertebrates from North America, they were first noted by Benjamin Silliman (1816) in Cleaveland's "Elementary Treatise on Mineralogy and Geology." Today, thousands of specimens are on exhibit or in museum collections worldwide, and they continue to be uncovered by avocational and professional paleontologists on a regular basis.

With very rare exceptions (e.g., Thorpe, 1936; McDonald et al., 2025), Hartford Basin fossil fishes are preserved in microlaminated sediments defined as having planar, very thin laminae (generally <1 mm) that commonly form regular couplets of contrasting composition and that can be traced over long distances (Fig. 2). Hartford Basin microlaminated strata sometimes also preserve crustaceans, notably clam shrimp (spinocaudatans) and ostracodes. The small thickness scale, regularity, and especially the lateral continuity of these laminae are important in distinguishing this facies from thin bedding in other contexts such as crossbeds, stromatolites, or microbial mats. Very similar microlaminated facies in other Late Triassic and Jurassic units of eastern North America yield fossil fishes and many other kinds of fossils, including complete insects and reptiles (Olsen and McDonald, 2026). Globally, this type of facies hosts some of the most significant fossil assemblages, including those of the Eocene Green River Formation, Early Cretaceous Jehol Biota, and Late Jurassic Yanliao Biota, famous for preserving feathered birds and non-avian dinosaurs.

The depositional context of the strata in which these spectacular fossils occur has been debated for over half a century (e.g., Eugster and Surdam, 1973), with a marked tendency for each occurrence to be interpreted as due to exceptional or even unique

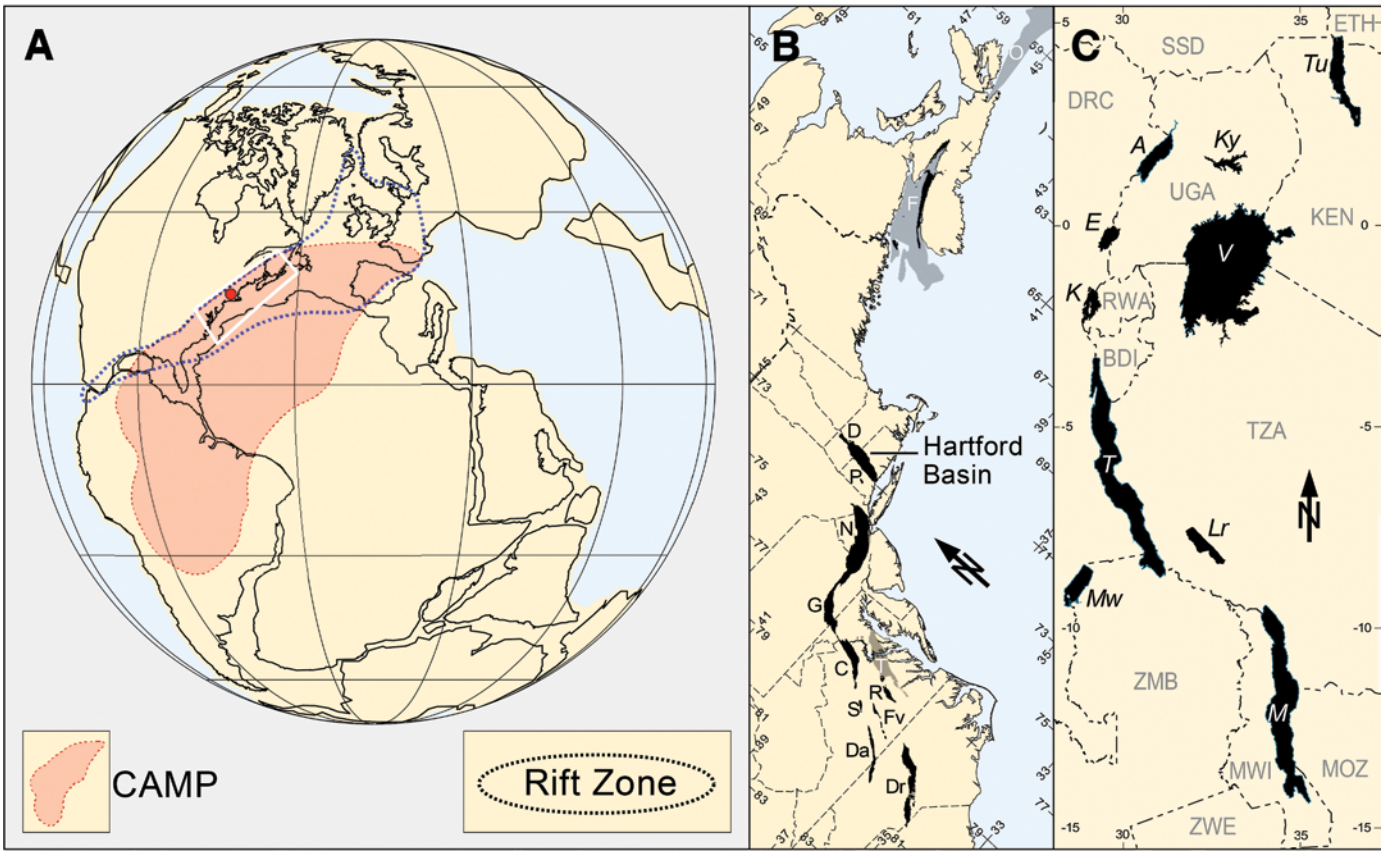

Figure 1. (A) Pangea at 202 Ma (red dot is Hartford Basin). White rectangle is for B. (B) Eastern North American Triassic–Jurassic Newark Supergroup Rifts. (C) East African Great Lakes, at the same scale as the Newark Rifts. Abbreviations for B: C—Culpeper Basin; D—Deerfield Basin; Da—Dan River Basin; Dr—Deep River Basin; F—Fundy Basin; Fv—Farmville and subsidiary basins; G—Gettysburg Basin; N—Newark Basins; O—Orpheus Basin; P—Pomeraug Basin; R—Richmond Basin; T—Taylorsville Basin. Abbreviations for C (lake abbreviation in italics): *A*—Lake Albert; BDI—Burundi; DRC—Democratic Republic of the Congo; *E*—Lake Edward; ETH—Ethiopia; *K*—Lake Kivu; Ken—Kenya; *Ky*—Lake Kyoka; *Lr*—Lake Rukwa; *M*—Lake Malawi; MOZ—Mozambique; *Mw*—Lake Meru; MWI—Malawi; RWA—Rwanda; SSD—South Sudan; *T*—Lake Tanganyika; *Tu*—Lake Turkana; TZA—Tanzania; UGA—Uganda; ZMB—Zambia; ZWE—Zimbabwe.

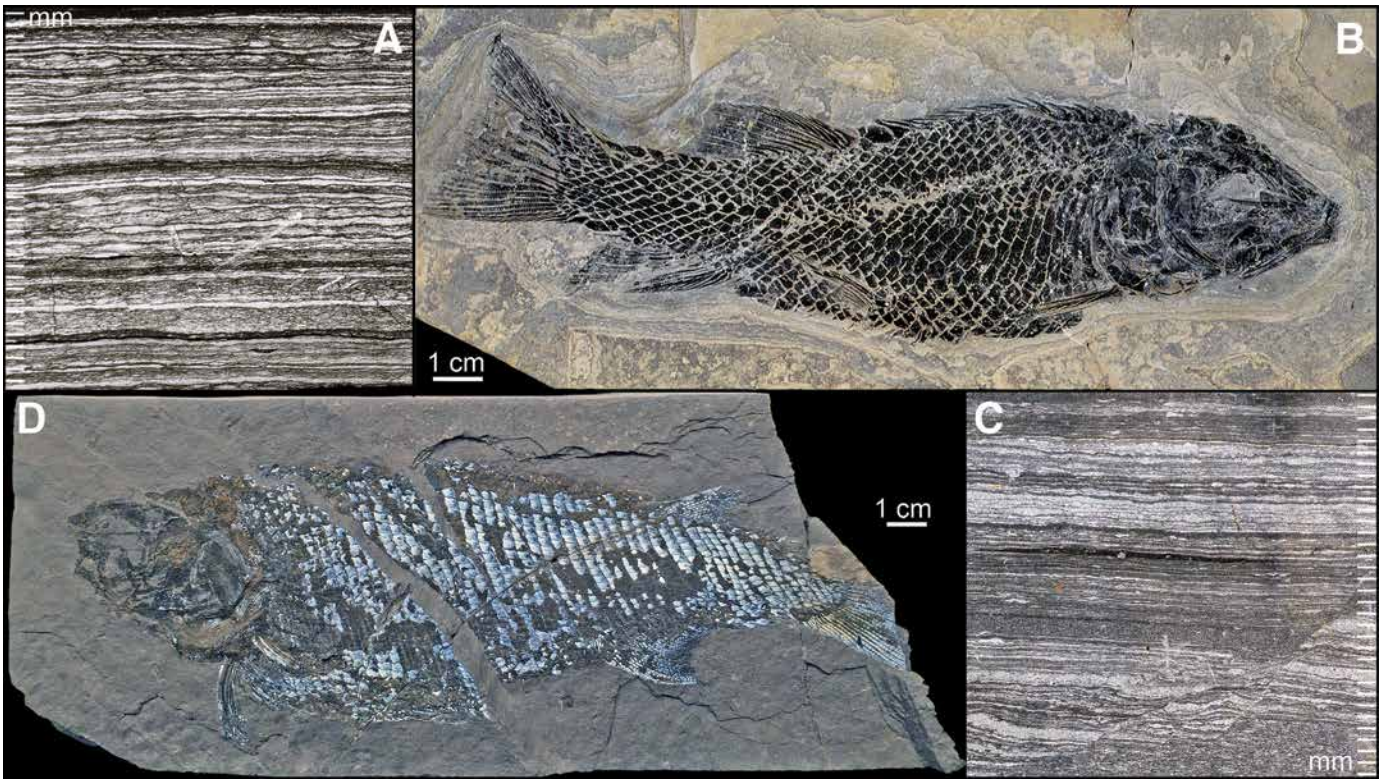

Figure 2. Examples of fishes and the microlaminated units that contain them in the Hartford Basin. (A) Slabbed block of the latest Rhaetian, Bluff Head Fish Bed, Shuttle Meadow Formation, Bluff Head, North Guilford, Connecticut. (B) *Semionotus* sp. from the same locality (YPM VP 8604). (C) Slabbed block of the Early Jurassic, Westfield Bed, just above the Westfield Turbidite (visible in the lower right), East Berlin Formation, Stevens Locality, Durham, Connecticut. (D) *Redfieldius* sp., same locality as C (uncatalogued Bruce Museum specimen).

circumstances. The purpose of this field guide is to explore this debate, focusing on direct observations that can be made within the Hartford Basin during a half-day field trip (Fig. 3).

GEOLOGIC SETTING

Tectonic Context and Stratigraphic Units

The Hartford Rift Basin is the southern subbasin of the Connecticut Valley Rift, part of a vast continental rift system extending from Greenland through to the Pacific that transected Pangea during its initial stages of fragmentation in the Late Permian to Early Jurassic (Fig. 1). Many of the individual basins, including the Hartford Rift, formed as half-graben along the major mostly normal faults that commonly reactivated older, low-angle Paleozoic compressional structures (Schlische, 1993). Within Hartford Basin half-graben, sedimentation started at least by 225 Ma and continued through 199 Ma, punctuated by less than 1 Myr of igneous activity at ca. 202 Ma of the Central Atlantic Magmatic Province (CAMP), which produced three lava flow formations (Talcott, Holyoke, Hampden) as well as intrusive sills and dikes. Lacustrine deposition was confined to the 202–199 Ma (latest Triassic to Early Jurassic) interval, beginning just before the oldest basalt flow, with both older and younger deposits being entirely fluvial (Fig. 1). This field trip focuses on profoundly cyclical lacustrine units (Fig. 4) between the oldest and youngest flows in the basin: the Shuttle Meadow and East Berlin Formations.

TAPHONOMIC AND PALEOBIOLOGICAL CONTEXT

Fossil assemblages in the microlaminated mudstones of the Hartford Rift Basin qualify as Konservat-Lagerstätten. Seilacher (1970) coined the now widely used term Lagerstätte (pl., Lagerstätten), German for "storage place" or "deposit," denoting exceptional fossil repositories. A classic example is the Late Jurassic Solnhofen Lagerstätte, the source of *Archaeopteryx*. The Shuttle Meadow and East Berlin microlaminated units preserve fishes in typical Lagerstätte fashion: abundant, complete, articulated specimens, some with soft-tissue preservation such as retinal melatonin (Fig. 2). This preservation mode implies that, with systematic and large-scale search, additional rare and informative fossils may be discovered.

Deposited soon after the end-Triassic extinction (ETE), the Shuttle Meadow and East Berlin Formations record continental biotas of reduced taxonomic and morphological diversity compared with Late Triassic tropical counterparts. Notably absent are

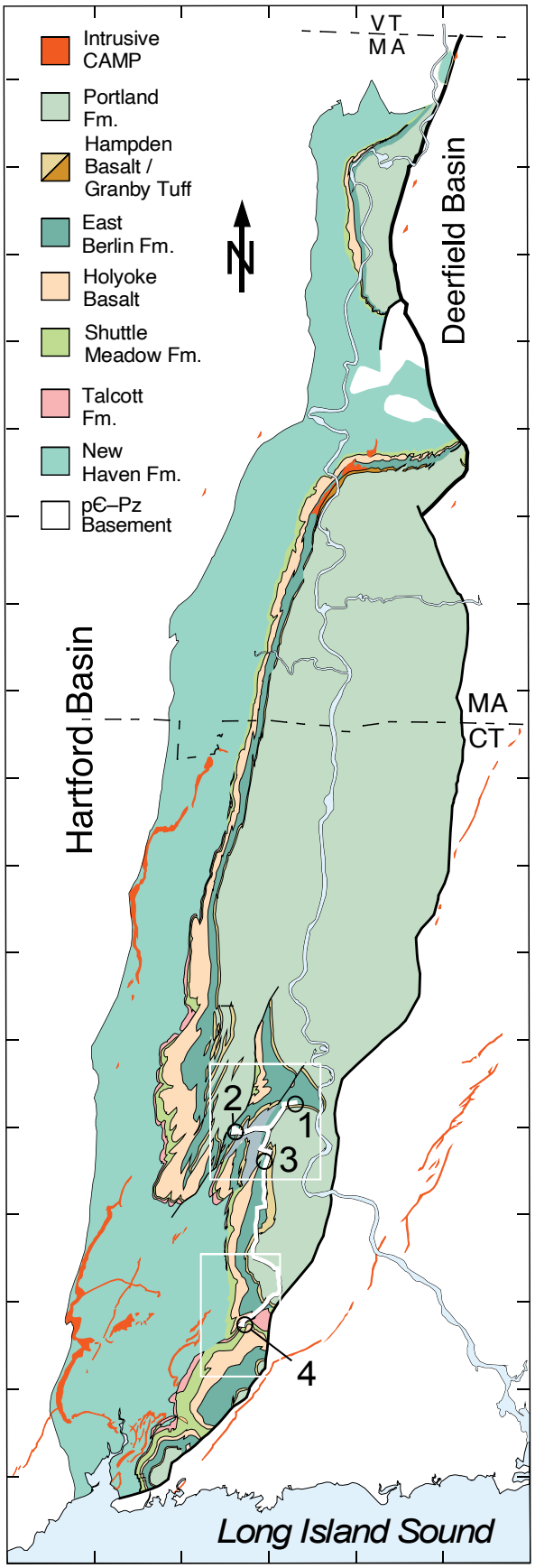

lacustrine tanystropheids and drepanosaurs (e.g., *Tanytrachelos* and *Hypuronector*: Olsen et al., 1978; Olsen, 2010; Colbert and Olsen, 2001), groups unknown from post-ETE strata globally. However, Hartford Basin microlaminated units could produce, yet to be found, terrestrial or aerial tetrapods such as sphenodontians, dinosaurs, and pterosaurs, elements of the fauna that survived into the Early Jurassic. Their apparent absence in these lacustrine strata is plausibly due to an insufficient collection effort.

STRATIFIED-LAKE MODEL—CONCEPTUAL BASIS AND APPLICATIONS

A survey of hypotheses concerning the conditions under which lacustrine Lagerstätten form reveals diverse interpretations despite similar patterns. The flattened lacustrine fauna of the Jehol biota in the Yixian Formation, including feathered non-avian dinosaurs, has been attributed to a "Pompeii"-like volcanic ash entombment (Benton et al., 2008; Zhong et al., 2021). In contrast, the preservation of insects and spiders in the "Solite" Lagerstätte has been linked to saline, groundwater-fed lake margins (Liutkus et al., 2010) (see Supplemental Material text 3.1.4, Fig. S4) and the tendency of fish in the Green River Formation toward burial within microbial mats (Hellawell and Orr, 2012). The "stratified-lake model" might seem at first to be another explanation of the same phenomena, which in relation to North American, temperate limnology could be viewed as just an additional ad hoc explanation.

The seemingly remarkable preservation of complete organisms with soft tissue can appear unusual or even miraculous—it is quite normal to seek extraordinary explanations for perceived extraordinary phenomena (with a nod to Carl Sagan). However, the stratified-lake model is best treated as a null hypothesis for comparison with other explanations. It provides a simple set of boundary conditions against which preservation modes can be tested.

Usually credited to Bradley (1929, 1963) and Bradley and Eugster (1969) (see Boyer, 1982), the model attributes microlaminae and articulated fossil preservation to the absence of physical disturbance and bioturbation within an anoxic hypolimnion (bottom waters lacking oxygen) (see terminology in Fig. 5). Initially developed for the Eocene Green River Formation, it has since been applied to many lacustrine deposits

Figure 3. Geological map of the Hartford and Deerfield Basins (Connecticut Valley Rift) and field-trip stops. Map and section adapted from Olsen and Davis (2022). Position of specific stops are shown by the black circles and numbers (1–4), and the white boxes show the position of the detailed maps for the stops. Formations of the Deerfield Basin colored as New Haven, Shuttle Meadow, Holyoke, East Berlin, and Portland Formations have their own names: Sugarloaf, Fall River Beds of the Sugarloaf, Deerfield Basalt, lower Mt. Toby Formation, Upper Mount Toby, respectively. Ticks are at 10 km intervals. CAMP—Central Atlantic Magmatic Province; Fm.—formation; MA—Massachusetts; CT—Connecticut.

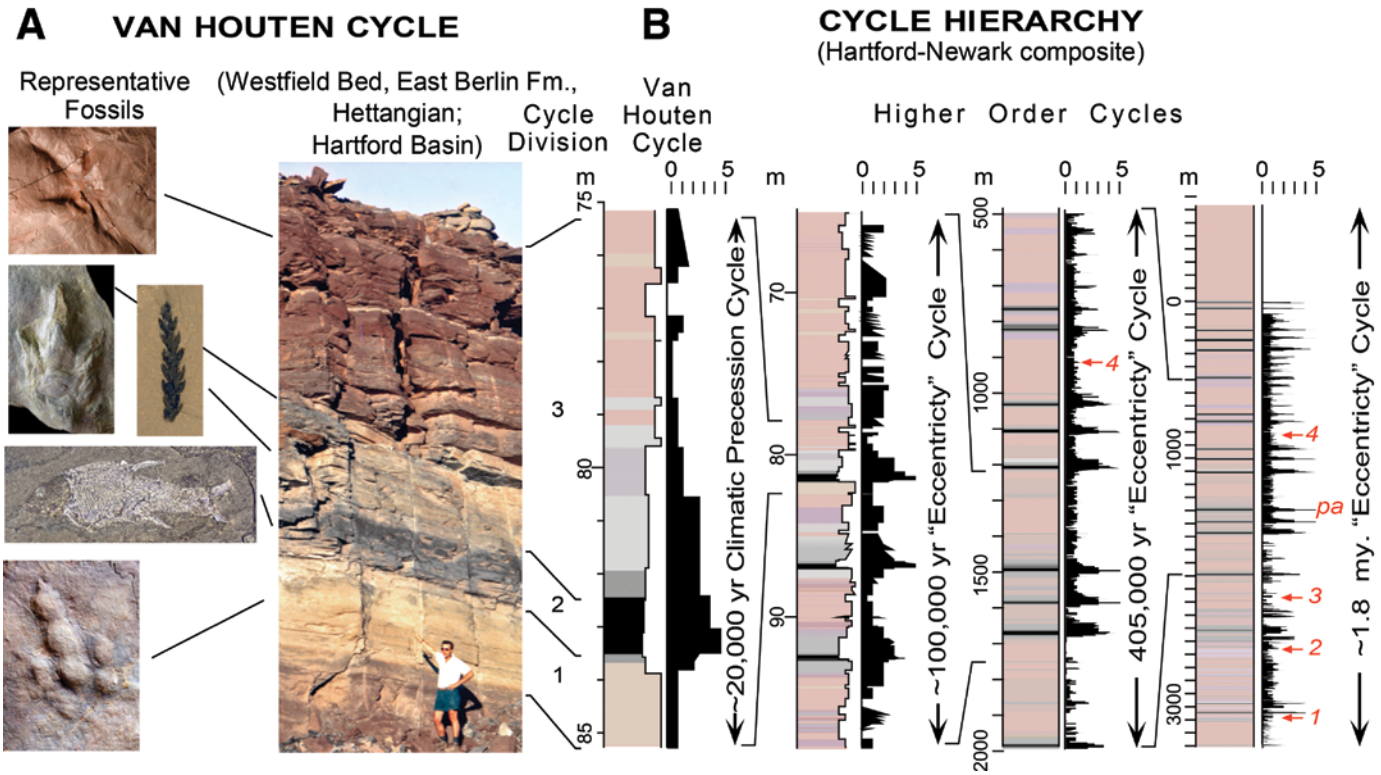

Figure 4. Precession- and eccentricity-related lacustrine cycles of the syn-CAMP (Central Atlantic Magmatic Province). Modified from Olsen and McDonald (2026). (A) Single Van Houten cycle in the East Berlin Formation, East Berlin, Connecticut (Peter LeTourneau for scale). (B) Cycle hierarchy of the Hartford–Newark composite sequence. Volcanic units: 1—Talcott and Orange Mountain Basalts; 2—Holyoke and lower Preakness Basalts; 3—top of upper Preakness Basalt; 4—Hampden and Hook Mountain Basalts. Scales 0–5 and black plots denote relative water depth, with 5 as deepest. Fm.—formation.

and Lagerstätten, including the Pleistocene Rita Blanca beds (Anderson and Kirkland, 1969), Eocene Grube Messel (Schulz et al., 2002), Early Cretaceous Yixian Formation (Hethke et al., 2013), Middle Jurassic Todilto Formation (Anderson and Kirkland, 1960), and Triassic Cow Branch Formation (Solite) (Olsen et al., 1978), among others, although several alternative models have been proposed.

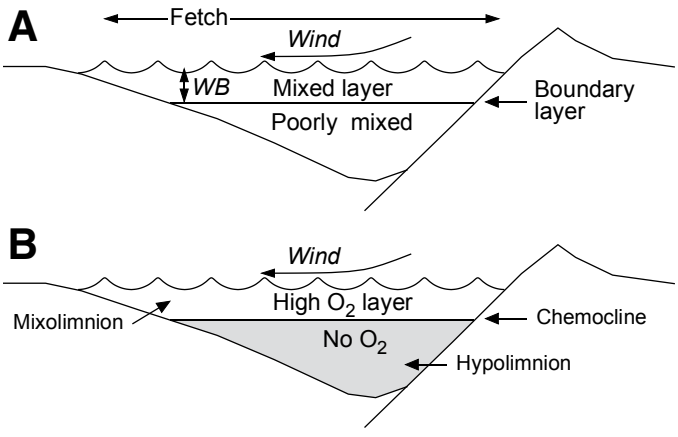

Figure 5. Lake morphology and terminology used in this paper. (A) Turbulent stratification in low-latitude lakes. (B) Oxygen stratification related to bacterial respiration of organic matter. WB—wave base.

A permanently stratified, chemically distinct lake with an anoxic lower water mass is called meromictic (Findenegg, 1935) and exhibits meromixis. Its upper layer, the mixolimnion, and lower layer, the hypolimnion, are separated by the chemocline (Hutchinson, 1937, 1957) (Fig. 5). In contrast, holomictic lakes mix seasonally or nearly continuously (Findenegg, 1935).

Physical Basis for the Stratified-Lake Model

A major strength of the stratified-lake model lies in its simplicity, as it is based on fundamental physical principles clearly described by Anderson et al. (1985): (1) Most important is the relationship between lake depth and surface area: the deeper a lake is relative to its area the less effective wind stress becomes at mixing it to the bottom. (2) Processes that increase the density contrast between shallow and deep water enhance resistance to wind mixing and promote stratification. (3) A lack of thermal overturn (at ~4° C) or limited inflow of denser water fosters meromixis.

Mixing, turbulent diffusion driven mainly by wind, is critical because it introduces oxygen into lake water from the atmosphere

or photosynthesis at rates several orders of magnitude greater than molecular diffusion (St-Denis and Fell, 1971; Bouffard et al., 2014). Heterotrophic bacteria consume dissolved oxygen while respiring particulate and dissolved organic matter that settles through the water column. Vertical turbulent mixing replenishes oxygen by transporting it from surface waters. When organic matter supply is sufficient, the water below the mixing front may become oxygen-depleted, producing meromixis with an anoxic hypolimnion.

Prolonged anoxia excludes all animals capable of macroscopic bioturbation, allowing preservation of primary suspension deposited stratification such as microlaminations (Anderson et al., 1985; Zolitschka et al., 2015). Seasonally varying microlaminations form varves, and the absence of scavengers leads to burial of intact organisms, while weak wind mixing prevents disturbance of laminae. Consequently, lakes with small surface areas relative to depth favor preservation of both microlaminations and whole, articulated organisms.

Although quantitative modeling of the relationship among lake depth, area, and meromixis remains difficult (e.g., Imboden and Wüest, 1995), semiempirical approaches (e.g., Olsen, 1990) provide useful insights. Specifically, the relationship between fetch, wind speed, and the depth of wave base scales similarly to what would be expected of the depth of the mixed part of the lake water column and predicts whether a modern lake is meromictic. This scaling offers a mechanism for estimating minimum lake depths in the Hartford Basin and other ancient microlaminated lacustrine deposits (Figs. 6 and 7).

Wave base is the depth below which wave-induced water motion becomes negligible, approximately half the wavelength (Dean and Dalrymple, 1991). Its depth depends on the distance over which the lake surface is exposed to wind (fetch) and on wind speed and duration. All else being equal, a lake with a larger surface area develops a deeper wave base than a smaller one. For lakes of equal area, the deeper lake will have a smaller proportion of its water column affected by wave mixing than the shallower lake.

For fresh water, the semiempirical equations of Bretschneider (1951) and Smith and Sinclair (1972) can be combined to yield (Manspeizer and Olsen, 1981; Olsen, 1984, 1990):

$$WB = 0.0062\ W^{0.881}\ F^{0.56}, \quad (1)$$

where WB is wave base (m), W is wind speed in (m/s^{-1}), and F is fetch (m). This defines the approximate depth to which wind-generated gravity waves mix the lake in deep water when wave action is fully developed. Figures 6 and 7 illustrate the relationship between fetch and wave-base depth for various lakes and seas (Table 1), for wind speeds of 20, 30, and 40 m/s^{-1} corresponding respectively to strong gale, violent storm, and lower-hurricane conditions (The Beaufort Wind Scale: https://www.rmets.org/metmatters/beaufort-wind-scale; Saffir-Simpson Hurricane Wind Scale: https://www.nhc.noaa.gov/aboutsshws.php). Under such storms, the chemocline migrates below the depth of wave base. For comparison, the 1975 storm that sank the ore freighter *Edmund Fitzgerald* on Lake Superior involved sustained winds of ~25–30 m s^{-1} with gusts approaching 35–38 m s^{-1} on 9–10 November 1975 (https://www.weather.gov/mqt/fitz_galesa). The African Great Lakes experience similar magnitudes winds, albeit rarely (e.g., Verburg et al., 1997).

Wave-base determinations are not physically rigorous measures of the potential depth of the mixolimnion, particularly under

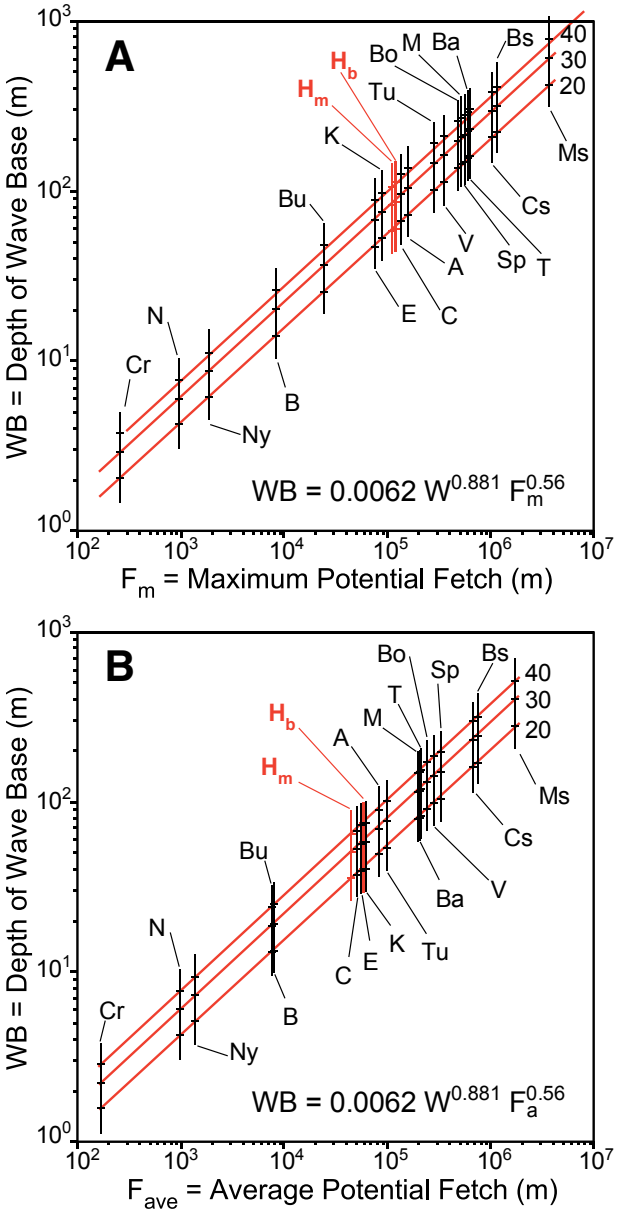

Figure 6. Calculated relationships between average fetch of a lake, wave base, and average depth for multiple wind speeds. (A) Wave base calculated using average potential fetch. (B) Wave base calculated using maximum potential fetch. Data from Wikipedia, HydroSHEDS (https://www.hydrosheds.org/), GLOBathy (Khazaei et al., 2022) and estimates from Ganz et al. (2024) (Table 1).

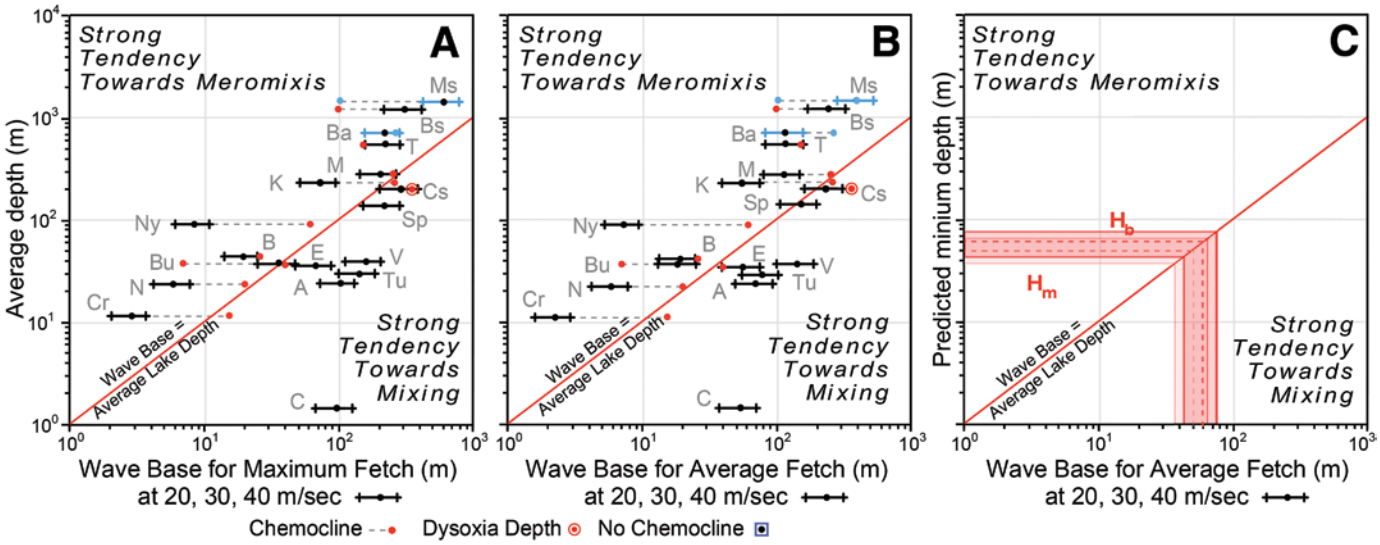

Figure 7. Observed and predicted wave base, fetch, and chemocline and predicted depths. (A) Relationship between calculated wave base and actual average lake depth for multiple lakes and seas using maximum potential fetch (data and abbreviations in Table 1). Lakes above the 1:1 line exhibit meromixis and preserve microlaminated sediments unless strong deep-water formation promotes mixing (e.g., Mediterranean Sea) or oxygen is maintained by low productivity (e.g., Lake Baikal). (B) Same as A except for average potential fetch. (C) Relationship between calculated wave base and the estimated depth below the mixed layer for Hartford Basin sediments. H_b is the minimum predicted depth using total preserved basin area; H_m is the minimum predicted depth using the area of the preserved East Berlin Formation, regarded as a minimal estimate. Data in Table 1.

steady-state conditions. Nevertheless, the wave-base estimate plausibly scales with the water motions that maintain a mixed layer, as shown by comparisons with chemocline depth in many lakes. These results are broadly consistent with those of Johnson (1980) and Håkanson (1977).

Olsen (1990) calculated wave-base depth using equation (1) and maximum potential fetch (the longest lake dimension) spanning several orders of magnitude in lake area (Figs. 6A and 7A). Figures 6B and 7B present a new survey of lakes and seas using a modified version of Olsen's (1990) comparison using average fetch and average depth for the same lakes. With some interesting exceptions (see below), lakes deeper than their predicted wave base are chemically stratified, with chemoclines often close to the calculated value, whereas shallower lakes were mixed to the bottom and lacked microlaminated sediments. The method also provides a means of estimating the depths of ancient lakes preserving microlaminated deposits (see Supplemental Material[1] text 1.0 for details of the method).

As shown in Figure 7, lakes spanning three orders of magnitude in area with average depths greater than predicted wave-base depths for 20–40 m s^{-1} winds tend to be meromictic and preserve microlaminated sediments, whereas shallower lakes do not (Figs. 8, S1).

Modern Exceptions and an Exemplar

Some exceptions: Among the world's large and deep lakes and inland seas, several lack deep-water anoxia and do not produce microlaminated sediments, even in their deepest subbasins; these include Lake Baikal, the Mediterranean Sea, the Caspian Sea, and the American Great Lakes (see Supplemental Material 1.0) (Figs. 6 and 7). These are worth describing because as exceptions they demonstrate both the strengths and limits of the stratified-lake model for ancient sediments. Examples of sediments in cores are shown in Figure 8 (Fig. S1).

Lake Baikal, though very similar in geometry to Lake Tanganyika and even deeper (1640 m—the World's deepest lake), certainly deep enough to permit meromixis, undergoes regular deep-water renewal driven by cold, dense surface waters formed during winter cooling and enhanced by thermobaric and wind-forced convection. This vigorous ventilation, together with low organic carbon flux to the abyssal basin, maintains high deep-water oxygen concentrations to the bottom and prevents development of a stable, permanently anoxic monimolimnion, despite warm-season turbulent stratification.

The Mediterranean Sea is on average far deeper than its wave base yet is normally well ventilated by dense-water formation and exchange with the Atlantic, yielding mainly bioturbated abyssal muds. Only during precessional minima, when enhanced monsoonal runoff and a low-salinity surface lid suppressed deep overturn, did the basin tip into quasi-meromictic states, recording microlaminated, organic-rich sapropels at depth (see Supplemental Material text 1.2.3; Fig. S1).

[1]Supplemental Material. Triassic–Jurassic great lakes of the Hartford Rift Basin. Please visit https://doi.org/10.1130/FLD.S.31692409 to access the supplemental material, and contact editing@geosociety.org with any questions.

TABLE 1. LAKE DATA FOR FIGURES 6 AND 7

Label	Lake	Area (m^2)	Maximum potential fetch (m) (Fm)	Average potential fetch (m) (Fa)	Max. / avg. depth (m)	Source	Wave base 20 F_m / F_a (m/sec)	Wave base 30 F_m /F_a (m/sec)	Wave base 40 F_m /F_a (m/sec)	Chemo-cline depth (m)
Cr	Crawford Lake	2.40E+04	270	1.75E+02	24 / 12	1	2 / 2	3 / 2	4 / 3	15.5
N	Lake Nkugute	8.00E+05	2590	1.01E+03	58 / 24	2	4 / 4	6 / 6	8 / 8	20
Ny	Lake Nyos	1.58E+06	1925	1.42E+03	208 / 95	3	6 / 5	9 / 7	11 / 9	60
Bu	Lake Bunyoni	4.60E+07	25,000	7.65E+03	40 / 39	4	25 / 13	36 / 19	46 / 24	25
B	Lake Bosumtwi	4.86E+07	8600	7.87E+03	81 / 45	5	14 / 13	20 / 19	26 / 24	25
C	Lake Chad	2.00E+09	142,500	5.05E+04	8 / 1.5	6	67 / 37	95 / 53	123 / 69	–
E	Lake Edward	2.33E+09	77,000	5.44E+04	112 / 37	7	47 / 39	68 / 56	87 / 72	40
K	Lake Kivu	2.40E+09	89,000	5.53E+04	485 / 240	8	51 / 39	73 / 56	95 / 72	60
A	Lake Albert	5.30E+09	160,000	8.21E+04	58 / 25	9	71 / 49	102 / 70	131 / 90	–
Tu	Lake Turkana	7.56E+09	290,000	9.81E+04	114 / 31	10	99 / 54	142 / 77	183 / 100	–
M	Lake Malawi	2.96E+10	560,000	1.94E+05	706 / 292	11	144 / 79	205 / 114	265 / 146	250
Ba	Lake Baikal	3.17E+10	636,000	2.01E+05	1642 / 744	12	154 / 81	221 / 116	284 / 149	–
T	Lake Tanganyika	3.26E+10	637,000	2.04E+05	1470 / 570	13	154 / 82	221 / 117	285 / 150	150
V	Lake Victoria	6.88E+10	359,000	2.76E+05	80 / 40	14	112 / 101	160 / 144	206 / 185	–
Sp	Lake Superior	8.21E+10	616,000	3.23E+05	406 / 147	15	152/ 106	217 / 151	279 / 195	–
Cs	Caspian Sea	3.71E+11	1,030,000	6.87E+05	1025 / 211	16	202 / 161	289 / 230	372 / 297	200
Bs	Black Sea	4.36E+11	1,175,000	7.45E+05	2212 / 1253	17	218 / 169	311 / 241	401 / 311	100
Ms	Mediterranean	2.50E+12	3,800,000	1.78E+06	5109 / 1500	18	420 / 275	600 / 393	774 / 507	
Hb	Hartford Basin (all)	3.22E+09	125,000	6.41E+04	–	here	62 / 43	89 / 61	114 / 79	–
Hm	Hartford Basin (just CAMP)	1.82E+09	121,000	4.81E+04	–	here	61 / 36	87 / 52	112 / 67	–
Bo	Lake Bonneville	5.10E+10	523000	2.55E+05	–	19	138 / 92	198 / 132	225 / 170	–

Sources:

1. Boyko (1973) and McCarthy et al. (2023) average depth calculated from bathymetry in these sources.
2. Beadle (1966) average depth calculated from bathymetry in this source.
3. https://en.wikipedia.org/wiki/Lake_Nyos (accessed 12 Dec. 2025).
4. https://en.wikipedia.org/wiki/Lake_Bunyonyi (accessed 12 Dec. 2025) and Denny (1972).
5. Lake dimensions from Boehrer et al. (2025) and https://en.wikipedia.org/wiki/Lake_Bosumtwi (accessed 24 Dec. 2025, citing LakeNet). Archived from the original on 28 Nov. 2003 (retrieved 18 Feb. 2007): http://www.worldlakes.org/lakedetails.asp?lakeid=10252. The chemocline varies between 7 m and 35 m with 25 m selected as something close to average (Beadle, 1981; Almond and Hecky, 2002; Puchniak et al., 2009; Boehrer et al., 2025).
6. Odada et al. (2006) and Buma et al. (2018), but note it is much smaller (Google Earth, accessed 30 Jan. 2025).
7. Russell and Johnson (2005) and Bagalwa et al. (2014).
8. Kranenburg et al. (2020).
9. Morana et al. (2014).
10. Obiero et al. (2023).
11. World Lake Database, Lake Malawi, https://wldb.ilec.or.jp/Lake/AFR-13 (accessed 25 Dec. 2025), and Eccles (1974).
12. Morphometric data, http://www.lin.irk.ru/intas_eng/morphometry.htm (accessed 25 Dec. 2025).
13. Cohen et al. (1997) and Edmond et al. (1993).
14. Renaut and Owen (2023).
15. Physical features of the Great Lakes: https://www.epa.gov/greatlakes/physical-features-great-lakes (accessed 25 Dec. 2025).
16. Caspian Sea, https://en.wikipedia.org/wiki/Caspian_Sea (accessed 25 Dec. 2025) and Peeters et al. (2000).
17. Islek et al. (2021) and Buesseler et al. (1994).
18. Black Sea, https://en.wikipedia.org/wiki/Mediterranean_Sea (accessed 25 Dec. 2025) and Google Earth (accessed 30 Jan. 2026), but it is irregular in shape, and fetch could be estimated at 1898 km if islands and peninsulas are in a straight line.
19. Gwynn (1996).

The Caspian Sea, with and average depth close to its predicted wave base, develops intermittent deep anoxia below ~200–350 m and centimeter-scale laminations in its deepest deposits, while shallower settings are mottled and bioturbated (see Supplemental Material text 1.2.4; Fig. S1).

The American Great Lakes and those African Great Lakes that have depths similar to or shallower than their wave bases experience vigorous seasonal mixing and accumulate massive to coarsely laminated sediments with no true microlamination, whereas those African Great Lakes whose average depths exceed their predicted wave base are meromictic and display microlaminated facies below the chemocline (Fig. 8) (see Fig. S1).

Exemplar: Lake Bosumtwi, Ghana (6.5° N), although small (10.5 km in diameter, 49 km^2), exemplifies and ground-truths the

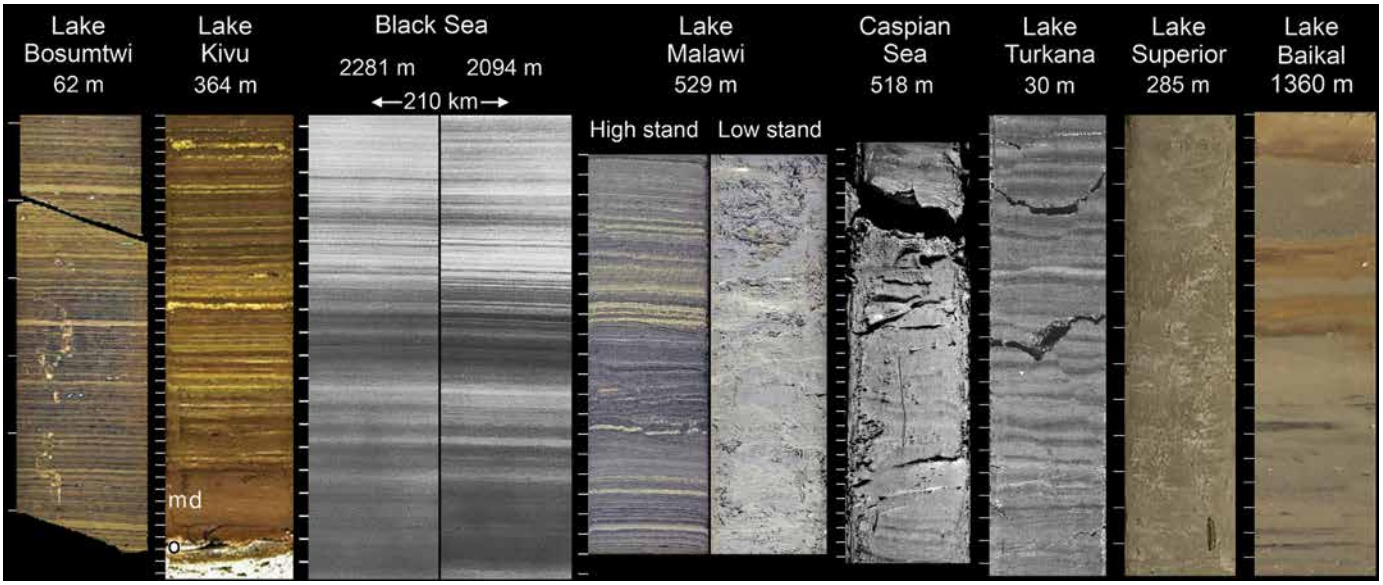

Figure 8. Photos of modern lake and sea sediments showing core water depths (scale = 1 cm): Bosumtwi, thin section core B2000-1P (Shanahan et al. (2012; used with permission of Elsevier Science © 2012); Lake Kivu, core KIVU12-14A (o, shallow water ooids at 8 m core depth; md—shallow water massive mud) (Wood and Scholz, 2017; used with permission of Elsevier Science © 2016). Black Sea, Box cores, sites 14 and 9 of Lyons and Berner (1992; published under Creative Commons CC BY-NC-ND 4.0). Malawi, Hole 1C, 592 m (lake high stand from upper section of hole, typical of modern deposits; low stand from middle part of core typical of megadrought intervals) (Scholz et al., 2011; used with permission of Elsevier). Caspian Sea, Core SR-9402 GS05, 31–60 cm (Jelinowska et al., 1998; used with permission of Blackwell Publishing). Turkana LT84-8P, 30 m water depth, 549–582 cm (Halfman and Johnson, 1988; used with permission of the Geological Society of America), Lake Superior, Thunder Bay Trough, core #533, 0.8–1.80 m (Hyodo, 2010; used with permission).

stratified-lake model. Its cores contain abundant articulated fossil fish preserved in microlaminated sediments deposited below a seasonally fluctuating chemocline in a modern meromictic lake, where alternating clastic and organic-carbonate varve couplets tracible across the basin thin downward by compaction (Figs. 8, 9; Supplemental Material text 1.2.5; Figs. S1–S3). The couplets are demonstrably annual varves, as ^{14}C dates from articulated fish collagen agree with ^{210}Pb ages and varve counts, providing one of the clearest confirmations of annually deposited non-glacial varves (see Fig. S2). These microlaminated strata display all the features anticipated by the stratified-lake model (Figs. 6 and 7) and are directly comparable to Hartford Basin deep-water lake strata and the lacustrine Lagerstätten.

Caveats

Using wave base as a proxy for the chemocline, or its absence, carries several caveats. It assumes chemocline depth tracks wind speed, yet in reality the chemocline responds dynamically to wind forcing and is better described as a depth range than a fixed boundary (e.g., Imboden and Wüest, 1995; Boehrer and Schultze, 2008). Stratification is also controlled by density contrasts driven by both salinity and temperature, with mixing work increasing sharply at higher temperatures (Wetzel, 2001), so tropical lakes stratify particularly easily. Oxygen depletion at depth depends on organic-matter flux and growing-season length, and some systems [e.g., ultra-oligotrophic (Sturm and Matter, 1978; Olsen, 1985) or chemically stressful lakes, or meromictic but oxygenated lakes like Crawford] can lack bioturbation for reasons other than anoxia (Llew-Williams et al., 2024), yet it still follows the wave-base and depth relationship (Fig. 7).

Long-term evolutionary and ecological changes further complicate interpretations: In the Archean, microlamination could develop without bioturbation regardless of oxygenation; early Mesozoic lakes largely lacked dysoxia-tolerant bioturbators; the Late Cretaceous appearance and late Eocene rise of freshwater diatoms and lacustrine grazers has altered sediment composition and the distribution of bioturbated facies through time (Olsen, 1990; Mustoe, 2005; Fox et al., 2015; Siver and Velez, 2023). Nevertheless, the link between basin geometry, mixing, and meromixis requires no special conditions beyond sufficient depth relative to mixing depth, minimal deep convective mixing, and a sufficient (but hardly unusual) flux of organic matter, so the stratified-lake model is a useful null hypothesis in warm climates. It should be rejected only when specific evidence demands alternatives—such as microlaminated facies restricted to margins rather than depocenters, adjacent very shallow facies incompatible with chemical stratification, highly discontinuous microlaminae suggesting local microbial mats, abundant macro-benthic traces other than mortichnia (Seilacher, 2007; Pokorný et al., 2025), repeated desiccation horizons, clear wave-base structures, or geochemical indicators of bottom-water oxygenation—none of which

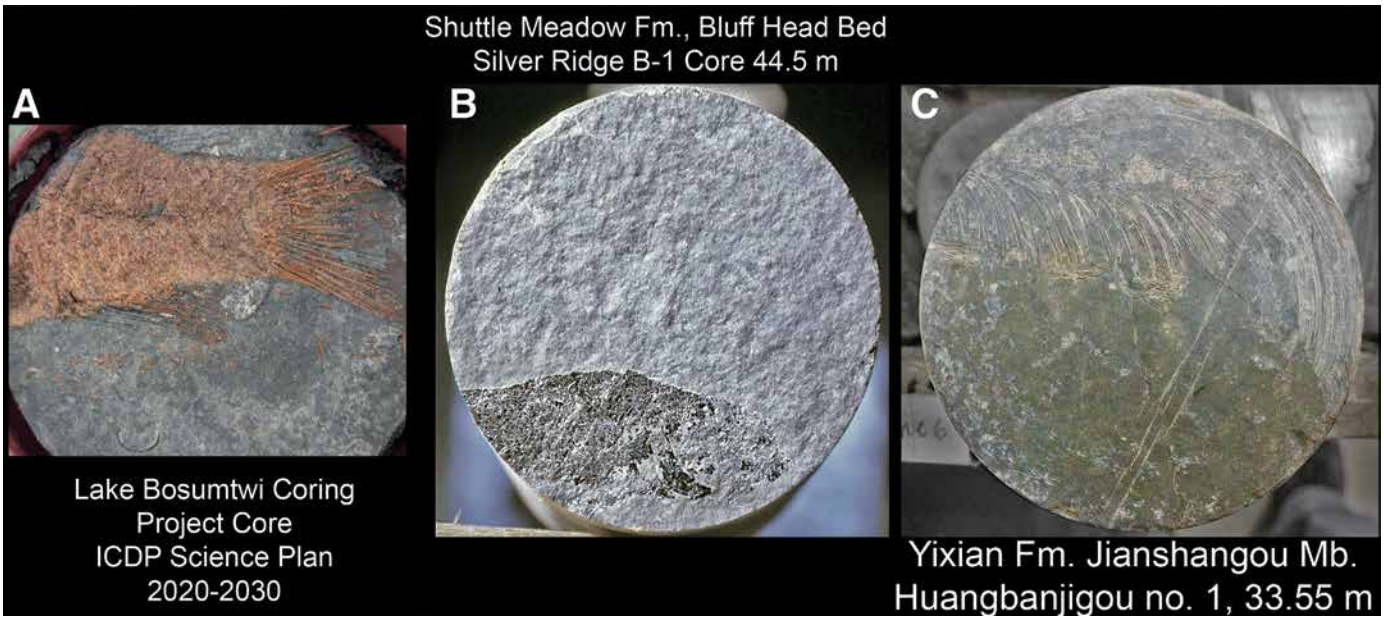

Figure 9. Fossil fish in cores of microlaminated lake sediments: (A) Holocene or Pleistocene cichlid sp. (Anselmetti et al., 2020; reproduced under Creative Commons Attribution 4.0 International License), Lake Bostumtwi coring project core; (B) latest Triassic (latest Rhaetian) *Semionotus* sp., Silver Ridge B-1 core, Bluff Head Bed, Shuttle Meadow Hartford Basin; (C) Early Cretaceous, Yixian Formation (latest Barremian–earliest Aptian), *Lycoptera* sp., Huangbanjiagou no. 1 core, Huangbanjiagou, Liaoning Province, China. Fm.—formation; Mb.—member.

are convincingly documented in facies otherwise matching the stratified-lake model.

The stratified-lake model explains the principal attributes of most lacustrine Lagerstätten: the preservation of articulated organisms in microlaminated strata and the absence of benthos. It also provides a means to infer minimum water depths during deposition of these exceptional layers.

Inverting the Paradigm—Lake Minimum Depth from Microlaminated Sediments

The relationship among predicted wave base, meromixis, and microlaminated sediment allows estimation of minimum water depths, assuming surface-mixing intensities were not markedly lower in the past. The stratified-lake model can thus be treated as an inverse problem: The area of preserved microlaminated strata reflects the part of the basin that lay beneath the mixed zone and below the chemocline. Based on Figure 7, the maximum length or average diameter of a microlaminated unit reflects the area over which wave base did not intersect the bottom. The depth predicted for that length or area then yields the minimum depositional depth using Equation (1) (Table 1).

The Westfield Bed, the fairly well-delimited microlaminated unit in the middle East Berlin Formation containing abundant fish and the Hartford Basin equivalent of the Pompton Ashes (Fig. 4 and Stops 1–3), has been identified at every examined stratigraphically appropriate locality and plausibly extends across the entire preserved formation. Using the relationships in Figure 6, the maximum potential fetch of 121 km or the average fetch of 48 km for the preserved East Berlin Formation gives predicted minimum lake depths of 61 m, 87 m, and 112 m or 36 m, 52 m, and 67 m for 20 m s^{-1}, 30 m s^{-1}, and 40 m s^{-1}, respectively. If the microlaminated Westfield Bed covered the entire preserved basin, those values would be 62 m, 89 m, and 114 m or 43 m, 61 m, and 79 m, respectively, for the same range of wind speeds (Table 1). Thus, the minimum lake depth required to preserve the microlaminated unit ranged between 36 and 114 m.

Because chemoclines often occur deeper than predicted under high-wind conditions (Fig. 7; Table 1), and because the Westfield Bed may once have extended beyond the Hartford Basin, these values are conservative. They correspond to a lake roughly comparable in size to Lake Kivu among the African Great Lakes, where sediments below the chemocline are microlaminated, as expected (Wood and Scholz, 2017). At highstand, the open waters of the Westfield Bed lake may have extended into adjacent basins—the Deerfield, Pomperaug, Newark, and Culpeper—each preserving coeval strata (see Stop 1). If so, its area and predicted chemocline depth could have rivaled Lakes Malawi or Tanganyika, reaching ≥100 m.

The same fundamental relationship applies to the Bluff Head Bed of the Shuttle Meadow Formation (Stops 1 and 4). Along the eastern extent of the formation, the lower part is locally absent where the unit onlaps onto the underlying Talcott Basalt or, where that is missing, the New Haven Formation. Although it is plausible that the microlaminated Bluff Head Bed originally extended into these areas and was later eroded during regression and low stands, no direct evidence supports this. Conservatively, the preserved area of the

bed is estimated at ~1600 km^2, implying a predicted minimum lake depth between 35 m and 65 m. Equivalent microlaminated strata appear absent in the Deerfield Basin but may occur in the Pomperaug Basin (Cass Formation) and are definitely present in the Newark Basin (Vosseler Bed, Feltville Formation) and the Culpeper Basin (Midland Bed, Midland Formation) (Whiteside et al., 2011). Onlapping of the Shuttle Meadow and Feltville Formations onto their respective underlying basalts indicates greater asymmetry and sediment focusing than in younger successions. The depositional system may have been narrower but nearly as long, suggesting the Bluff Head Lake's minimum depth could have exceeded estimates derived from the Hartford Basin alone.

The stratified-lake model remains highly effective for explaining Lagerstätten within microlaminated strata because of its simplicity. In relatively warm climates, lake geometry and basin size are the principal variables. Notably, it is the only model verified by a modern example of articulated fish preservation in a microlaminated lake of known type.

Key Specific Fossil Examples of the Stratified-Lake Model

Several key lacustrine Lagerstätten illuminate the stratified-lake model and show how alternative interpretations can be reconciled within it. The similarities of these occurrences to the Hartford Basin Lagerstätte requires they be examined. These examples, described in more detail in Supplemental Material text 1.3 include the Eocene Green River Formation (Wyoming, Colorado, Utah, USA), strata containing the lacustrine components of the Early Cretaceous Jehol and Late Jurassic Yanliao biotas (northeastern China), and the Triassic Solite assemblage of the Cow Branch Formation (North Carolina and Virginia, USA) (Fig. 10). These examples also frame the model's broader implications for understanding and predicting future fossil discoveries in the Hartford Basin and other eastern North American rifts.

Across the Green River, Jehol, Yanliao, and Solite Lagerstätten, microlaminated strata and exceptional fossil preservation are most parsimoniously explained by deposition in deep, stratified, and commonly meromictic lakes. In each system, alternative interpretations, whether shallow, saline (Liutkus et al., 2010; Fraser et al., 2017), playa-lake (Eugster and Surdam, 1973), or microbial-mat models (Schieber, 2007; Hellawell and Orr, 2012), and in the Asian examples, volcanically induced mortality (Benton et al., 2008; Jiang et al., 2011, 2014; Wang et al., 2019; Yang et al., 2019; Zhong et al., 2021) have been advanced to explain the same suite of features: fine lamination, articulated skeletons, and soft-tissue preservation. Yet none of these alternative models withstand detailed sedimentological or taphonomic scrutiny (e.g., Boyer, 1982; MacLennan et al., 2024; Vastano, 2025; Supplemental Material text 1.3).

Modern shallow or shallow hypersaline lakes are not known to generate microlaminated couplets traceable over kilometers, nor have they been shown to preserve complete vertebrates and arthropods. Supposed evidence for microbial binding is better explained by post-depositional deformation rather than pervasive benthic mats. Likewise, dolomite and clam shrimp occur in a wide range of lacustrine settings and do not diagnose hypersalinity or shallow water. Claims of volcanically driven mortality fail where ash horizons cannot be specifically linked to fossil concentrations, and even in the volcanogenic Chinese basins, exceptional preservation occurs independent of direct volcanic influence. Instead, all four Lagerstätten share key hallmarks of stratified lakes: laterally persistent microlaminae, preservation in the depocenter of the lake basin, presence of articulated animals, and absence of in situ benthic animal activity.

Taken together, objections to the stratified-lake model in these cases are unsupported by direct evidence, while its predictions, laterally persistent laminations, and exceptional fossil preservation, lack of benthos, etc., are uniformly met across these Lagerstätten. It remains the simplest and most robust framework for explaining their shared depositional and taphonomic character.

Conclusions from Specific Examples

Two main conclusions emerge. First, the stratified-lake model provides an appropriate null hypothesis for microlaminated Lagerstätten. Shared sedimentary and taphonomic features across these deposits, such as continuous lamination, articulated skeletons, and soft-tissue preservation, are best explained by deep, stratified lakes with anoxic bottom waters. This model requires only that the basin exceeded its mixing depth and sustained organic flux sufficient for hypolimnetic anoxia, conditions common in temperate and tropical lakes. It should be rejected only when clear evidence supports alternatives such as shallow saline or microbial-mat systems with falsifiable predictions. For the Hartford Basin and other examples, no such evidence exists, and the stratified-lake interpretation remains most parsimonious. Second, shoreline proximity strongly influences the occurrence of terrestrial biotas. Narrow, steep-sided basins bring the anoxic hypolimnion close to land, enhancing preservation of terrestrial and aerial organisms. Deep, stable basins such as those of the Green River, Jehol, and Yanliao systems provided more frequent opportunities for nearshore anoxia than the more cyclic lakes of the Hartford Basin, with Solite representing an intermediate case. The extent of collection effort, especially intensive private collecting by local farmers in the Jehol and Yanliao Biotas (Fig. 11), has a major effect on the discovery of rare vertebrates such as birds, mammals, or feathered dinosaurs, emphasizing both depositional and sampling controls on exceptional preservation.

WALTHER'S LAW IN RELATION TO ORBITALLY PACED LAKE CYCLES

For educational institutions across eastern North America, the early Mesozoic lacustrine successions of the eastern United States provide readily accessible examples of vertical facies sequences and appear to exemplify Walther's Law. Yet their continental rift-basin context requires caution. Walther's principle—that only facies laterally contiguous in space can stack vertically in time—arose from open, marine shelf systems where shifting shorelines and

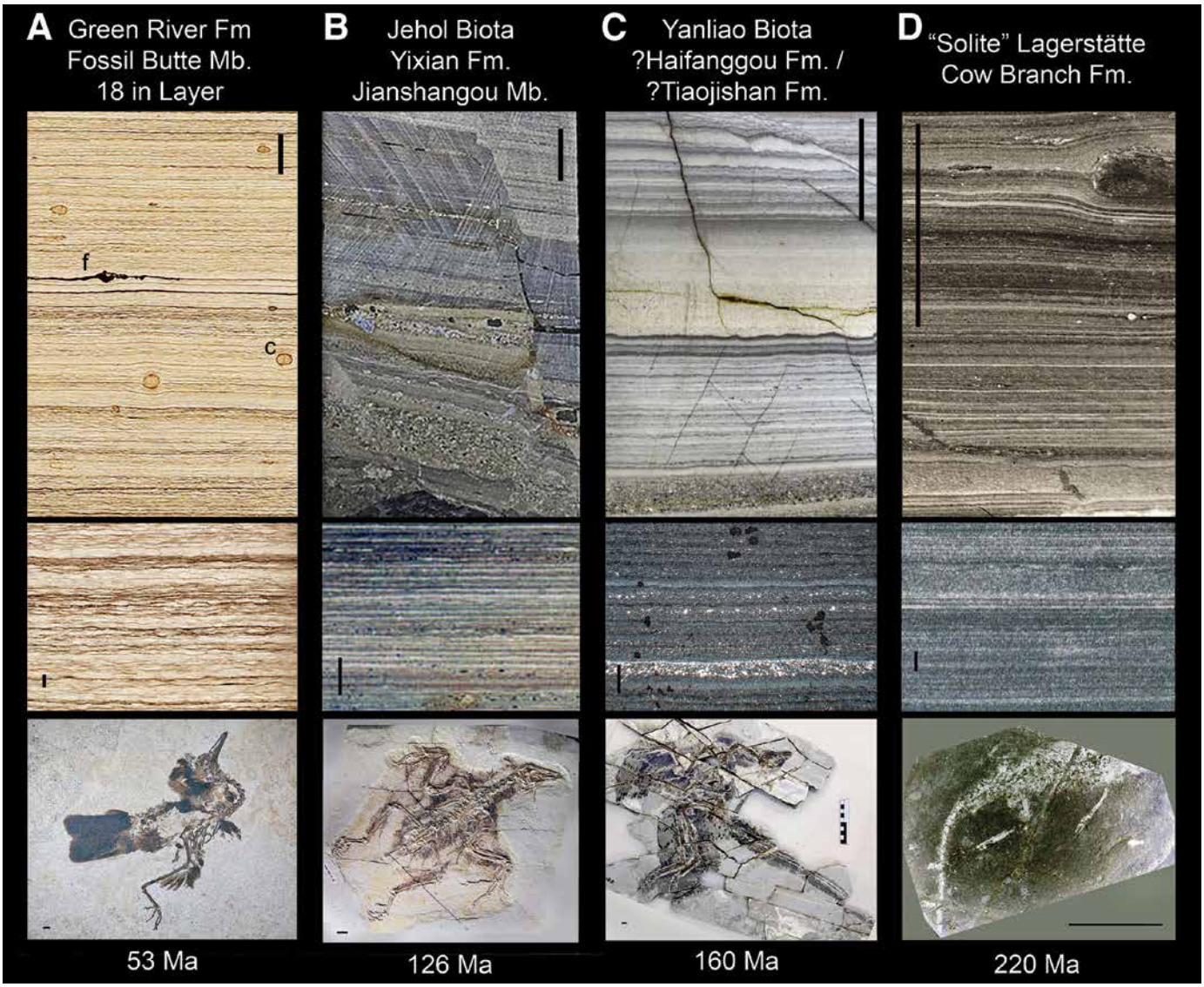

Figure 10. Example of microlaminated facies from major lacustrine Lagerstätten. (A) Green River Formation (Wyoming, USA): top, portion of 18-inch layer (c is coprolite, f is a fish; middle, slabbed portion of 18-inch layer; bottom, neoavian bird, *Nahmavis grandei*, Field Museum (FMNH PA778). (B) Jehol Biota (Liaoning Province, China): top, Anjiagou Bed, Sihetun no. 1 core, 32.5 m; middle, thin section Sihetun Fossil Museum section; bottom, pygostylian avialan bird, *Confusiusornis sanctus,* Royal Tyrell Museum TMP98.14.01. (C) Yanliao Biota: top and middle (Inner Mongolia, China); bottom, non-avian, paravian, theropod dinosaur, *Anchiornis huxleyi* Shandong Tianyu Museum of Nature (Pingyi), STM0-214 (Liaoning Province, China). (D) Solite Lagerstätte (North Carolina, USA): top, *Tanytrachelos*- and fish-bearing laminate; middle, "insect bed," VMNH 211653; bottom, very small reptile with soft tissue preservation, VMNH120045. Scale for upper and lower is 1 cm; scale for middle is 1 mm. Fm.—Formation; Mb.—member. Figure credits: (A) Top, courtesy National Park Service (Jamie P. Kennedy); middle, courtesy Lance Grande, Field Museum; bottom, Musser and Clark (2020: Fig. 1; used with permission of G. Musser). (B) Middle, Zhang and Sha (2012; their fig. 6A3; used with permission of Elsevier © 2012); lower, image courtesy of the Royal Tyrrell Museum, Drumheller, AB). (C) Upper and middle, Yang et al. (2019; their figs. 4A and 5A; used with permission of Elsevier © 2019); lower (https://www.eurekalert.org/multimedia/827048; credit: Xiaoli Wang). (D) Lower, courtesy Virginia Museum of Natural History, www.vmnh.net).

accommodation changes translate laterally connected facies into vertical sequences. In contrast, rift-lake strata formed in structurally confined, largely closed basins are governed by climate rather than eustasy. Here, successive lake levels reflect major climatic oscillations, not lateral facies shifts within a single depositional system. Modern analogues such as Lake Bonneville and the Great Salt Lake show that deep, freshwater, and shallow, hypersaline facies can occupy the same basin at different times but were never contemporaneous; their vertical superposition violates the spatial premise of Walther's Law. Similarly, orbitally paced lake cycles in the eastern North American rifts record climatic transitions between humid, deep-water and arid, playa phases, each with its own set of

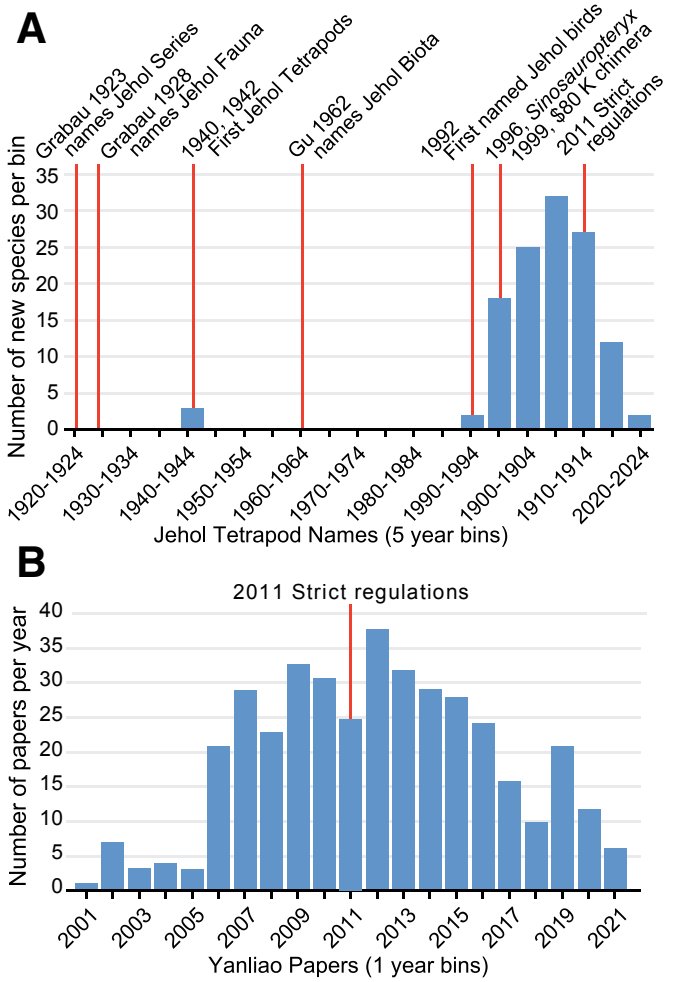

Figure 11. Histograms of frequency of proxies for charismatic fossil discoveries in relation to government laws regulating excavation, sale, and export in China. (A) New tetrapod names in five-year bins from 1923, when Grabau (1923–1924) first named the Jehol Series, to the present. Fossil occurrence data were downloaded from the Paleobiology Database (https://paleobiodb.org; accessed December 2025) with the following filters: Amphibia, Reptilia, Mammalia, Aves, Liaoning, Hebei, Inner Mongolia Provinces, Yixian, Jiufotang Formation, Early Cretaceous (Uhen et al., 2023). All exclusively Lujiatun taxa were manually excluded, and three occurrences otherwise missing were added. (B) Histogram of the number of references about insects at Daohugou each year (redrafted from Lian et al., 2021).

lateral facies relations. Walther's Law thus applies only within individual lake phases and not across entire climate-driven successions (Supplemental Material text 2.0). We will spend time discussing specific field cases of Walther's Law in the field where appropriate.

Implications of Microlaminated Strata

Microlaminated, fish-bearing strata of the Hartford Basin exemplify the stratified-lake model as a default null hypothesis. They formed during the most humid, deepest-water phases of their respective lacustrine cycles, and the only fundamental requirement of the model is that the lake became sufficiently deep in a warm climate (minimal seasonal overturn). Other proposed explanations for the same phenomena require additional, more complex assumptions and evidence. Strata with different facies above and below the microlaminated intervals record different climatic contexts and, except for those immediately adjacent to the microlaminated beds, would not be expected to have existed laterally alongside them, so Walther's Law does not apply.

Globally renowned Lagerstätten such as the Jehol assemblage share essentially the same facies type as Hartford Basin microlaminated strata. It is therefore reasonable to suspect that, if comparable collection effort were focused on Hartford microlaminated units near basin margins, where the likelihood of capturing nearshore and terrestrial faunal components is highest, rare elements such as feathered non-avian dinosaurs or densely proto-feathered pterosaurs might eventually be recovered.

In 1868, Thomas Henry Huxley, nine years after the publication of *On the Origin of Species*, anticipated this potential. Commenting on what are now recognized as very latest Triassic and Early Jurassic strata, he wrote:

> … It is true that these have yielded neither feathers nor bones; but the creatures which traveled them when they were the sandy beaches of a quiet sea have left innumerable tracks which are full of instructive suggestion. … The important truth which these tracks reveal is, that at the commencement of the Mesozoic epoch bipedal animals existed which had the feet of birds, and walked in the same erect or semierect fashion. These bipeds were either birds or reptiles, or more probably both; and it can hardly be doubted that *a lithographic slate of Triassic age* would yield birds so much more reptilian than *Archaeopteryx*, and reptiles so much more ornithic than *Compsognanthus*, as to obliterate completely the gap which they still leave between reptiles and birds. (Huxley [1868], p. 74, emphasis ours)

STOPS AND DESCRIPTIONS

Trip will begin at Dinosaur State Park, which is Stop 1 (Figs. 12 and 13).

Stop 1. Dinosaur State Park, Rocky Hill, Connecticut (400 West St., Rocky Hill, Connecticut 06067; 41.652639°, -72.656194°; 41°39′9.5″N, 72°39′22.3″W)

We will examine and contextualize main track surfaces and lacustrine fossils. We will also have lunch, and during the 2026 GSA meeting, examine cores and samples.

Main Points

1. Dinosaur State Park anchors discussion of orbitally paced lacustrine cycles, microlaminated sediments, stratified lakes, and limits of Walther's Law.

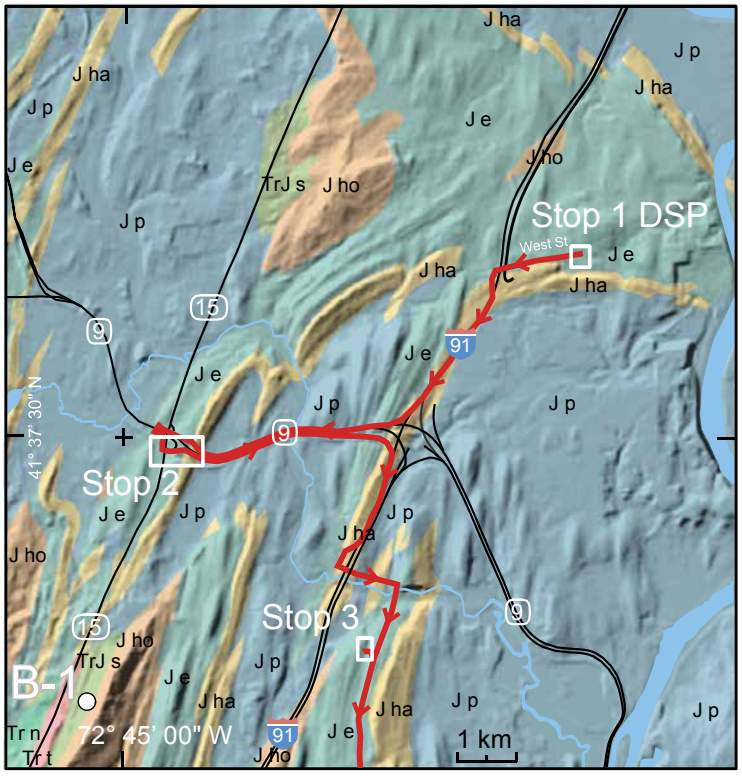

Figure 12. Geologic map showing locations of Stops 1–3 in the East Berlin Formation. Key to their stratigraphic abbreviations (in order of oldest to youngest): Tr n—Triassic New Haven Formation; Tr t—Triassic Talcott Basalt; TrJ s—Triassic–Jurassic Shuttle Meado Formation; J ho—Jurassic Holyoke Basalt; J e—Jurassic East Berlin Formation; J ha—Jurassic Hampden Basalt; J p—Jurassic Portland Formation. Geology from Lehmann (1959); Drzewiecki et al. (2012); Hanshaw (1968); and Simpson (1966); Lidar from The National Map. B-1—location of the Silver Ridge B-1 core hole. DSP—Dinosaur State Park.

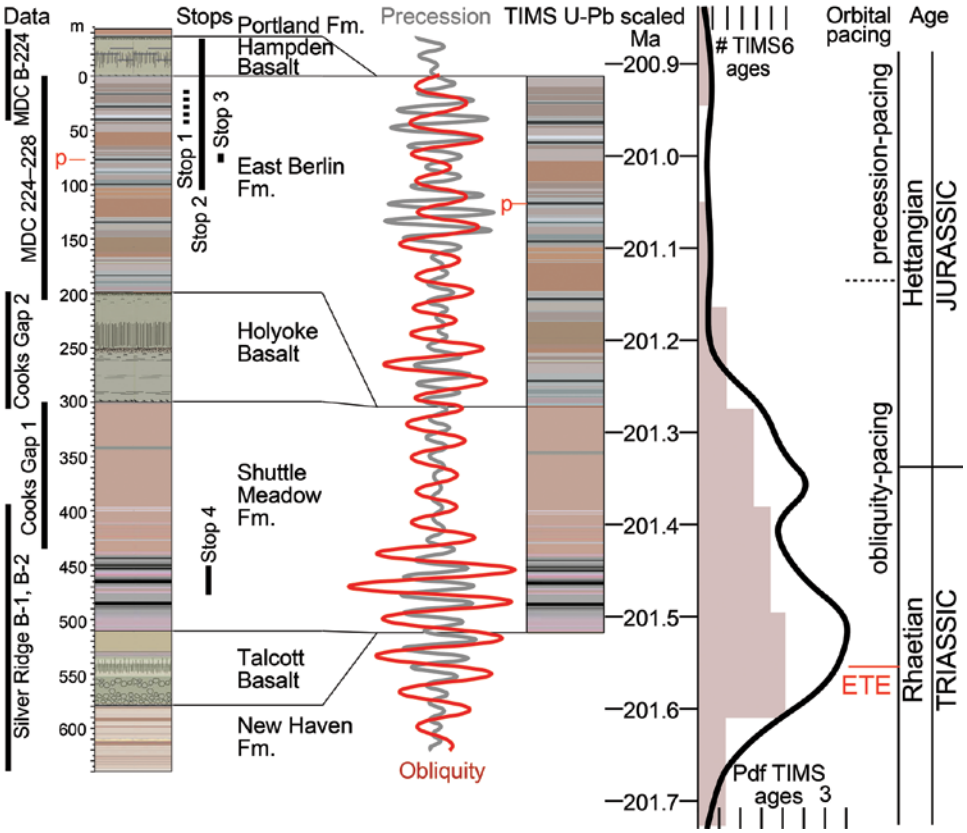

Figure 13. Stratigraphic and temporal context of syn-CAMP (Central Atlantic Magmatic Province) lacustrine units in the Hartford Basin and field stops. Zircon U-Pb and chemical abrasion–isotope dilution–thermal ionization mass spectrometry (CA-ID-TIMS) ages from entire area of the CAMP (Blackburn et al., 2013; Wotzlaw et al., 2014; Davies et al., 2017, 2021). ETE—end-Triassic mass extinction; and p shows position of the Pompton Ashes. Stratigraphic data sources: Hampden Basalt and basal Portland data from photographs of core MDC BD-224 (AECOM, 2015); MDC cores 224–228 adapted from Conti (2016)—compilation colors retained but lightened; Cooks Gap 2 (Plainfield, Connecticut), outcrops from Gray (1982); Cooks Gap 1 (Plainfield, Connecticut), adapted from Hubert et al. (1978); Silver Ridge B-1 core from Whiteside (Whiteside et al., 2011). Scaling of Cooks Cap 1 to the Silver Ridge core remains uncertain and is here based on Olsen et al. (2003). Preliminary filtered obliquity and precession, time scale, and probability density function adapted from Olsen et al. (2025b) by S.T. Kinney based on CA-ID-TIMS ages from Blackburn et al. (2013). Fm.—formation.

2. Track-bearing sand sheets formed in a shallow, wave-dominated perennial lake with thick microbial mats and no evidence of desiccation.
3. Microbial-mat features and modern analogs argue against ephemeral, subaerial sand-sheet models.
4. Fishes document trophic structure and water-column and sediment chemistry.
5. Cores reveal orbitally paced lacustrine cycles and permit secure regional correlations.
6. Shuttle Meadow thickness variations indicate syndepositional small half-grabens.
7. East Berlin cycles are much more laterally uniform, implying a change in subsidence style.
8. Westfield Bed turbidite and the Pompton Ashes demonstrate flat lake floors, support long-range correlations, and indicate deep perennial lake conditions.
9. Evidence at Dinosaur State Park indicates a climate-driven transition from deep to shallow perennial lake and eventual desiccation, contradicting simple Walther-style shoreline equivalence.

Discussion

Dinosaur State Park (DSP) will serve as our lunch stop and is the site where the famous in situ dinosaur footprints can be examined in the context of a single precession paced lacustrine cycle (Fig. 14). This stop will also set the stage for the remaining three stops by examining cores and slabbed sediment block that reveal their orbitally paced sedimentary-cycle context, which will be compared with modern lake deposits that also preserve fish.

The history of the park and detailed documentation of the tracks and associated sedimentary structures have been presented in multiple papers, including Ostrom (1967), Ostrom and Quarrier (1968), Ostrom (1972), Galton and Farlow (2003), Farlow and Galton (2003), Farlow et al. (2025b, 2025a), Hyatt et al. (2025), Drzewiecki and Hyatt (2025), Brinkman and Hyatt (2025), Ross et al. (2025), McDonald et al. (2025), and numerous guidebooks. Here, however, the emphasis will be on the Park's context for microlaminated sediments, the stratified-lake model, and Walther's Law.

The exposures within the exhibit center dome are unequivocally part of the regressive phase of a lake-level cycle in the East Berlin Formation. Although this could be inferred from nearby outcrops, it is most clearly demonstrated by three short cores taken early in the history of DSP, described by Zangler (1969) and Byrnes (1972) (Fig. 14). The first two, 3.7 cm BQ cores drilled in 1967, were used to determine the attitude and displacement of a fault on the south side of the main track area and have since been severely damaged. The third, a 6.4 cm HQ core drilled in 1969 and described in Zangler's (1969) unpublished report, is much better preserved. All three show that the track beds lie in the upper part of a "sandwich" of very dark-gray to black microlaminated mudstone between gray mudstones and sandstones, unmistakably representing the regressive portion of a cycle in the upper half of the East Berlin Formation.

Stop 1 is divided into two stations within the exhibit center and one outside (Fig. 14): Station 1 focuses on the main track beds and overlying strata inside the Exhibit Center; Station 2 examines exhibits of fossil fish, many from the East Berlin Formation; Station 3, at the Picnic Area outside the Exhibit Center, is where lunch will be held and DSP Core 1-1, relevant fossil fish, and slabbed sections of the East Berlin Formation will be inspected, along with segments of the B-1 core of the Shuttle Meadow Formation in preparation for Stop 4.

Station 1

Look over the two main track surfaces in the exhibit center. About one-fourth of the originally exposed track-bearing surface at Dinosaur State Park is visible here, with nearly all the remaining area in the larger excavation east of the building carefully covered and reburied in 1978 for protection. The principal track layers are two stratigraphically adjacent beds of light gray, fine- to coarse-grained, micaceous sandstone, separated from each other and the surrounding strata by thin mudstone partings (Fig. 15). The lower bed is termed Layer 0 and the upper bed, Layer 1 (Farlow et al., 2025b). Many Layer 1 tracks are infilled by sandstone with oscillatory ripples ("pancakes," Layer 2; Farlow et al., 2025b). Numerous Layer 1 tracks are transmitted into Layer 0, which is almost completely covered by oscillatory ripples. On both layers, note the absence of desiccation cracks and the general smoothness of most of the surface. Climb down onto the track surface (only with advance permission from park staff).

Most researchers interpret the footprint-bearing beds as shoreline deposits of a perennial lake (e.g., Byrnes, 1972; Hubert et al., 1976; Coombs, 1980; Farlow and Galton, 2003; McDonald, 2010; LeTourneau et al., 2015). In a simple transgressive–regressive marine-shelf analogy, one might infer that the underlying black microlaminated mudstones (Fig. 14) are laterally adjacent deep-lake deposits, following Walther's Law. This conceptual framework underlies the well-known *Dilophosaurus* diorama and mural at Dinosaur State Park, which show a perennial lake with a lush, forested shoreline.

However, bed-by-bed temporal correlations across the basin are not yet precise enough to demonstrate that the track-bearing sandstones pass laterally into a truly contemporaneous laminated dark-mudstone sequence representing a perennial lake. Microlaminated intervals in Hartford Basin lacustrine cycles thicken dramatically toward the eastern border-fault system (LeTourneau and McDonald, 1985), suggesting such a correlation if thickness alone is a proxy for time. Extending this reasoning upward into the red beds toward the next cycle exposes a problem with Walther's Law: if applied strictly, a continuous microlaminated mudstone sequence should span an entire cycle, including the red beds, yet basin-wide data show the lake dried out many times during red-bed deposition. The climatic and hydrologic conditions that sustained a deep lake no longer existed in the regressive phase, so it is essential to distinguish what is actually observed from what is inferred as lateral equivalents, and to understand how those hypotheses can be tested.

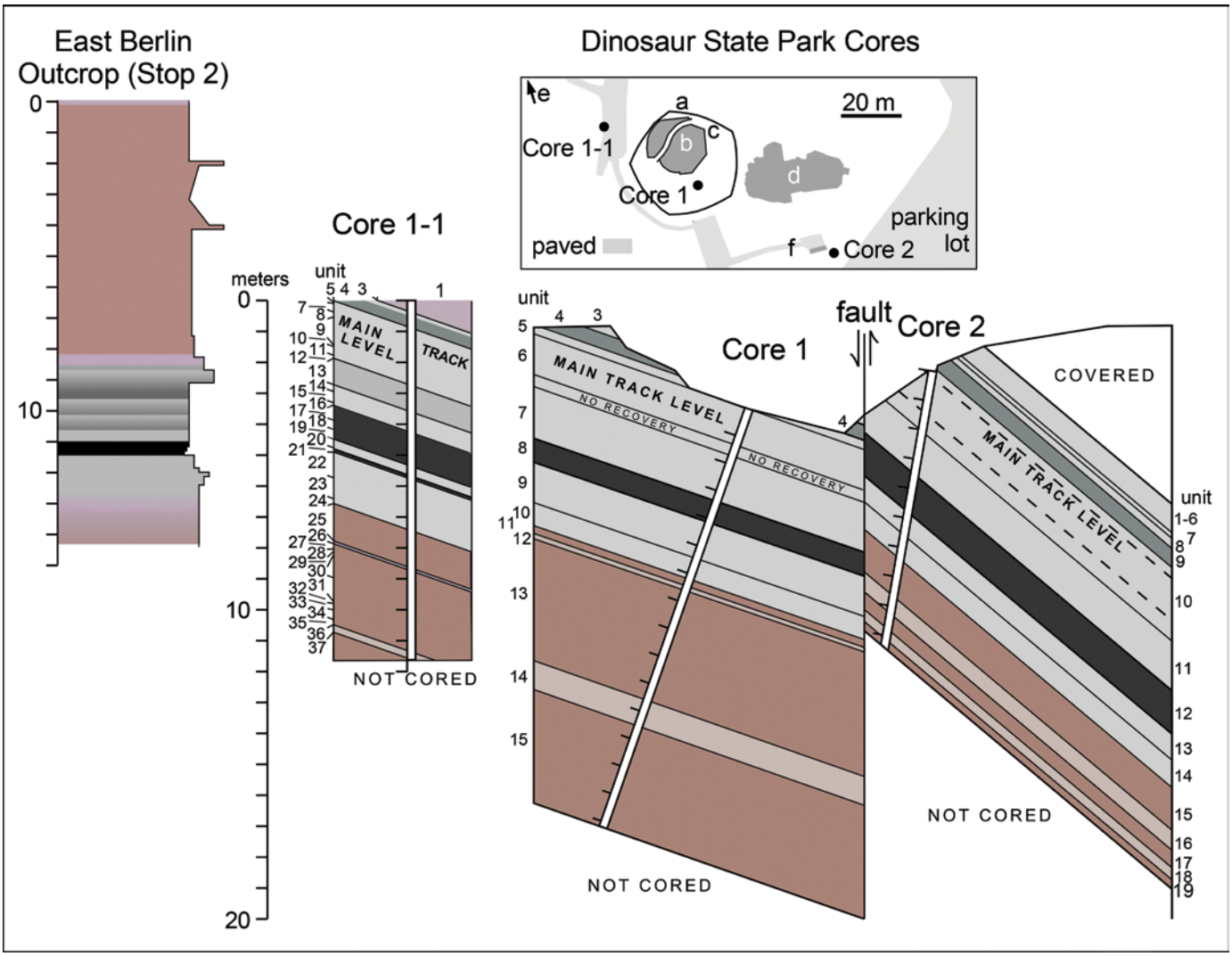

Figure 14. Cores from Dinosaur State Park (DSP) (after Byrnes, 1972, plate 6B; as modified by McDonald et al., 2025) showing strata encountered in the DSP Cores 1 and 2 compared to DSP Core 1-1 and a single cycle at Stop 2. The very dark unit ~3 m below the track beds is a fossiliferous, gray-black, microlaminated shale: unit 8 of Byrnes (1972) and units 17–19 of Zangler. Tick marks on cores are in meters; vertical exaggeration is 5× for the DSP sections. Inset shows locations of cores and track areas (based on historical imagery and models of Hyatt et al., 2025): a—Exhibit Center; b—in situ track area and adjacent overlying stratigraphy (Station 1); c—area with exhibit of fishes and other fossils (Station 2); d—covered track area; e—picnic area (Station 3); f—small additional track area (Station 4).

1. The thin sand sheet comprising Layer 1 has been heavily modified by microbial-mat processes (P.M. LeTourneau, 2019, personal commun.; Drzewiecki and Hyatt, 2025; McDonald et al., 2025; Olsen and McDonald, 2026; Drzewiecki et al., 2026). Mat tears, wrinkle and roll structures, and gas bubbles are key to the environmental interpretation.

2. Cracks and fissures in the tracks support a thick microbial mat on Layer 1 at the time the tracks were made, consistent with extension of a cohesive mat during implantation. Thick mats suppress fine anatomical detail (e.g., pads, scales), and the lack of such detail on DSP ichnites is similar to footprints on modern thick microbial mats (Marty et al., 2009; McDonald et al., 2025). These are true tracks (Farlow et al., 2025b); if they were undertracks, overlying true tracks should occur on counterpart slabs, which they do not. The enigmatic footprints described by Coombs (1980) may record interactions between flexed toes of a swimming dinosaur and a thick microbial mat. They do not resemble, proportionally, what you would expect of a full digitigrade footfall of a *Eubrontes*-type trackmaker (presumed digit III appears too far forward).

3. Coombs (1980) argued the unusual three-part tracks mentioned above were made by swimming theropods in 1.5–2.5 m of water, but this interpretation remains disputed (e.g., Farlow et al., 2025b; McDonald et al., 2025; Drzewiecki et al., 2026).

4. There is no convincing evidence of desiccation in Layers 0–2. Drzewiecki and Hyatt (2025) and Drzewiecki et al.

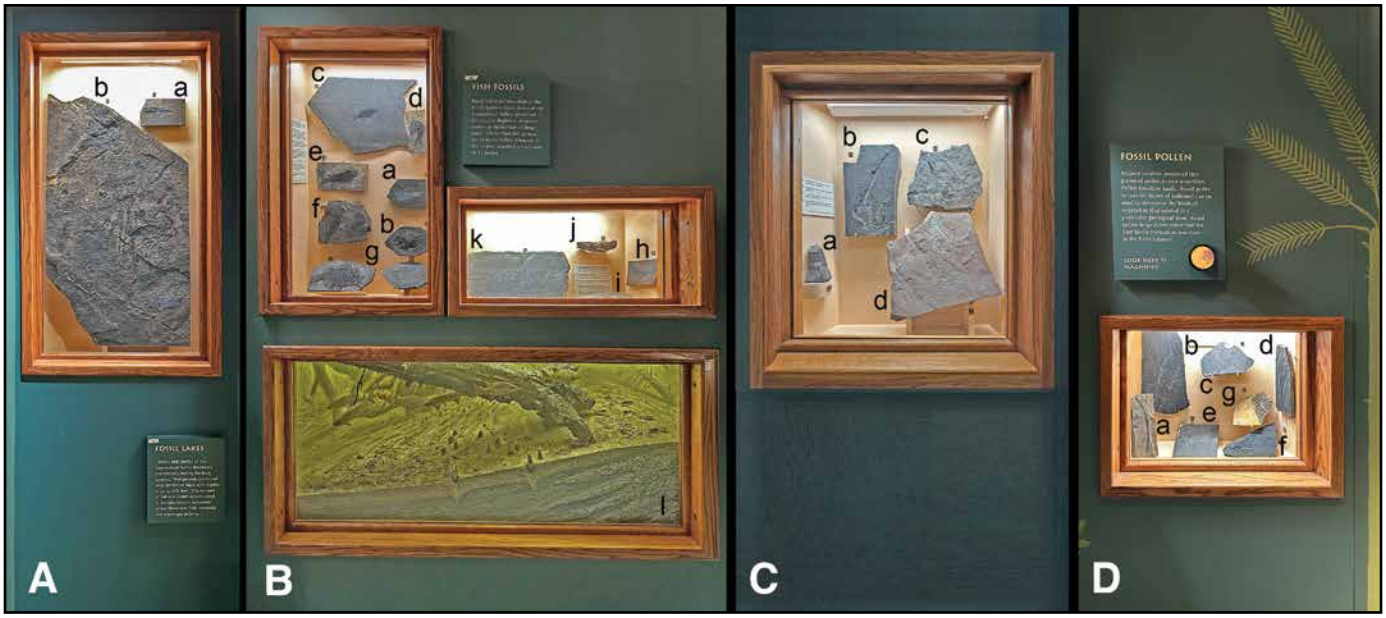

Figure 15. Key to display of fossils at Station 2 (c in Fig. 14): (A) the coelacanth *Diplurus* and its putative coprolite (Westfield bed); (B) fishes, clams, a clam escape structure, and coprolite from Shuttle Meadow, East Berlin, and Portland Formations and a shoreline diorama; (C and D) fossil plants from all Hartford Basin formations. See text for detailed explanation. Photos courtesy of Michael Ross, Dinosaur State Park.

(2026) cite small (~10 cm) "sand cracks" on Layer 1 as desiccation and microbial-mat tearing. McDonald et al., (2025) interpret the same features as roll structures produced by tears in the microbial mat under subaqueous shear stress (Bose and Chafetz, 2009; Mariotti et al., 2014; Peterffy et al., 2016; Tu et al., 2016).

5. At times, water was shallow enough for large dinosaurs to walk and leave tracks (probably <~2 m for Layer 1), and the scarcity of small tracks on the upper main track layer may indicate water depths of 1–2 m that excluded smaller trackmakers. Smaller dinosaur tracks in Layer 0 indicate shallower water, ~1 m or less, when those tracks formed.

6. The oscillatory-ripple wavelength (~3–4 cm, crest-to-crest) indicates shallow water, on the order of decimeters to roughly 1–2 m at most (e.g., Komar, 1974; Takeda, 1992; Mondro et al., 2025), although no single precise depth can be calculated. These constraints apply only to the oscillatory-rippled sand in Layer 0 and the ripple-bearing "pancakes" infilling tracks in Layer 1, and only to the times when the tracks were made.

7. Layer 1 is very planar, ~3–5 cm thick, and traceable across at least the entire western and eastern track areas at DSP (~80 m). Oscillatory ripples are not obvious on its surface, but in cross-section uncommon tilted grain lineations (identified by Drzewiecki and Hyatt, 2025, as current-ripple forsets) and wavy surfaces occur; overall, the bed appears massive to indistinctly bedded with sorted grain layers. Drzewiecki and Hyatt (2025) interpret Layer 1 as deposited by unconstrained flow (i.e., sheet floods), and the dimensions do fit within the range for such events (Fisher et al., 2007). However, in lakes with tens of kilometers of fetch, non-breaking storm waves in 5–20 m water depth can generate 3–5 cm planar sand beds extending for kilometers (Fagherazzi and Wiberg, 2009; Green and Coco, 2014; Roberts et al., 2019). The same reasoning can apply to Layer 0, the main difference being that its surface was not fully stabilized by a thick microbial mat as in Layer 1, so lower-energy wave reworking, perhaps in slightly shallower water, continued over most of the surface. A patchy microbial mat nevertheless developed, as shown by ripple-free sand patches previously interpreted as subaerial surfaces (Farlow et al., 2025b) (see McDonald et al., 2025).

8. The "pancakes" were interpreted by Farlow et al. (2025b) as either remnants of a once-continuous bed that remained attached to Layer 1 during excavation or as originally patchy, with the continuous-bed model favored because ripple crests are aligned. Drzewiecki and Hyatt (2025) also supported a continuous Layer 2. However, if Layer 2 had been continuous, most blocks preserving counterpart surfaces of Layer 1 tracks should retain a thin rippled sand layer above the track surface, which is not the case. An alternative model (Fig. 16) invokes a microbially bound surface that limited wave traction and erosion but still allowed sediment to accumulate in low spots such as deep footprints. Olsen and McDonald (2026) propose that the oscillatory-rippled infill represents sand migrating across a cohesive, thick microbial mat on the main track-bed surface; wave-transported sand largely bypassed the mat-stabilized surface and accumulated only in depressions (the deep *Eubrontes* tracks) where it could form oscillatory ripples because the sand there was not cohesive. Similar interpretations for unstabilized patches within otherwise microbially bound surfaces have been advanced by Schieber (1999) and Noffke et al. (2019), and in such

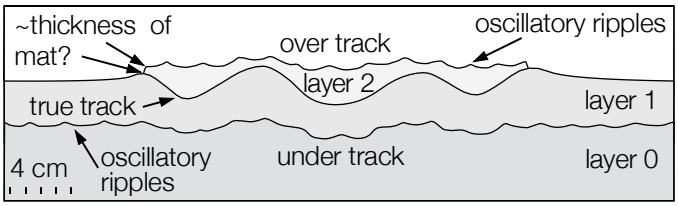

Figure 16. Diagram of the main track layers in cross section, illustrating how tracks infilled with wave-transported sand develop a raised lip that records mat thickness at the time of track formation (minus compressed and stretched mat within the track). After sand buries the Layer 2 infill, the mat decays and thins to near-zero thickness, leaving a silty-clay layer.

cases ripple crests align, as observed for the pancakes (Noffke et al., 2019; Buntin et al., 2025). The distinct lip around many pancakes is here interpreted not as the breakaway edge of a formerly continuous bed but as preserving the former thickness of the now-compacted microbial mat that once covered the main track layer (Fig. 16).

9. Rare pebbly beds and the overall coarseness of the sandstones suggest that the DSP site received detritus from nearby highlands ~4.3 km to the east, although longitudinal transport is also possible. This implies that the sediment surface at DSP was not the lowest point in the basin during deposition.

10. Layers with desiccation cracks and footprints occur a few decimeters above Layers 1–2, and desiccation features become increasingly abundant upward. This pattern reflects progressive lake shallowing, with repeated fluctuations, from the time of maximum depth when the microlaminated bed ~3 m below Layers 1 and 0 was deposited (Fig. 14) to the overlying red beds, when complete desiccation was common.

11. There is no evidence for hypersalinity.

In sum, Layers 0 and 1 formed in a wave-dominated lake that did not desiccate at DSP. Water depths likely fluctuated between less than a meter and perhaps ~20 m, with depositional events during deeper-water stages, followed by gentler wave reworking in Layer 0 and development of a thick, plausibly photosynthetic microbial mat on Layer 1 before dinosaurs crossed the surface during lower-water stages.

The time represented by Layers 1 and 0 remains uncertain. If the entire sand package is ~7 cm thick and the full precession cycle is ~11 m thick (see Stop 2), the interval could be as short as ~127 years. If the sands are event beds, most of that time would reside in intervening muds. If ~1 cm of mud accumulated at the same rate as in the microlaminated interval, it could represent only ~42 years (Kominz et al., 1991), although sediment bypass over the microbial mat under wave action could mean a longer effective duration.

African Great Lakes such as Kivu, Turkana, and Edward can fluctuate in depth by tens of meters over a few centuries during phases of rapid climate change (Morrissey and Scholz, 2014; Wood and Scholz, 2017). Comparable lake-level falls are documented for Great Basin lakes such as Bonneville and Lahontan, attributed to climatic forcing (Benson and Thompson, 1987; McGee et al., 2018). On this basis, simple scaling suggests that depth changes on the order of ~0.5–6.5 m could reasonably be expected over similar time scales under Quaternary-like conditions.

We conclude that Layers 0–2 were deposited in a perennial lake that fluctuated by a few meters over several decades; on human time scales this would still appear as a persistent lake not a playa. If, however, the sand beds of Layers 1 and 0 formed by unconstrained flow under essentially subaerial conditions, the oscillatory ripples, microbial mats, and dinosaur tracks would instead record deeper-water episodes, the opposite interpretation. Lake Eyre, where sand-sheet deposition is well documented, can show meter-scale rises or falls in water depth within about two years (e.g., ~0.8 m rise and fall from 2021 to 2025: https://earth.gsfc.nasa.gov/gwm/lake/10068), leaving sand sheets submerged for only months or less and exposed for years to decades. Such rapid oscillations would promote desiccation and fragmentation of a thick microbial mat into curled flakes (Noffke, 2021), unlike the smooth, well-preserved mat surface inferred for Layer 1.

Testing these alternative models requires detailed, bed-scale observations that trace individual units laterally over substantial distances. This may be difficult using only outcrops but could be achieved with modest coring campaigns. The critical question is what lateral facies relationships should be observed from this site to decisively reject one or both models. After considering these issues, return to the walkway and proceed to Station 2 at "c" in Figure 14.

Station 2

A series of cabinets display fossils from the Connecticut Valley, many directly relevant to this field trip and derived from units examined at Station 3 and Stops 2, 3, and 4 (Figs. 15 and 17). *Semionotus* (Figs. 15Ba–15Bd, 15Bf, 15Bg, and 17) is a ray-finned fish (Osteichthyes, Actinopterygii) closely related to living gars (Lepisosteidae) (Olsen and McCune, 1991; Grande, 2010). Named by Louis Agassiz in 1832, famous for recognizing the Pleistocene Ice Ages (Agassiz, 1840), now known to be paced by the same orbital cycles that paced the East Berlin cycles (Stop 2) (Hays et al., 1976), it was the second Jurassic fish genus found in the Connecticut Valley and in North America, after *Redfieldius*. *Semionotus* is by far the most abundant fish genus in post-ETE, syn-CAMP, latest Triassic–Early Jurassic lacustrine strata of eastern North America, where a few riverine species diversified into species flocks analogous to those of the African Great Lakes (McCune et al., 1984; McCune, 2004).

The *Semionotus* specimens on display come from three deep-lake microlaminated units (Figs. 13, 14): the latest Triassic Bluff Head Bed of the Shuttle Meadow Formation, Hartford Basin (Figs. 15Bd, 15Bf, 15Bg, and 17; Stop 4); the Westfield Bed of the East Berlin Formation, Hartford Basin (Figs. 15Ba, 17; Stops 2 and 3); and "Lake Bed # 3" of the Mount Toby Formation, Deerfield Basin (Wise, 1988) (Fig. 15Bb), the last preserved in

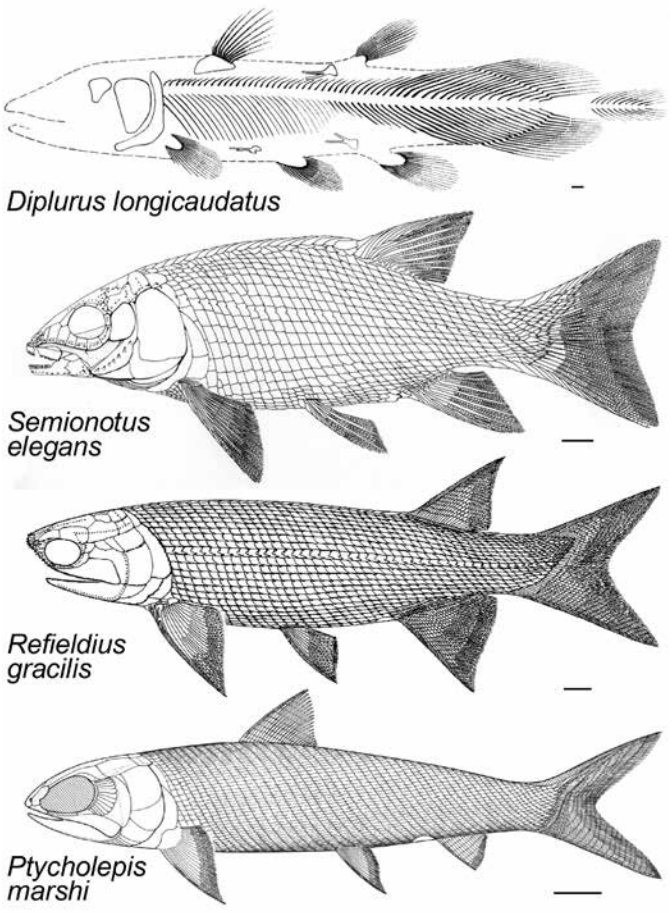

Figure 17. Reconstructions of the fishes in Figure 15. Sources are from top to bottom: Schaeffer (1948; used with permission of American Museum of Natural History); Olsen and McCune (1991); Schaeffer and McDonald (1978); Schaeffer et al. (1975). Scale bar is 1 cm.

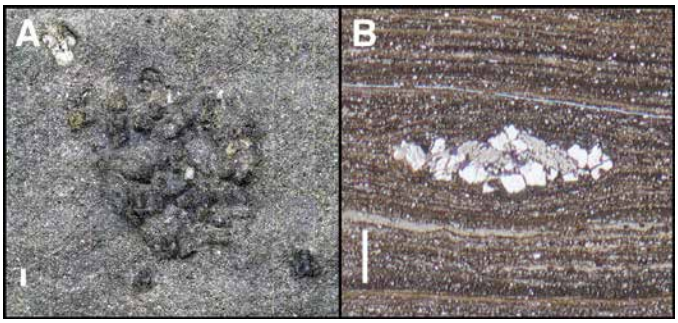

Figure 18. Blebs from the East Berlin Formation: (A) plan view large bleb (Keyence digital microscope image), same locality as Figure 15Bc; (B) thin section of small bleb, Dinosaur State Park, same locality as Figure 27. Both photos from Chang (2024; used with permission). Scale bars are 1 mm.

a split carbonate nodule. Shuttle Meadow *Semionotus* show the characteristic Bluff Head preservation style typical of sites near the eastern border-fault system, with robust, relatively uncrushed bone in a silty, medium-gray, calcareous microlaminated matrix. The East Berlin *Semionotus* (Figs. 15Ba and 17) are preserved differently: although fully articulated, like most Shuttle Meadow specimens, the skeleton is nearly flat, with bones extensively dephosphatized (McDonald and LeTourneau, 1989; McDonald et al., 2025). In the Eocene Green River Formation, similarly preserved specimens are termed "ghost fish" (Meacham, 2016, 2017) (Supplemental Material text 3.2, Fig. S5); we use "ghost fishes" here in the same descriptive sense. Similar preservation affects a number of units elsewhere in the Green River and in other taxa such as reptiles and amphibians (Grande, 1984). A bluish mineral, apparently calcite (Leonard, 2013), replaces the normally robust ganoid scales, skull bones are almost invisible, and only dark organic traces outline the skeleton. This dephosphatization characterizes the mid-basin taphonomic style of fishes and coprolites from the Westfield Bed (and other East Berlin microlaminated units). Most fishes lack the bluish trace and are mostly organic films, whereas calcareous fossils and plants in the same bed are well preserved, posing a geochemical puzzle discussed at Stop 3. Fishes nearer the eastern border fault in siltier lithologies, such as the Westfield Bed specimen in Figure 15Bc, resemble the Bluff Head material on display. Based on jaw morphology, *Semionotus* species were probably selective feeders (Whiteside et al., 2011) occupying a wide variety of niches.

Small (<1 cm), irregularly shaped protuberances and their impressions on the slab bearing the Westfield Bed *Semionotus* from near the border fault (Fig. 15Bc) are termed blebs (McDonald, 1975, p. 59). Internally, they are sand- to granule-sized clusters of lithic clasts, commonly quartz but also rock fragments (Fig. 18), interpreted as clasts trapped by filamentous algal mats along shorelines or rivers and rafted into open water, where they coalesced into pods as the mats sank (Chang, 2024).

A specimen of *Redfieldius* (originally *Catopterus*; Schaeffer and McDonald, 1978) from the Westfield Bed was among the fossil fishes reported in 1816 that formed the first early Mesozoic vertebrate record from North America (discussed in detail at Stop 3). *Redfieldius*, named for botanist John Howard Redfield, commemorates his work on *Catopterus gracilis* from a microlaminated lower Portland Formation unit as well as his father William Charles Redfield's broader contributions to Triassic–Jurassic geology; the original generic name was preoccupied and later replaced with their family name (Hay, 1902).

Redfieldius belongs to an extinct group of uncertain affinity, possibly near the origin of Neopterygians (gars + Amia + teleosts, excluding polypterids, sturgeons, and paddlefish). The specimen on exhibit (Figs. 15Be and 17), from the Bluff Head Bed, has a wide gape, small teeth, and an inclined jaw apparatus reminiscent of anchovies and paddlefish, suggesting a planktivorous lifestyle (Whiteside et al., 2011). It is the second most common fish genus in the Shuttle Meadow and East Berlin Formations.

Ptycholepis is much rarer than *Semionotus* or *Redfieldius* (Figs. 15Ch and 17). It bears distinctive, dorsoventrally narrow, strongly ribbed body scales on a fusiform body, and its

relationship to Neopterygians is also uncertain. Known originally from marine early Mesozoic deposits in Europe (including the Early Jurassic of Lyme Regis, UK), the American species *P. marshi* Newberry (1888) was first recognized from Bluff Head Bed material at the classic Durham locality (Stop 4) (Schaeffer et al., 1975) and is now known from both the Shuttle Meadow and East Berlin formations. Eastern U.S. rift-basin *Ptycholepis* have not been studied in detail, but their large eyes, fusiform bodies, and anterior dorsal fins suggest mid-water cruising and visual predation.

Diplurus cf. *D. longicaudatus* is a large coelacanth (Figs. 15Ab and 17). On the Westfield Bed display slab from the East Berlin Formation, the characteristic three-lobed tail fin and ovoid scales are evident. This specimen is almost completely dephosphatized and shows patches of bluish mineral on the skull bones. The genus was erected on material from the Boonton Formation (post-CAMP in the Newark Basin); the type remains unprepared, and it is unclear whether Shuttle Meadow and East Berlin *Diplurus* are conspecific with the Boonton holotype.

Diplurus cf. *D. longicaudatus* (Fig. 17), like other mawsonian coelacanths, was a large lacustrine apex predator, capable of ingesting all other Hartford Basin fishes except perhaps the largest *Semionotus* (McDonald, 2010). Abundant phosphatic coprolites (Figs. 15Aa and 15Bi), some containing fish scales and bones, are attributed to *Diplurus* as the only fish large enough to produce them, although other predators cannot be entirely excluded (McDonald et al., 2025).

Shallower-water lacustrine associations are also represented in the Hartford Basin and include bivalve molluscs, clam shrimp, ostracodes, and fishes such as *Semionotus* and coelacanths. Examples here are an internal bivalve cast (Fig. 15Bj), a bivalve escape trace associated with an intraformational conglomerate containing fish fragments (Fig. 15Bj), and a shallow-shoreline diorama. Although tempting to treat this assemblage as a lateral equivalent of deep-lake microlaminated units following Walther's Law, these strata come from the uppermost cyclical member of the Portland Formation (Stony Brook Member), which lacks microlaminated beds; a Shuttle Meadow example likewise comes from a non-microlaminated interval. These assemblages are more simply interpreted as facies marginal to or part of relatively shallow, perennial lake successions rather than direct lateral equivalents of deep-water microlaminated units.

Plants displayed here are mostly from microlaminated strata and include the large, distinctive, palmate-leaved fern *Clathropteris meniscoides* from the Bluff Head Bed (Fig. 16Cf), a fern fiddlehead from the Westfield Bed of the East Berlin Formation (Fig. 16Cb), the cycadeoid (Bennettitales) *Otozamites* from the Bluff Head Bed (Figs. 15Db, 15Dc, and 15De), and the ginkgoalean *Baiera* (Fig. 15Dd). Another *Clathropteris meniscoides* specimen comes from fluvial strata in the lower Shuttle Meadow Formation (Fig. 15Dg). *Clathropteris* is notable because, in eastern North America, it is confined to the ETE and syn-CAMP equivalents of the Shuttle Meadow and lower East Berlin formations; given its high-latitude abundance from the Late Triassic to Middle Jurassic, these occurrences may record an equatorward range shift during CAMP-related volcanic winters (Olsen et al., 2025b).

Conifers and horsetail rushes (*Equisetites*) are nevertheless much more common than ferns, cycadeoids, or ginkgoes. Examples include conifer wood from the uppermost New Haven Formation, enclosed by pillow lavas of the Talcott Basalt (Fig. 15Ca); *Equisetites* from non-microlaminated lacustrine strata of the South Hadley Falls Member of the lower–middle Portland Formation (Kent and Olsen, 2008) (Fig. 15Dg); and conifer wood, shoots, and cones from shallow-water red and gray lacustrine strata of the Stony Brook Member of the middle Portland Formation (Figs. 15Cc and 15Cd). The Stony Brook Member also yields clam shrimp, ostracodes, and insects, again without evidence that these shallow-water deposits are lateral equivalents of deep-water microlaminated units.

Proceed outside to the picnic area and Station 3 (Fig. 14).

Station 3

Segments of the Silver Ridge B-1 core (Shuttle Meadow Formation), DSP Core 1-1 (Zangler, 1969), and additional core intervals, slabbed sections, and fossil specimens will be available here as preparation for Stops 2–4 (Figs. 13, 14, and 19). Before 2002, the cycle-level stratigraphy of syn-CAMP lacustrine sequences in the Hartford Basin was inferred mainly from a single quarry in the upper Shuttle Meadow Formation (Hubert et al., 1978), a few large road cuts in the upper half of the East Berlin Formation (Hubert et al., 1976, 1978; Olsen et al., 1989), and several small, isolated outcrops that were difficult to integrate into a composite section. The cores now provide a basin-scale view of cycle stratigraphy, allowing detailed intervals to be placed in consistent stratigraphic, environmental, and temporal context.

Shuttle Meadow lakes. The Silver Ridge cores were recovered in January 2002 as part of a sandstone-reservoir assessment project and span the uppermost New Haven Formation and Talcott Basalt (Silver Ridge B-1 and B-3) and the lower half of the Shuttle Meadow Formation (Figs. 13 and 19). In terms of lower Shuttle Meadow stratigraphy, the cores were revelatory: what sparse outcrops had suggested were two lacustrine cycles proved to be four, and facies differences previously interpreted as lateral variation within cycles largely reflect differences between distinct cycles; Shuttle Meadow cyclicity could not be convincingly documented before these cores.

The most important points revealed by Silver Ridge B-1 are (Fig. 19): (1) the Shuttle Meadow is, in places, much thicker than previously recognized (~200 m versus ~100 m or less; Lehmann, 1959; Olsen et al., 2003; Whiteside et al., 2011); (2) the classic Durham fish bed (Stop 4) is only one (third from the base) of four microlaminated intervals, each with distinctive lithologies, within four lacustrine cycles, allowing isolated outcrops to be ordered stratigraphically; (3) the large-scale cyclicity has a 2:1 ratio to the smaller-scale cycles (Whiteside et al., 2011), demonstrating that correlative cyclicity in the Newark Basin had been misinterpreted; and (4) the large-scale

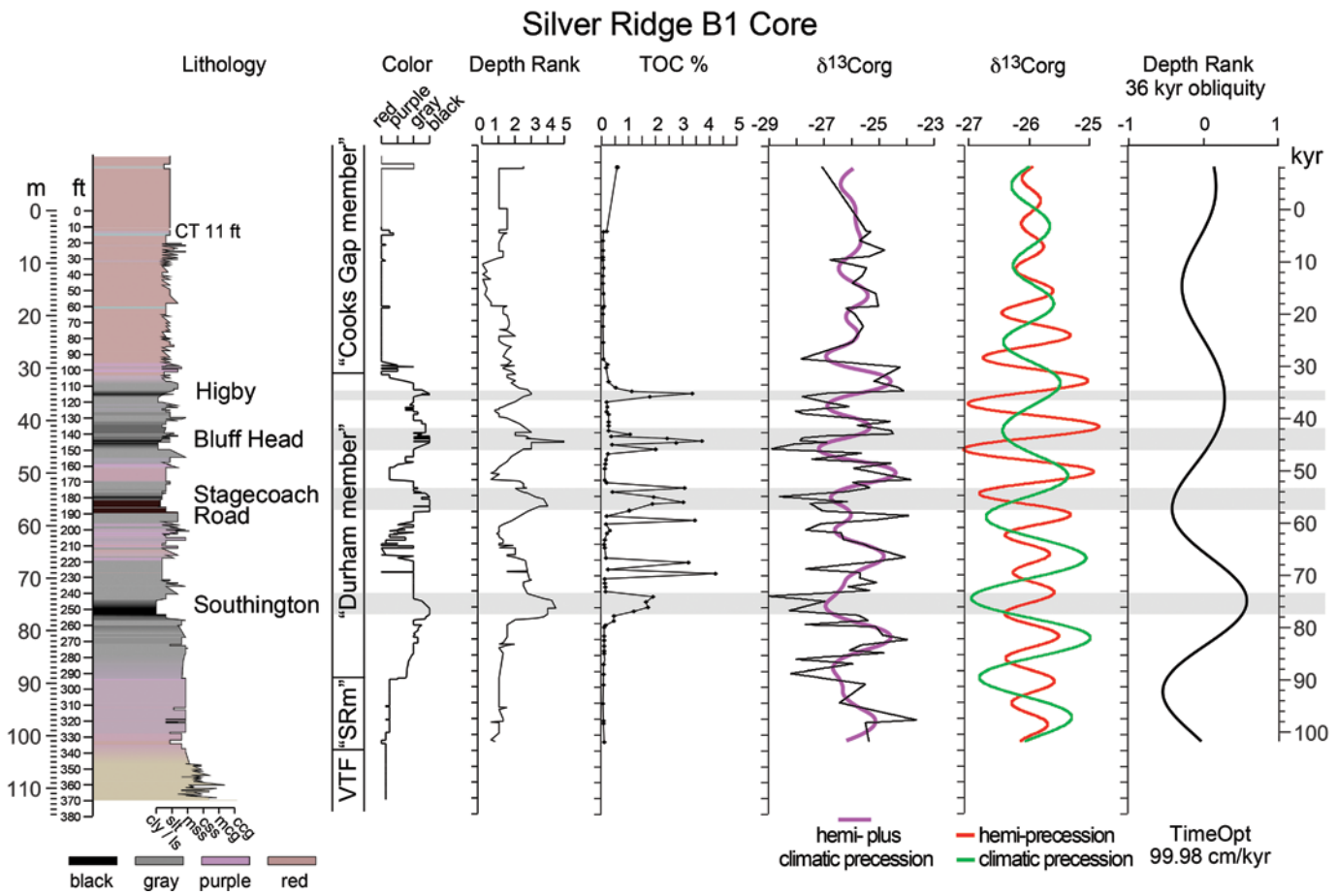

Figure 19. Silver Ridge B-1 core, lower Shuttle Meadow Formation and upper Talcott Basalt pyroclastics showing climatic precession (~19 kyr), hemi-precession (~10 kyr) and obliquity (36 kyr) cyclicity. Modified from Whiteside et al. (2011) with addition of new data (filtered obliquity). TOC—total organic carbon; org—organic. Informally, the Stagecoach Road Bed is known as "the crinkle bed."

cycles are paced by obliquity rather than precession (Olsen et al., 2024a, 2024b, 2025a).

Fossil fishes are best known from the Bluff Head Bed in the lower Shuttle Meadow, a carbonate-rich microlaminated interval that yields very well-preserved specimens (Figs. 2 and 19). Its microstratigraphy was described by Whiteside et al. (2011) based on materials collected by Bruce Cornet, Philip Huber, and Nicholas McDonald in the 1970s–1980s. Apart from being medium gray to nearly black, the Bluff Head Bed closely resembles the Westfield Bed and the 18-inch layer of the Fossil Butte Member of the Eocene Green River Formation, with wavy but laterally continuous microlaminae (Fig. 20), although their lateral extent is unknown. As in most microlaminated beds of the Shuttle Meadow, carbonate content can be high, up to ~64 wt% (Whiteside et al., 2011).

The lowest microlaminated bed, the Southington Bed, is more coarsely laminated, with a flocculant and pelleted appearance, and forms a limestone locally so pure it supported a hydraulic-cement industry in the early nineteenth century (Andrews, 1924; Wiley, 1933; Olsen et al., 2024b). Fishes in this unit tend to be less well preserved, and both fish and limestone are lighter in color, ranging to reddish brown and light gray to tan. These traits persist from the southernmost exposures at Bluff Head, Connecticut, to the northernmost at Northampton, Massachusetts, and characterize homotaxial equivalents in the Feltville Formation

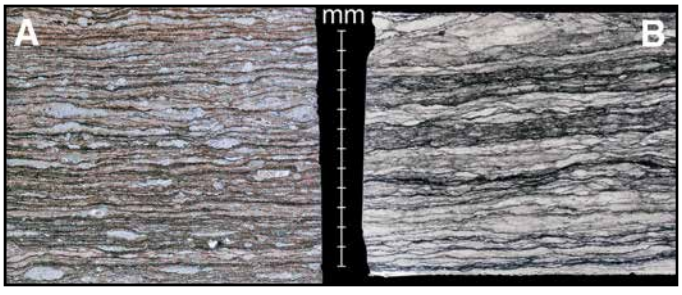

Figure 20. Thin sections of Hartford Basin microlaminated units: (A) Westfield Bed between Pompton Ashes, Stevens locality, Durham, Connecticut; (B) Bluff Head Bed at 146.25 feet in Silver Ridge core, Berlin, Connecticut.

of the Newark Basin (Olsen et al., 2024b), implying that the responsible water-column chemistry was regionally pervasive.

A major contrast between the cyclostratigraphy of the lower Shuttle Meadow and that of the middle and upper East Berlin is that, although individual microlaminated beds can be traced basin-wide, overall formation thickness changes dramatically over only a few kilometers. At some localities (e.g., Farmington River Gorge, where the section is fully exposed), the entire lower part of the Shuttle Meadow is absent and the formation is only ~17 m thick (Gray, 1987; Olsen et al., 2024b). At Higby Mountain, only the Higby Bed is complete, and the inferred Bluff Head Bed rests directly on Talcott Basalt, infiltrating a conglomerate of basalt clasts (41°33′1.63″N, 72°44′43.55″W). This site lies only ~3 km northwest of the Silver Ridge core site. About 5.4 km south from the Silver Ridge site and 5.6 km west Higby Mountain site is a Meriden locality lacking all fish-bearing cycles of the lower part of the formation (41°33′13.92″N, 72°48′42.63″W). Because these three sites lie in different fault blocks (Higby, Lamentation, and Cathole Mountain blocks) and contacts with the underlying basalt vary inconsistently from east to west, the bounding faults must have been active during deposition, creating structural highs against which microlaminated units pinched out rather than simple across-dip variation in a single half-graben (Olsen et al., 2026).

Comparable along-strike changes in outcrop width define lens-shaped Shuttle Meadow lithosomes onlapping highs at their margins (Olsen et al., 2024b), consistent with depocenters localized along normal faults with length scales of ~10 km. This implies that the faults now marking the trap ridges of the Hanging Hills of Meriden were active in the Triassic, generating top-Talcott relief of ~100 m, as indicated by missing stratigraphy, even though the lake floor at any given time could have been nearly flat. Accommodating the lower Shuttle Meadow in these lows requires very rapid subsidence, on the order of ~1 m kyr^{-1}, whereas Talcott Basalt thins much less along strike, suggesting that just before Shuttle Meadow deposition the basin floor was comparatively flat.

Thus far, there is no indication that the East Berlin Formation, or, for that matter, the Holyoke and Hampden basalts and the Portland Formation, exhibits the kind of highly irregular thickness changes seen in the lower Shuttle Meadow (Olsen et al., 2024b), even across some of the same fault blocks. This suggests that movement on the internal basin faults had largely slowed by that time, with most subsidence taken up on the major eastern boundary faults, although the internal faults clearly cut these post–Shuttle Meadow strata and thus must have been reactivated later.

The absence of lower Shuttle Meadow strata on structural highs does not necessarily imply that lakes failed to inundate these areas at maximum depth. It may instead record erosion during low stands, although the dark-gray sediment intercalated with upper Talcott rubble at Higby Mountain is not microlaminated, implying that this point lay above wave base during deposition and providing the clearest evidence for locally shallower water on some highs. Comparable detail is lacking elsewhere in the lower Shuttle Meadow, but the lake that deposited the Bluff Head Bed can be envisaged in cross section as onlapping up-dip highs across multiple fault blocks, much like the geometry in seismic lines from Lake Tanganyika and Lake Malawi (Fig. 21) (Scholz and Rosendahl, 1988; Specht and Rosendahl, 1989).

The occurrence of non-microlaminated strata onlapping Talcott at Higby, together with missing intervals on other highs, means the wave-base method for estimating lake depth cannot be applied as straightforwardly to the Shuttle Meadow Formation as to the Westfield Bed of the East Berlin Formation. Nonetheless, the similarity in lamination style among successive cycles in contemporaneous strata of the Newark and Hartford basins suggests that, at times, a single lake may have extended across both basins.

East Berlin lakes. Cores acquired in 2012–2013 for the Metropolitan District Commission's South Hartford Conveyance and Storage Tunnel (hereafter MDC cores) span the entire East Berlin Formation, plus the upper Holyoke, all of the Hampden Basalt, and the lower Portland Formation. They proved as revelatory as the Silver Ridge core (Figs. 22 and 23). They show that the lower East Berlin Formation (Olsen, 1988; Olsen et al., 1989) had been largely misinterpreted, whereas the stratigraphy of the upper East Berlin had been correctly interpreted and is consistent over large distances (Figs. 13, 22, and 23).

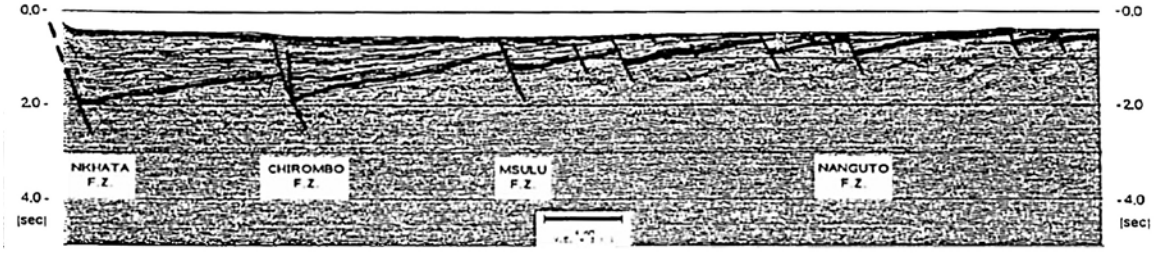

Figure 21. Seismic line across Lake Malawi showing faulted half graben with onlap onto updip highs, analogous with internal faulting in Hartford Basin during Shuttle Meadow time. Horizontal scale is 4 km; vertical exaggeration 3:1. Abbreviations: FZ—fracture zone; sec—seconds. From Specht and Rosendahl (1989; used with permission of Elsevier Science and Technology © 1989).

The main observations from the MDC cores are: (1) cycle stratigraphy in the upper half of the East Berlin Formation was correctly recognized nearly 60 years ago (Hubert et al., 1976), and cycle thickness is remarkably uniform at least along strike (Fig. 22); (2) the lower half of the East Berlin contains far more section and cyclostratigraphy than previously inferred by comparison with the Towaco Formation of the Newark Basin (Olsen, 1988), with the lower East Berlin having no sedimentary counterpart there and instead replaced by the upper Preakness Basalt (Olsen et al., 2019); (3) the confirmed northward extent of the 2-cm-thick turbidite in the Westfield Bed, already known to be widely present in the southern Hartford Basin (Olsen, 1988), is doubled to 32 km by its presence in MDC cores BD-225 and BD-226 (Fig. 24); (4) the Pompton Ashes occur with the Westfield Bed in both cores, with boudinage of the lower ash in BD-226; (5) the microlamination pattern is consistent over at least tens of kilometers; (6) the distribution of possible saline-lake minerals (e.g., magnesite of Gierlowski-Kordesch and Rust, 1994) within single cycles is inconsistent even over <200 m, suggesting a local, patchy diagenetic origin; and (7) and there is a basaltic intrusive sill locally injected into the basal East Berlin Formation (first noted by Steinen et al., 2015).

Hereafter termed the Westfield Turbidite, after its best exposure at Stop 3, a comparison of slabbed outcrop blocks and two cores (Fig. 24) shows that it thins northward and then maintains nearly constant thickness over 32.5 km. The bed also extends at least ~5 km eastward and may continue ~60 km farther north to Mount Tom in Massachusetts (Olsen et al., 2025b), implying a total length approaching 90 km. Such areal extent is highly unusual and comparable only to much thicker turbidites traced over similar distances in Black Sea microlaminated sediments (Degens et al., 1978; Lyons and Berner, 1992). A single turbidite continuous on that scale implies an extremely flat lake floor.

A particularly striking feature of the Westfield Bed is the pair of thin air-fall ash beds, the Pompton Ashes, named from an outcrop at Pompton, New Jersey, in the Newark Basin. These ashes are known from 10 sites (four cores, six outcrops) in the Newark and Hartford basins and have been characterized petrographically (Olsen et al., 2016, 2024b). In addition to their relevance for CAMP volcanism and atmospheric effects, they are critical for testing correlations within and between basins (Fig. 25). Their presence within microlaminated sediment demonstrates: (1) correlation of the Westfield Bed across the Hartford Basin; (2) minimum distances over which wave base did not intersect the lake floor; and (3) that homotaxial cycles of the East Berlin (Hartford Basin) and Towaco (Newark Basin) formations correlate not only at millennial and centennial scales but down to annual or seasonal resolution.

Thin sections of the Westfield Bed (Fig. 20) closely resemble those of the Shuttle Meadow Bluff Head Bed and the 18-inch layer of the Fossil Butte Member of the Green River Formation, and bundles of microlaminae can be matched laterally on slab surfaces. At the couplet scale, some laminae appear to merge laterally from the southern high-accumulation area (Durham) toward northern, lower-accumulation sites (Fig. 24). This trend parallels a west-east gradient in fish preservation, from strongly dephosphatized, low-relief "ghost fishes" near the basin center to fully phosphatized, high-relief skeletons near the eastern margin (Fig. 26).

On display is the "Zangler core" (Zangler, 1969), DSP Core 1-1. Unlike the relatively small diameter "Byrnes" cores taken in 1967 to delimit the track-surface distribution, this 2.5-inch-diameter (HQ) core was intended for public display in the original "bubble building" and any future exhibit halls, and was sited just northwest of the building so that it would intersect the trackway and the units exposed in the northwest corner (S. Quarrier, 2025, personal commun.). Zangler's (1969) log records 38 ft of section in 36 lithologic units and includes slightly modified logs of Byrnes's two 1967 cores, noting she had access to a 1969 draft of his thesis, although Byrnes (1972), did not cite Zangler or this core. Despite some damage and loss, DSP Core 1-1 is in much better condition than the small-diameter 1967 cores and clearly shows the track bed within the regressive phase of a black, microlaminated-bearing cycle.

A temporary trench along the south side of West Street, just west of the Park's service-entrance road, exposed this laminite, which contains dephosphatized fishes, clam shrimp, and blebs. It also includes at least one thin turbidite that should help identify which specific cycle is represented (Fig. 27). Notably, a wispy lamina of light-colored coarse silt occurs at the base of the turbidite, an unusual feature. Drzewiecki et al. (2026) illustrate several intervals from the Zangler core, including part of the deeper-water dark mudstone (Drzewiecki et al., 2026, their fig. 4A), but the illustrated interval lies above the microlaminated bed, which is only partly sampled in the core. Instead, their illustrated core segment represents a postdepositional but early interbed mélange, fragments of which were also recovered from the West Street trench. Additional examples will be on display, and the interbed mélange will be discussed further at Stop 2.

What cycle do the strata at DSP belong to? Given the large distances over which the cycles remain consistent (Fig. 22), the DSP beds most likely represent one of the already recognized cycles. On trigonometric grounds and proximity to the Hampden Basalt, the simplest interpretation is that the DSP cycle is one of the upper triplet of dark mudstone-bearing cycles, and (Hubert et al., 1976, 1978) correlated the DSP beds with the second cycle from the top (without elaboration). If thickness does not change toward DSP relative to the MDC cores or the East Berlin and Cromwell exposures, the only plausible candidate among the upper three would be the lowest cycle, because red beds in the cores would overlap the gray beds of the next lower cycle; yet the gray beds at DSP are thicker than in any East Berlin, Cromwell, or MDC-core cycle. Conversely, if the section thickens by ~47% eastward, the DSP beds could represent any of the three cycles. Assuming an 11° dip and the distance from the microlaminated unit at West Street, that unit should lie ~57 m below the Hampden Basalt—lower than any of the upper triplet—but with 47% thickening, the DSP microlaminated unit aligns with the second

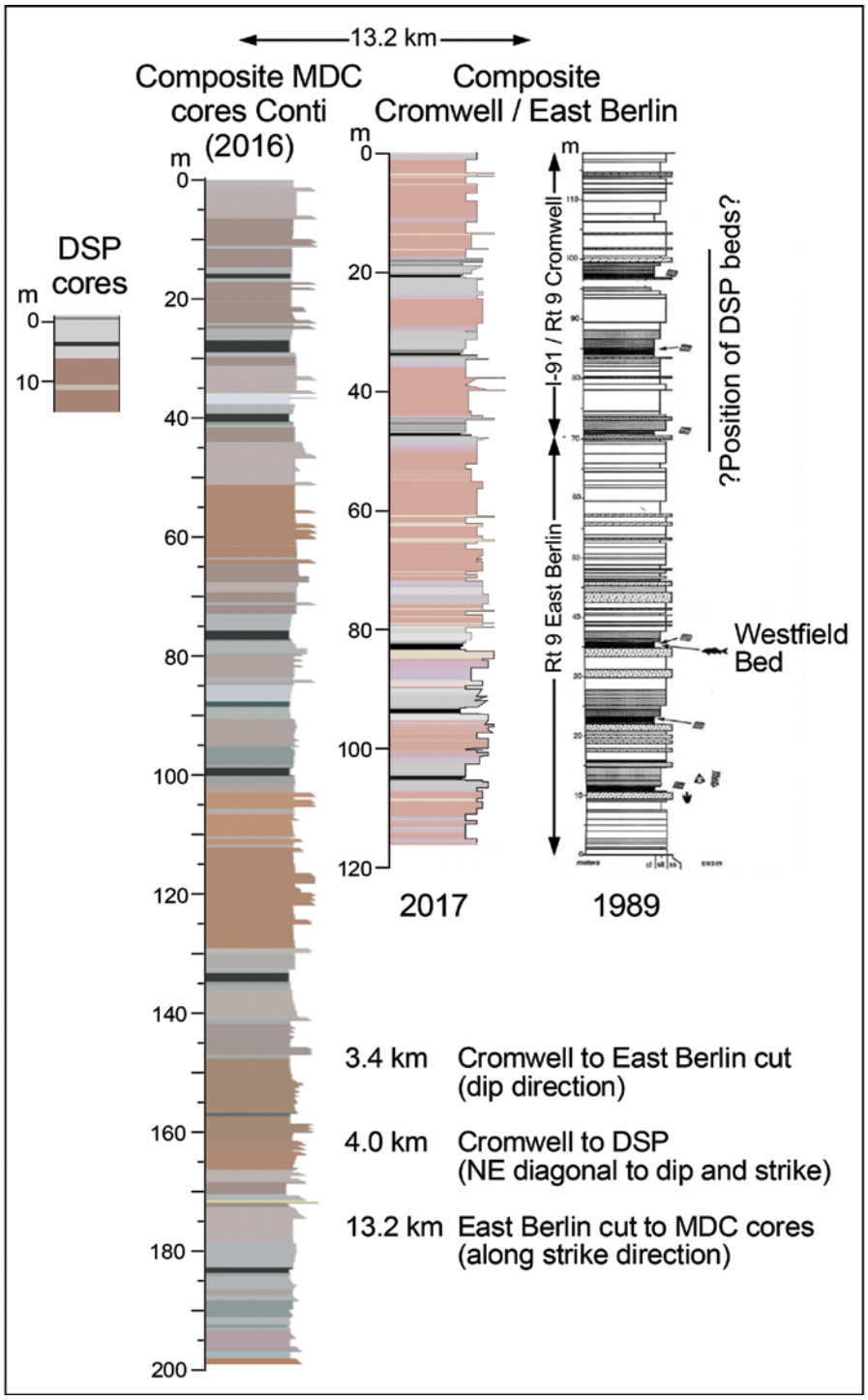

Figure 22. Comparison between the composite Metropolitan District Commission (MDC)-core section (Conti, 2016), the composite East Berlin plus Cromwell sections (Olsen et al., 1989; Olsen, 2017), and the section at Dinosaur State Park (DSP). The ~4% thickness discrepancy likely reflects compositing the I-91/Rt 9 Cromwell and Rt 9 East Berlin sections, with west-east thickening by a factor of ~1.26 over 3.4 km along Rt 9; note the I-91/Rt 9 Cromwell thickness matches Hubert et al. (1976).

cycle from the top, as proposed by Hubert et al. (1976, 1978). Small, poorly constrained faults, dip uncertainty, and uncertain eastward thickening, however, mean the cycle at DSP cannot be confidently identified by trigonometry alone.

The cycle's character may offer further clues. A dark mudstone bed near the gray-to-red transition at DSP resembles one in the East Berlin Formation exposures of the third cycle down in the upper triplet, although the intervening gray beds there are only about half as thick as those at DSP, again implying substantial thickening toward the border fault if the correlation is correct. Another possibility is that the small turbidite within the DSP microlaminated unit (Fig. 27) is laterally persistent and recognizable in one of the MDC or East Berlin/Cromwell cycles, but no detailed search has yet been made. Without

Figure 23. Composite of core boxes for Metropolitan District Commission (MDC) core BD-226, 36.2–156.2 ft, in 5-ft boxes; P–P—Pompton Ashes (Fig. 34); T–T—turbidite. Photographs from AECOM (2015). Used with permission of the Metropolitan District Commission.

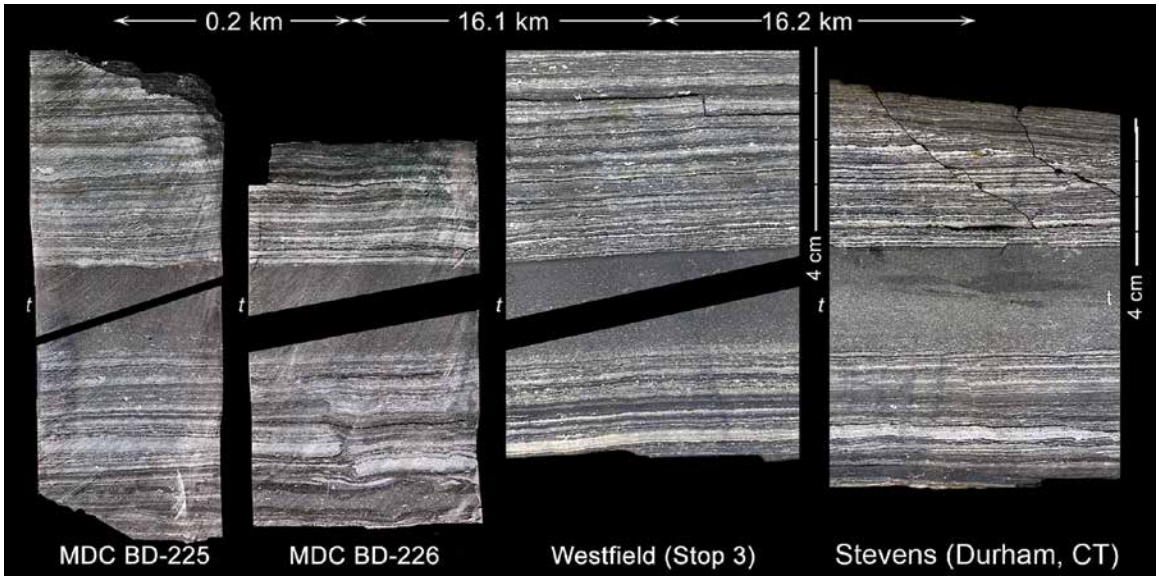

Figure 24. Westfield Turbidite "t" in the East Berlin Formation traced over 32.5 km from south (Durham, Connecticut [CT]) to north (Metropolitan District Commission cores, Hartford, CT); because laminae thin northward more slowly than the turbidite, the latter has been digitally split so laminae can be aligned. Core scales match those for the Westfield; note the matching bundles of microlaminae.

Figure 25. Pompton Ashes in microlaminated sediments from outcrop and core separated by 142 km: upper, Stevens locality, Durham, Connecticut (Hartford Basin); lower, ACE core PT-14, Newark Basin. L—lower ash; U—upper ash.

coring downward from the Hampden Basalt, this problem may remain unresolved.

Directions to Stop 2

Mileage starts as the gate from the DSP parking lot onto West Street (41°39′09.5”N, 72°39′22.4”W).

Cum. mileage	*Directions*
0	Turn left onto West Street (CT 411) heading west.
0.9	Turn left onto entrance ramp onto I-91 S.
1.2	Merge onto I-91 S.
2.6	Take exit 22N and merge onto CT-9 N toward New Britain.
4.8	Take exit 31 for CT-372 W.
5.0	Turn right onto CT-372 W.
5.6	Turn left to stay on CT-372 W, keeping left to cross U.S. 5/CT-15 onto the ramp for CT-RT 9 S.
5.9	Park on gravel/dirt area on right.

Stop 2. CT Rt 9 and U.S. 5/CT-15 Roadcut East Berlin (CT Rt 9 South on-ramp: 41.622222°, -72.740472°; 41°37′20.0″N, 72°44′25.7″W)

Cyclical, Early Jurassic middle to upper East Berlin Formation lacustrine strata and the overlying Hampden Basalt are exposed at this site (Figs. 22 and 27). Portions of the following summary are adapted from Olsen and Douglas (2022) and Olsen et al. (2024b). A permit from the Connecticut Department of Transportation (CT DOT) is required for parking and research access, and highway crossings are not allowed without separate DOT authorization.

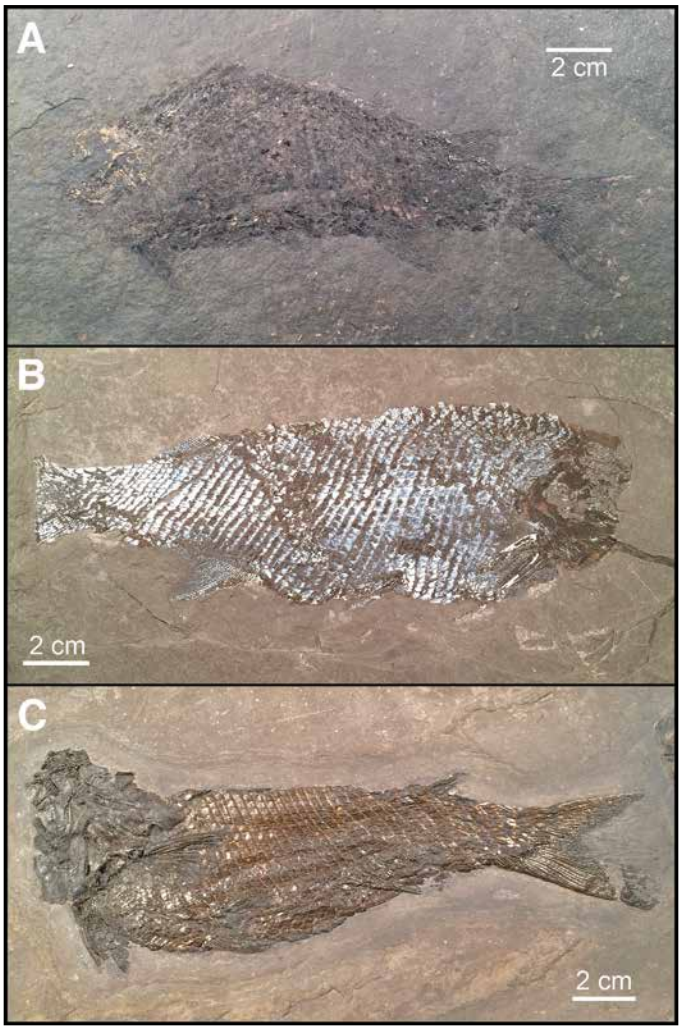

Figure 26. Trend in dephosphatization (McDonald and LeTourneau, 1989; LeTourneau et al., 2016) from near the basin center to the eastern margin, from top to bottom (modified from Olsen and McDonald, 2026): (A) Miner Brook, Westfield, Connecticut (Stop 3), near basin center, with almost no skeletal relief; (B) Stevens locality, Durham, Connecticut, with partial phosphate loss and bluish (?calcite) coatings; (C) North Branford, Connecticut, near the eastern margin, with no phosphate loss and robust skeletal relief.

Main Points

1. The upper East Berlin Formation displays stacked Van Houten lake-level cycles paced by climatic precession and grouped into short-eccentricity packets.
2. Cycle with Dinosaur State Park track bed is exposed—but which one is it?
3. The middle redbed-dominated interval, showing muted cyclicity, reflects damped precessional lake-level variability during ~100-kyr low-eccentricity phases.

Figure 27. Dinosaur State Park: fishes, microlaminated bed, turbidite, and bleb. (A) At least three fishes, the most obvious a partially dephosphatized *Semionotus*. (B) Thin section of the microlaminated bed with a turbidite, cut by an irregular fault and containing a bleb (light grain cluster); see Figure 18B for detail.

4. The Westfield Bed contains an organic-rich, microlaminated Division 2, deposited in a deep (~40–80 m), perennial, chemically stratified rift lake that likely spanned multiple basins.
5. The Pompton Ashes record large, distant CAMP eruptions that may have produced volcanic winters, potentially linked to the Moroccan Foum Zguid Dike.
6. Post-depositional interbed mélanges within dark mudstone cycles record shear and liquefaction rather than event beds or slumps. The mélange in the Westfield Bed preserves ripped-up fragments of an otherwise missing Westfield Turbidite.

Discussion

Overview. Exposures of the middle and upper East Berlin Formation and the overlying Hampden Basalt along CT 372 (old CT 72), at the intersections of CT 15 and CT 9, and within the I-91/CT-9 cloverleaf, have been key sites in Connecticut Valley geology since the first CT-72 roadcut was made in the late 1950s (Lehmann, 1959). Lehmann (1959) designated the CT-372 exposure as the East Berlin type section, and the I-91/CT-9 cloverleaf cuts, excavated in the 1960s, were later used by Karl M. Waage (Yale) for stratigraphy instruction in 1972, including an exercise distinguishing lithologic repetition caused by faulting from cyclicity. John Sanders (Barnard) famously called these roadcuts "The Grand Canyon of Connecticut." Additional cuts built in the mid-1980s, especially the large on-ramp from CT-15 to CT-9 (Fig. 28), revealed the Westfield Bed cycle—the focus of this stop. Although now largely obscured by vegetation and microbial coatings, the rocks can still be examined effectively in winter and early spring, and the Westfield Bed remains visible year-round.

After parking, we will walk east along the south side of the road, moving up-section toward the Hampden Basalt. There we will examine the basalt before descending through the sedimentary section to the Westfield Bed, noting key features along the way.

The highway cuts at the East Berlin intersections of U.S.-15/CT-9 and I-91 reveal sections of the upper half of the East Berlin Formation repeated in two fault blocks separated by ~3 km. Lacustrine cyclicity at this site was first recognized in the 1950s (Krynine, 1950; Klein, 1968) and later quantified by Olsen (1986), who proposed pacing by Milankovitch cycles. This interpretation was strongly supported by U-Pb dates (Blackburn et al., 2013). The section vividly illustrates these precessional to eccentricity-scale cycles on an extraordinary scale (Figs. 4 and 22); the unusual clarity of the orbitally paced cycles invites explanation.

About 117 m of sedimentary section is exposed on the south side of the cut (Fig. 22). The most conspicuous cycles include a dark-gray to black, finely laminated, deepest-water interval typified by the Westfield Bed (Figs. 4, 13, and 20). Similar meter-scale lithologic cycles were described by Van Houten (1962, 1964, 1969) in the Triassic Lockatong Formation of the Newark Basin and interpreted as precession-paced lake-level variations, at a time when many thought Milankovitch theory was disproved. Olsen (1986) named these transgressive–regressive successions Van Houten Cycles. They comprise three divisions defined by sedimentary features indicating relative water-depth change (Fig. 4): Division 1 (transgression), marked by upward loss of desiccation cracks or roots; Division 2 (highstand), often represented by finely laminated mudstone; and Division 3 (regression and lowstand), showing renewed exposure indicators such as roots and desiccation cracks. In the Westfield Bed cycle, these transitions and color contrasts are easily recognized; in other cycles, they are subtler or lack color change, but all are defined by relative changes in water depth rather than absolute rock types.

Hampden Basalt. Although tangential to our main topic, we begin our traverse at the 200.9 Ma Hampden Basalt (Blackburn et al., 2013), representing the youngest known CAMP flows in eastern North America and Morocco. The Hampden Basalt is controversial for two main reasons (Supplemental Material text 3.1.1). First, how many individual flows it comprises—estimates range from one to eight, despite common field criteria such as vesicular zones often reflecting segregation sheets rather than true flow boundaries (Chapman, 1965; Colton and Hartshorn, 1966; Moumou et al., 2024; Olsen et al., 2024b). There is no compelling evidence for more than one flow here. Second, how a relatively thin, laterally extensive unit could drive one of the

Figure 28. Three middle East Berlin precession paced lacustrine cycles at the CT-15/CT-9 on-ramp, East Berlin, Connecticut, in 1988, 1993, and 2023. Dark mudstone behind the left lamp post is the Westfield Bed. Light poles are ~11 m tall.

largest inferred CAMP-related CO_2 pulses recorded in paleosol carbonates (Schaller et al., 2011, 2012).

Cyclicity and orbital pacing. Perhaps the most striking feature of this outcrop is the clear cyclicity linked to Milankovitch climatic pacing, a feature described multiple times in the literature (e.g., Olsen et al., 1989, 2005, 2025b; Olsen, 2017). U-Pb dates as well as state-of-the-art time series techniques confirm the orbital pacing of these cycles strongly dominated by climate precession (Fig. 29). Independently derived accumulation rate models match the Early Jurassic precession period of ~19.1 kyr (Figs. 22, 29). A weak 41.6-kyr signal suggests a minor obliquity component, unlike the lower East Berlin and Shuttle Meadow Formations (Figs. 22 and 29) (Supplemental Material text 3.1.2). The precessionally paced cycles are bundled in two ~100 kyr short eccentricity cycles in the high eccentricity phase of a 405-kyr-long eccentricity cycles (Figs. 13 and 22).

Walking west and down-section, red strata occur below the basalt, followed by a gap in exposure. Seen also across the highway, this gap marks a glacially scoured valley that channeled along the uppermost black-shale-bearing cycle of the East Berlin, as shown by the more complete ~50-m-thick section ~3.5 km east at the CT-9/I-91 interchange (Fig. 22) (Olsen et al., 1989). Two additional underlying cycles also contain black mudstones, with the third resembling the Dinosaur State Park footprint cycle (Stop 1) (Figs. 14 and 30), corresponding to the gray regressive portion of Division 3, although this correlation remains very uncertain. Together, these three cycles and subjacent red beds represent most of an ~100-kyr short-eccentricity cycle (Supplemental Material text 3.1.3).

Westfield Bed. At roughly 82 m below the Hampden Basalt lies Division 2 of the cycle shown in Figure 4—the Westfield Bed (Fig. 31A). It contains a calcareous, organic-rich, microlaminated interval bearing ghost fishes (Fig. 32), clam shrimp, and the Pompton Ashes (Fig. 31B).

In order of abundance, the Westfield Fish Bed has produced *Semionotus* spp. (holostean gar relatives), *Redfieldius* spp.

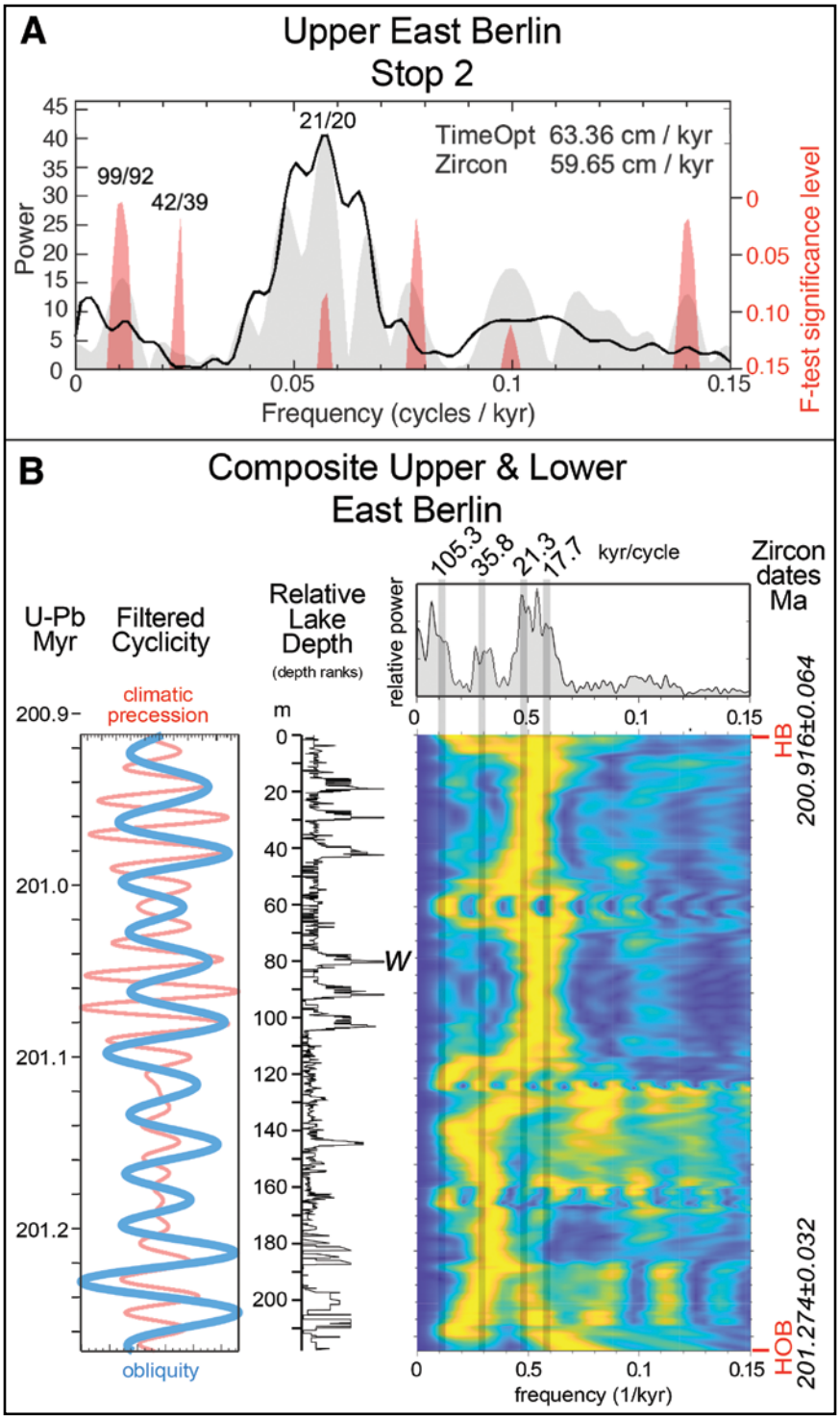

Figure 29. Power spectra of East Berlin Formation cycles showing precessional dominance in the upper section and obliquity dominance in the lower section: (A) upper East Berlin Formation, dominated by precessional pacing, based on the composite of the depth rank series from the Cromwell and East Berlin sections; (B) evolutive spectrum of composite of all of the East Berlin plus Towaco and filter cycles, showing the dominance of obliquity pacing in the lower East Berlin, followed by precessional pacing. Abbreviations: HB—Hampden Basalt; HOB—Holyoke Basalt.

(paleonisciforms), *Diplurus* cf. *longicaudatus* (a coelacanth), and *Ptycholepis* (another paleonisciform, from a different site in the same bed) (Fig. 17). The fishes here, as at most Westfield Fish Bed localities, are "dephosphatized" ghost fish typical of the central-basin facies (Stop 1), their bone phosphate having dissolved early in diagenesis (McDonald and LeTourneau, 1989), a process that may be widespread and is discussed further at Stop 3. Also present are the spinocaudatan (clam shrimp) *Bulblimnadia froelichi*, carbonate remains of possible charophyte green algae, and land-plant fragments of various sizes.

A striking feature here is the distinct bundling of dark and light couplets (varves) (Fig. 33). Although merging carbonate

Figure 30. Lacustrine cycle at Stop 2 (north side of Rt 9 on-ramp) in ca. 2000, before microbial coatings obscured coloration. Note the second dark-gray mudstone, which resembles that in the Dinosaur State Park section. Photo by Richard Bergen, from McDonald (2010).

laminae complicate counting, the Westfield Bed shows rhythmically banded microlaminae possibly reflecting solar periodicities such as the ~11-year Schwabe, ~22-year Hale, ~80–100-year Gleissberg, or ~200-year de Vries/Suess cycles (see Hathaway, 2015, for a review of solar cycles. Schwabe and Hale periodicities appear in microlaminae of the Newark Basin Feltville Formation (Olsen, 2023), and other geological records suggest similar solar pacing, so such modulation here would not be unexpected (see review by Glenn and Kelts, 1991).

Giant chemically stratified lakes. The Westfield Bed represents a distinctive facies that typically preserves whole fishes and occasional terrestrial vertebrates and insects, consistent with the stratified-lake model. Its microlaminated strata comprise alternating carbonate-rich and carbonate-poor laminae forming couplets most simply interpreted as annual lacustrine varves, and individual couplets and their patterns can be traced across the entire Westfield Fish Bed, implying wave base never reached the bottom and the lake remained perennially stratified.

The preserved microlaminated extent of the Westfield Bed is ~18,200 km^2; if it once covered the entire basin, it would have spanned ~32,220 km^2 (Table 1). This implies a minimum chemocline depth between 36–114 m and greater total lake depth. The lake may have extended from the Hartford into the Deerfield and possibly the Culpeper rift basins, reaching >700 km in length (larger than any modern lake except the Caspian and Black seas), and such fetch would imply a deeper chemocline, plausibly >100 m.

Microlaminae commonly show small-scale structural deformation, including brittle normal and thrust faults, duplexes, ductile folds, micro-brecciation, liquefaction structures, and clastic dikes. The absence of erosional or draped tops indicates formation within sediment rather than at the sediment-water interface, so these are not event beds or slumps, and their lack of mineralization shows they formed early in diagenesis; such deformation is typical of layered lacustrine strata adjusting to local stresses and may reflect post-depositional seismic events (e.g., Törő and Pratt, 2015), although not correlatable with specific earthquakes, and at this outcrop scale synsedimentary and post-depositional features can be readily distinguished.

The Pompton Ashes and CAMP mega-eruption. The lower ~10 cm of the Westfield Bed contains a thin, graded basaltic crystal tuff overlain by a thinner ash layer—the Pompton Ashes (Olsen et al., 2016). The graded basaltic-to-andesitic ash consists

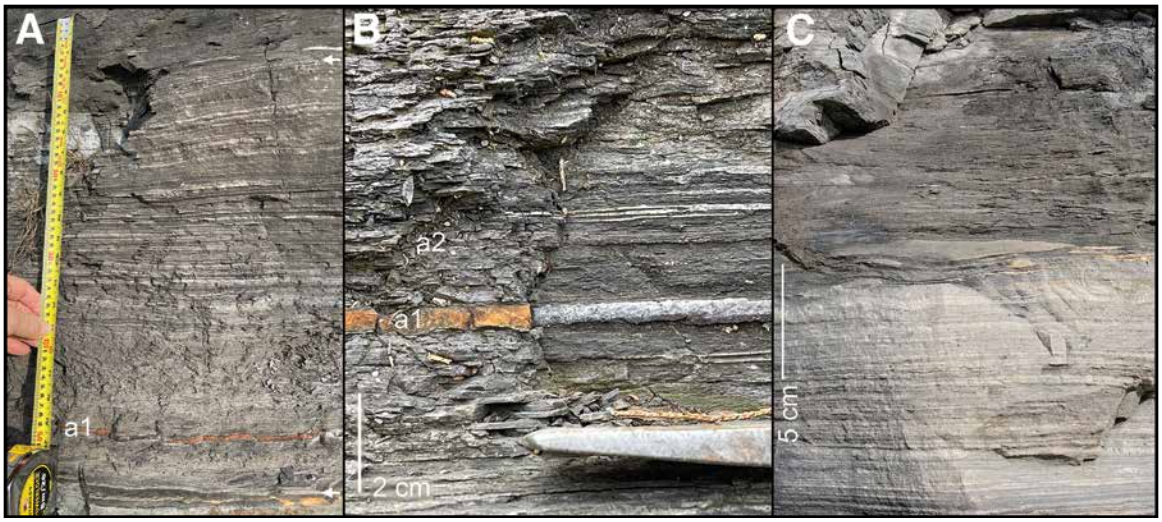

Figure 31. Aspects of the Westfield Bed at Stop 2. (A) Microlaminated portion between arrows: scale in inches and centimeters; a1—lower Pompton Ash (orange). (B) Pompton Ashes: a1—lower, main ash weathers orange, where fresher it has a white, ?sulfate efflorescence, but its fresh color is nearly black; a2—upper, smaller gray ash. (C) Top of microlaminated bed with mélange clast of the Westfield Turbidite, normally present higher in the laminite (Fig. 24).

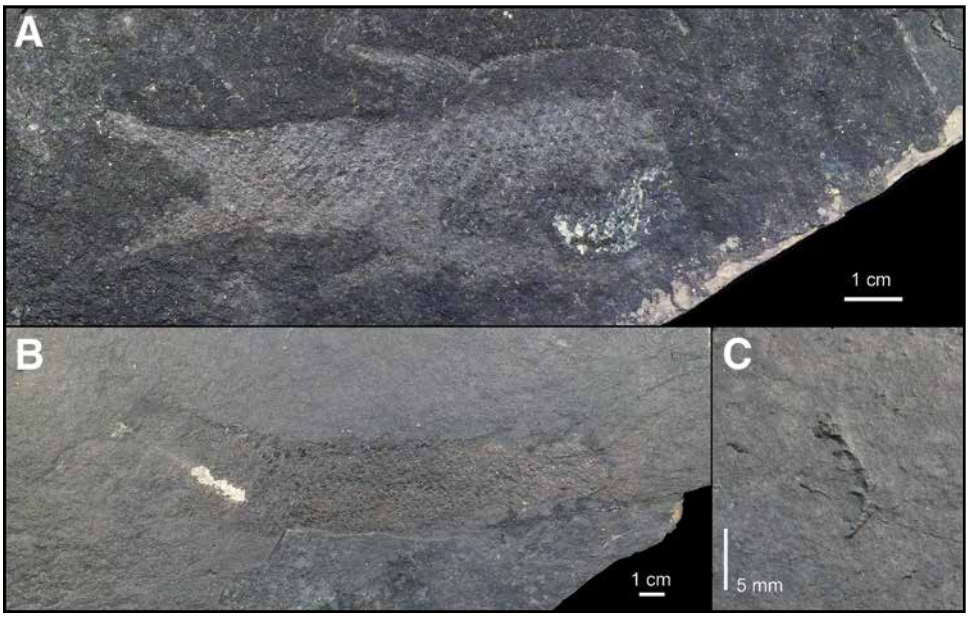

Figure 32. Representatives of the Westfield Bed biota, Stop 2, East Berlin, Connecticut: (A) complete, dephosphatized *Semionotus* sp. (ghost fish) with dark gut area with some pyritization; (B) complete, nearly completely dephosphatized *Redfieldius* sp. (ghost fish) with some gut area pyritization; (C) possible charophyte thallus.

of euhedral plagioclase laths in a clay- or chalcedony-rich matrix derived from volcanic glass, fine feathery feldspar, carbonate, and distinct sub-millimeter spherule-like grains at the base; pyrite is abundant, locally >20 wt% (Stüeken et al., 2019), producing bright-orange jarositic weathering, whereas fresh interiors are dark gray to black; the ash darkened with early gypsum efflorescence when first exposed in 1988 but developed vivid orange coloration by 2007 as pyrite oxidized (Fig. 31).

Astrochronologic correlation tied to U–Pb zircon ages from Newark Basin equivalents of the Hampden and Holyoke basalts gives an age of 201.050 ± 0.020 Ma for the Pompton Ashes, midway between the Preakness/Holyoke and Hook Mountain/Hampden flows (Figs. 13 and 22). The U–Pb zircon CA-ID-TIMS (chemical abrasion isotope-dilution thermal ionization mass spectrometry) age of 201.111 ± 0.071 Ma from part of the 400-km-long Foum Zguid Dike in Morocco (Morocco) (Davies et al., 2017) falls within analytical uncertainty of this age, potentially linking it to the Pompton Ashes.

Figure 33. Bundling of microlaminae (varves) into broader bands possibly related to solar cycles. Right-hand side of the image vertically spans ~16 cm.

Several aspects of the ash are notable. First, its thickness is remarkably uniform across >200 km and 10 sites (Fig. 34), implying deposition from either a massive distant eruption or a smaller, optimally positioned source; second, the <1 mm upper ash a few centimeters higher also shows little lateral variation. Third, beyond confirming decades-old inter-basin lake-cycle correlations, the Pompton Ashes are enclosed by identical microlaminar patterns over comparable distances (Fig. 25), implying either a single interconnected Newark–Hartford lake or basin-wide climatic synchrony. Fourth, the lower ash shows a minor Ir anomaly, suggesting that similar basaltic ashes mixed into sediment could explain subtle Ir signals in other Triassic–Jurassic strata. Collectively, these attributes permit correlation not only at the ~20 kyr cycle scale but down to annual–seasonal resolution, constraining eruption timing to within about a year.

Sulfate derived from the eruption and reduced to pyrite by sulfate-reducing bacteria while still in the upper ocean–atmosphere system could have driven volcanic winters via enhanced albedo, potentially one for each ash layer. A concentrated episode of such CAMP-related volcanic winters could temporarily override CO_2-driven global warming (Landwehrs et al., 2020) and has been implicated in the end-Triassic mass extinction (Olsen et al., 2022).

Interbed mélange. Overlying the microlaminated part of the Westfield Fish Bed is a unit comprising a mélange of small (<20 cm) quadrangular, rounded, or folded clasts with truncated, oblique-to-bedding laminae in a poorly bedded matrix

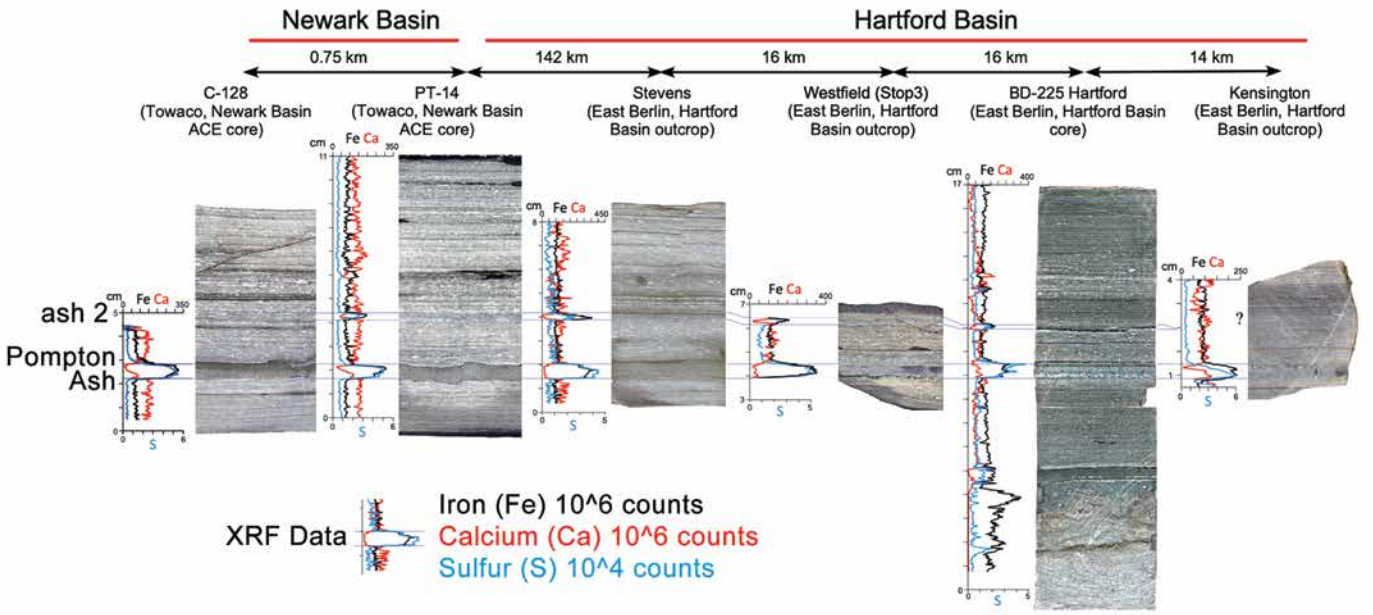

Figure 34. Slabbed Pompton Ashes from six localities spanning 189 km in the Newark and Hartford Basins all to the same scale. X-ray fluorescence spectroscopy (XRF; ITRAX) data (in counts) shows high pyrite content and consistent ash thickness (data courtesy of Clara Chang and Sean Kinney, 2015, personal communication).

(Fig. 35). Every black-mudstone interval in this section includes such a bed. Olsen et al. (1989), informally termed these clasts "dead horses," adapting the structural term horse to emphasize their sheared or prone geometries. These mélanges, often mistaken for turbidites, rip-up clasts, slumps, or seismites, were reinterpreted by Olsen and Kinney (2016) as early shear- and liquefaction-related deformation formed well below the sediment–water interface. They occur throughout many Triassic–Jurassic lacustrine successions in the eastern United States, and nearly every dark-gray to black mudstone cycle includes one. Comparable layers in the Eocene Green River Formation (Dyer-Pietras, 2020) and other laminated organic mudstones are commonly misidentified as depositional.

Treating these mélanges as depositional units yields major paleoenvironmental errors. Formed post-depositionally between preexisting beds, they reflect specific rheological conditions at variable depths and pressures, perhaps with local triggers. Each represents interbed deformation rather than a discrete event, making stratigraphic sequences of such beds unsuitable for event reconstruction.

Conspicuous here by its absence is the distinctive Westfield Turbidite normally seen in the upper part of the microlaminated unit of the Westfield Bed (Figs. 23 and 24; Stop 3). At Stop 3, it lies ~40 cm above the main ash, yet only that thickness of laminae remains here. Rhombic clasts of the Westfield Turbidite in the mélange base (Fig. 31C) show the bed was sheared into the mélange along with the laminae top.

Not every layer records a true depositional event; sedimentary appearances can reflect post-depositional rheology rather than sedimentology. Also, late post-depositional, brittle, mineralized bedding-parallel faults, mostly near microlaminated-unit bases, break strata into polished, slickenlined blocks. These often seep water in outcrop and are easily distinguished from the older interbed mélange intervals.

The rest of the section. Continue west to two additional Van Houten cycles, each with a black-shale-bearing Division 2. A bedding-plane fault cuts the upper cycle, disrupting most of Division 2's laminations. The lower cycle's Division 2 contains abundant magnesite (magnesium-carbonate) crystals (Gierlowski-Kordesch and Rust, 1994), whose limited distribution in cores adjacent to each other suggests a local diagenetic origin. Although largely poorly laminated, its basal laminae are distinctive and traceable for at least 5 km southeast.

Directions to Stop 3

Cum. mileage	*Directions*
5.9	Go straight continuing on the ramp onto CT-9 S.
6.2	Merge onto CT-9 S.
8.3	Take exit 30 to merge onto I-91 S toward New Haven/New York City. (This is the cloverleaf with the Cromwell exposures; Fig. 22.)
9.5	Take exit 21 for CT-372 toward Cromwell/Berlin.
9.9	Turn left onto CT-372 E/Berlin Rd.
10.6	Turn right onto CT-217 S/East St.
11.4	Turn right onto Town Colony Dr.
11.5	Turn left and park (41°35′30.3″N, 72°42′04.2″W).

Leave vehicles and walk back to Town Colony Drive, walk 185 ft (56 m), then turn left following the banks of Miner Brook north another 185 ft (56 m) to field stop.

Stop 3. Miner Brook, Westfield (Middletown), Connecticut (41.592275°, -72.700517°; 41°35′32.19″N, 72°42′1.86″W) (Fig. 12)

Permission from the landowners is required in advance to visit this site.

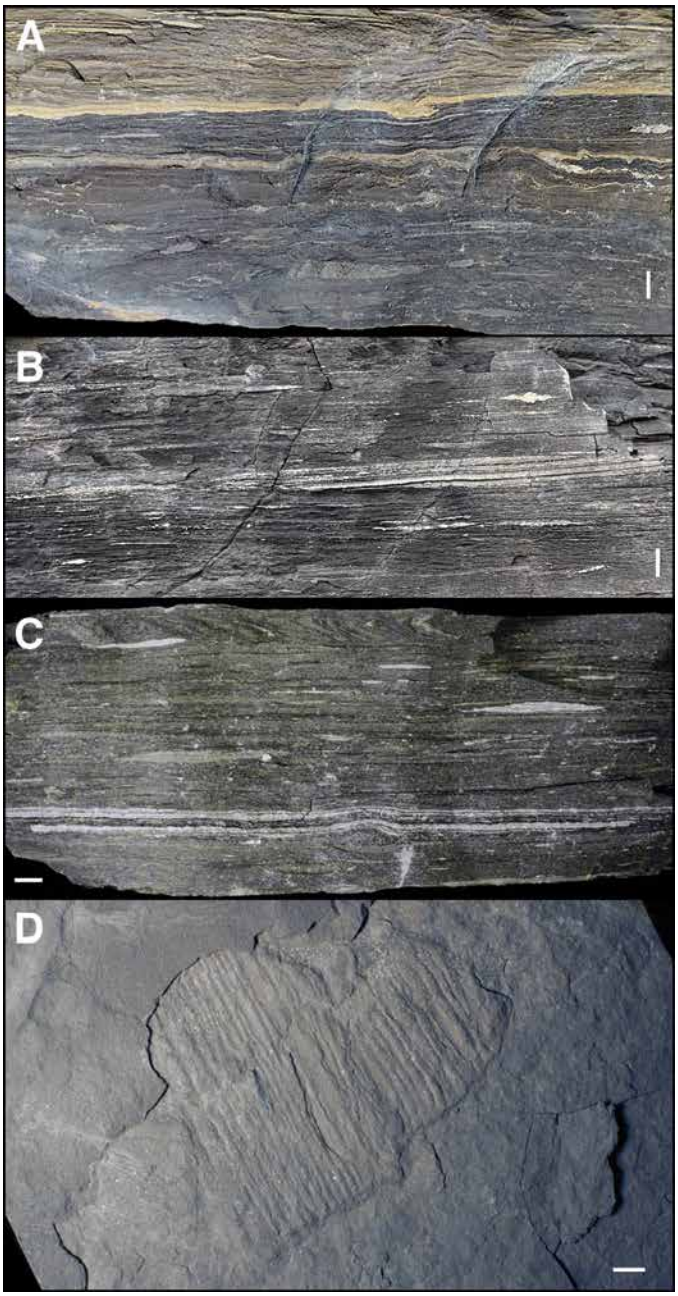

Figure 35. East Berlin cut (Stop 2). Interbed mélange in upper Westfield Bed (all scale bars 1 cm). (A) Block sample with transition mélange upward into overlying strata; note downward truncation of uppermost laminae, clasts with very high aspect ratios lower down, and clasts with thick, vertical, highly compacted laminae. (B) Outcrop photo of large laminated clast with laminae truncated above and below. (C) Block sample with many small clast with oblique laminae, and two high aspect ratio clasts, the upper of which has truncated recumbent folding. (D) Plan view of hand sample with high aspect ratio fitted but displaced, rhombic clasts; ribbing reflects differential compaction of obliquely cut carbonate microlaminae.

Main Points

1. Nearly along-strike exposure of the Westfield Bed at its type locality.
2. Close to the coal prospect that yielded fish described in 1816—the earliest record of articulated fossil fishes in the United States.
3. Pompton Ashes and Westfield Turbidite exceptionally exposed; oblique fractures accentuate apparent tuff and lamina thickness.
4. Interbed mélange weakly developed, preserving a thicker microlaminated interval and better-defined Westfield Turbidite.
5. Numerous ghost fishes and coprolites exhibit strong dephosphatization plausibly linked to carbonate-rich pore-water chemistry.

Discussion

Overview. This site, the Westfield locality, exposes ~5 m of the Westfield Bed and adjacent strata (Fig. 36). It typifies eastern U.S. Triassic–Jurassic lacustrine successions, where otherwise recessive deep-water beds form resistant ledges in streams. Unlike roadcuts, this well-exposed this brook section has large, flat ledges, and offers exceptional observation opportunities. All key features of the Westfield Bed, including the Pompton Ashes and widespread Westfield Turbidite, are visible here (Fig. 37).

History. The timing of the first fossil-fish discoveries along Miner Brook is uncertain. The earliest record is a notice by Benjamin Silliman in (1816), describing fish "impressions" at Westfield near Middletown, Connecticut (Brignon, 2017) (Fig. 38). As Brongniart and Silliman (1821, p. 221) later recounted, "The person who brought them, obtained them at the depth of about 40 feet, while exploring for coal … [and] brought his chaise box full of them then to New-Haven…". At that time, many supposed coal excavations, possibly based on the presence of coalified wood, yielded fossil fish instead (Percival, 1842). Silliman added (Brongniart and Silliman, 1821, p. 222) that "… no more fish have been obtained at Westfield, because the pit has long been filled with water…" The pit's exact location is unknown, but it plausibly targeted wood in the Westfield Bed along Miner Brook.

By 1842 the site was well known for fossil fishes. Percival (1842) and Davis and Loper (1891) documented it specifically,

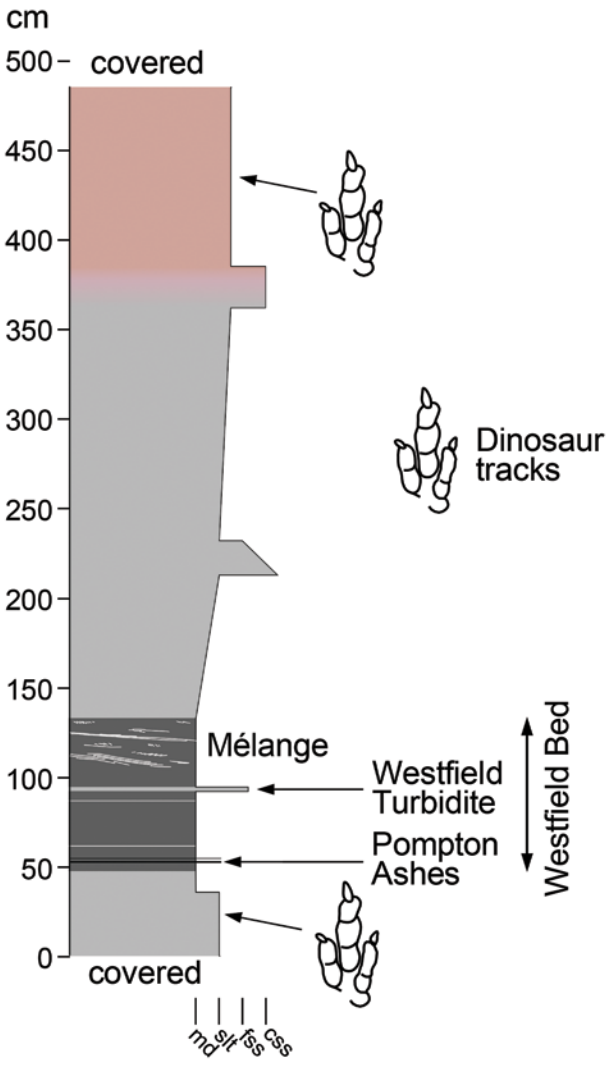

Figure 36. Measured section at Westfield (Stop 3).

Figure 37. Westfield Bed with prominent and resistant Westfield Turbidite (middle of image) outcropping at Stop 3, Miner Brook, Westfield, Connecticut. Hammer rests on Pompton Ashes and is 28 cm high.

noting long-standing awareness of Miner Brook outcrops. Another nearby site, the Stevens locality in Durham (Davis and Loper, 1891), first targeted for coal, also exposes the Westfield Bed with both Pompton Ashes and Westfield Turbidite (Figs. 24, 25, and 34). Despite frequent nineteenth-century mentions (McDonald, 1996), the Westfield site's detailed geology was never described, yet it is the type locality from which the Westfield Bed is named (McDonald, 1975; Olsen, 1988).

Pompton Ashes and Westfield Turbidite. Both units are well exposed here (Figs. 24, 34, 37, and 39), this being the best site for the Westfield Turbidite. The lower Pompton Ash is darker and less conspicuous than at Stop 2, reflecting reduced weathering. Unique oblique fractures here thicken the apparent tuff and microlaminate sections (Fig. 39), hindering sampling. The ashes confirm correlation of this microlaminated unit with Stop 2, the MDC cores, and other occurrences (Fig. 34).

Interbed mélange. The microlaminated interval is thicker than at Stop 2 because mélange deformation is weaker, leaving the Westfield Turbidite preserved well below its top. Sparse mélange clasts occur as occasional rhombs in dark massive mudstone above (Fig. 40). Eastward, mélange diminishes toward the border-fault system and disappears into siltier strata, where shear becomes bedding-parallel recumbent folds (Olsen and Kinney, 2016).

Dephosphatized ghost fishes and coprolites. The Westfield Bed here has yielded hundreds of ghost fishes showing various degrees of dephosphatization—a pattern also seen in coprolites (Figs. 38 and 41). Dephosphatization removes bone, scale, and coprolite relief, sometimes entirely. A thin whitish-blue Mg-calcite or dolomite coating (Leonard, 2013), possibly tinted by uranium-related radiation (Calderon, 1983), replaces original phosphatic tissues.

Articulated but flattened skeletons indicate bone dissolved within sediment during early diagenesis, not after lithification. As previously noted, dephosphatization decreases eastward—from Westfield and Stop 2 to deeper lacustrine facies (Fig. 26), and similar patterns occur elsewhere (Supplemental Material text 3.2, Fig. S5). These trends suggest basin-scale gradients in pore-water chemistry tied to facies and burial depth.

Calcite is thermodynamically more soluble than hydroxyapatite across normal environmental pH ranges, so in simple aqueous systems calcite should dissolve more readily than bone. Intuitively, this is why a chicken eggshell, composed mainly of calcite, dissolves in vinegar, whereas our teeth, composed mainly of low-solubility hydroxyapatite, do not. In carbonate-rich, Ca-scavenging settings, phosphate solubility may rise

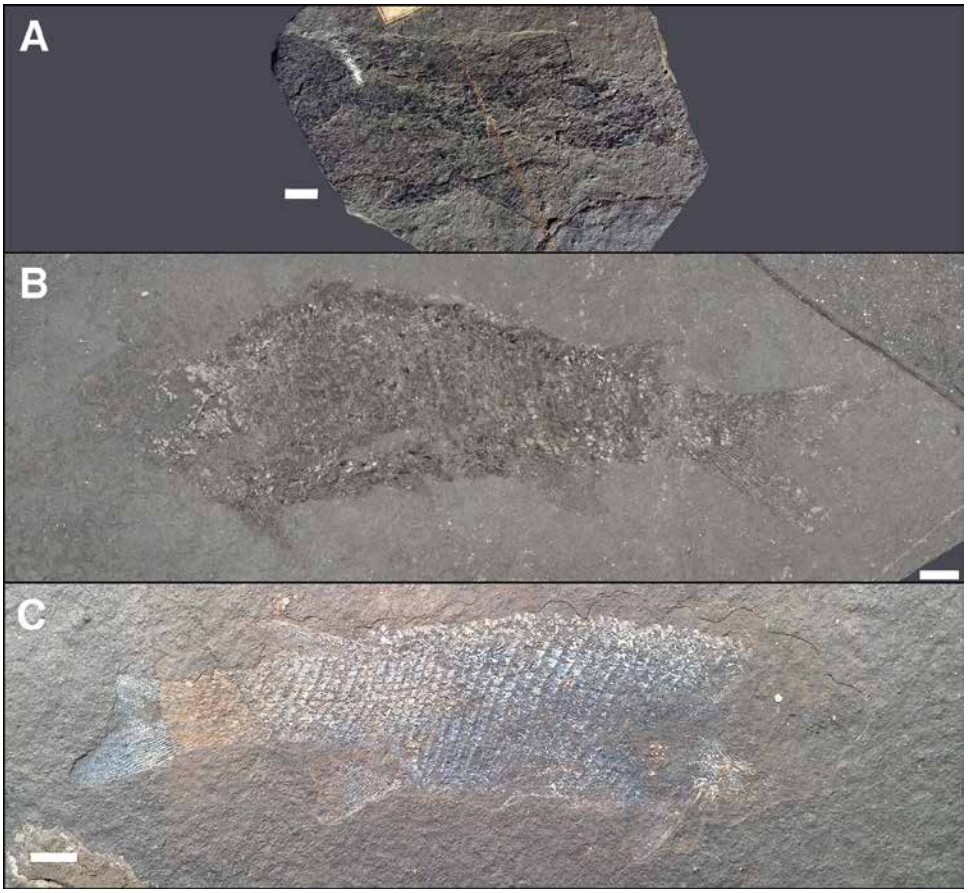

Figure 38. Examples of degrees of dephosphatization of Westfield (Stop 3) fish (*Redfieldius*): (A) Brongniart collection, UPMC.PAL.2017.0.1.7, old number 12879 (from Brignon, 2017; used with permission of Elsevier © 2017); (B) *Recurvirostra*, Bruce Museum, Gift of Nicholas G. McDonald, 2017.11.58, photograph by P. Olsen (this is the most common mode of preservation at Westfield); (C) *Redfieldius*, Bruce Museum, Gift of Nicholas G. McDonald, 2017.11.59, photograph by P. Olsen. Note the slight darkening of the eye area in B and C and darkening of the gut area in B. Scale is 1 cm.

Figure 39. Oblique cut through Pompton Ashes, Westfield (Stop 3): a1—lower, thicker ash (note slickenlines); a2—upper ash. Hammer head is 2.4 cm in height.

Figure 40. Rhombic clast of microlaminated bed floating in massive mudstone at Westfield (Stop 3). Hammer head is 17 cm across.

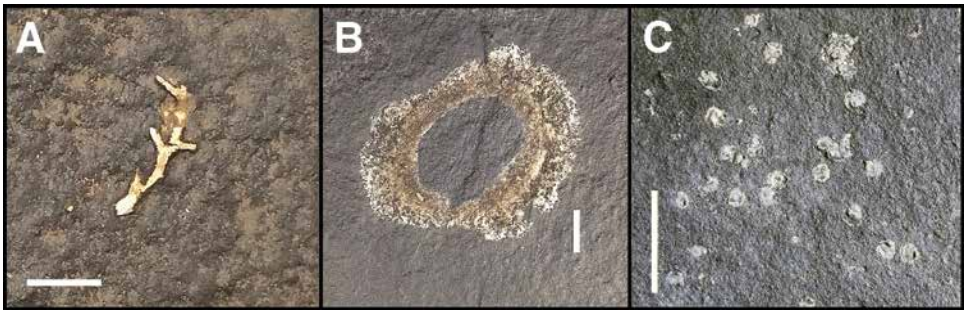

Figure 41. Other fossils from Westfield (Stop 3): (A) Possible carbonate charophyte; (B) completely dephosphatized coprolite with carbonate halo; (C) clam shrimp (*Bulbilimnadia froelichi*) with carbonate valves.

enough for apatite to dissolve while calcite remains stable (Meacham, 2017). Less affected bone preservation near the border fault (LeTourneau, 1985; LeTourneau and McDonald, 1985), a feature that needs to be explained by any viable model, may reflect thicker lacustrine muds that trapped phosphate-rich pore waters, briefly stabilizing bone (details in Supplemental Material text 3.2.1). This pattern predicts stronger dephosphatization near bed tops, consistent with field relations.

Dark organic stains in eye and gut areas (Supplemental Material text 3.2.3, Fig. S3) may indicate residual melanin (Lindgren et al., 2012; Dubey and Roulin, 2014; Prado et al., 2025), showing partial pigment preservation despite dephosphatization. Comparable melanin retention in *Sinosauropteryx* suggests pigment patterning could likewise survive in a future feathered dinosaur find from these beds.

Return to the vehicles.

Directions to Stop 4

Cum. mileage	*Directions*
11.5	Turn right onto Town Colony Dr.
11.6	Turn right onto East St.
13.5	Continue onto CT-217 S/Ballfall Rd.
14.6	Turn right onto CT-66 W.
15.2	Turn left onto Jackson Hill Rd.
17.3	Continue straight onto CT-157 S.
18.5	Continue onto CT-147 S.
19.8	Slight right onto Middlefield Rd.
20.6	Turn right onto Main St.
22.1	Continue onto CT-17 S/New Haven Rd.
25.9	Turn left onto Stage Coach Rd.
26.1	Destination will be on the right (Bluff Head from New Haven Rd Mattabassett Trail).

Park at around 41°25′46.5″N, 72°43′39.0″W and proceed 160 ft (49 m) to creek and enter on east to walk up creek bed, which we will walk along.

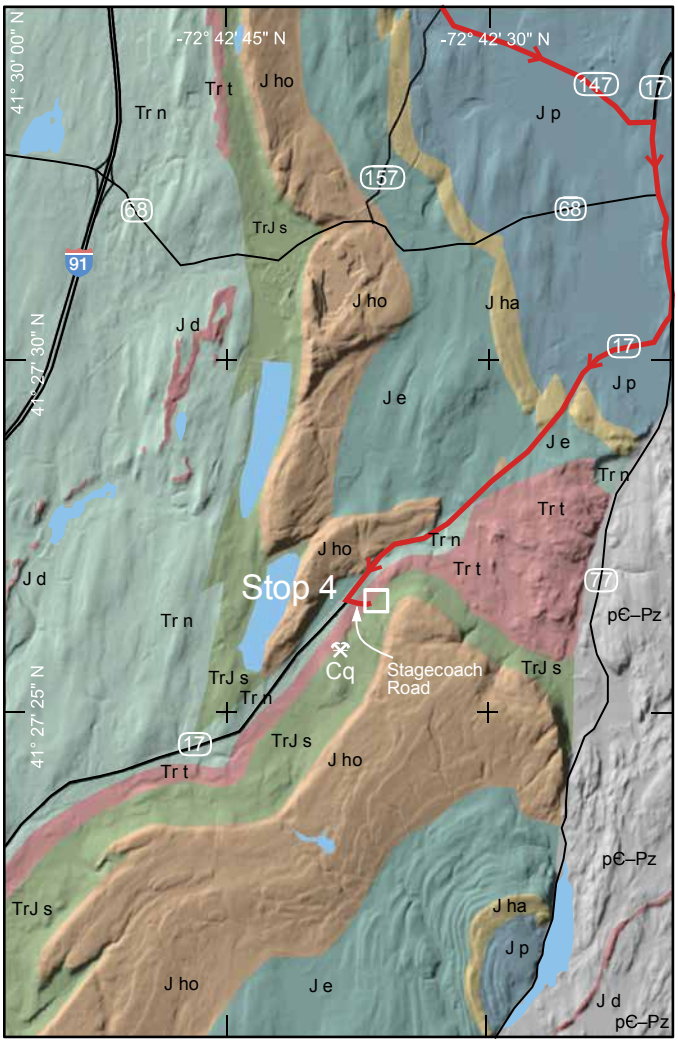

Figure 42. Geological map for Stop 4. Lidar topography from The National Map; geology modified from Simpson (1969), Rogers (1985), and Steinen and Charney (2020). Cq. indicates filled Coe's Quarry (position from Simpson, 1969).

Stop 4. Classic Durham Locality: Shuttle Meadow Formation (Transect begins at Bluff Head from New Haven Rd., Mattabassett Trail, Durham, Connecticut; James Velley Preserve, 41.429792°, -72.726989°; 41°25′47.25″N, 72°43′37.16″W)

Main Points

1. Most renowned fossil-fish locality in the Hartford Basin, with a history dating to the early nineteenth century.
2. Site of limited nineteenth- and early twentieth-century quarrying, small in scale compared with the Green River Formation or Chinese feathered-dinosaur deposits.
3. Important to concept of hypothetico-deductive lateral traceability of fish-bearing lacustrine units.
4. Basic stratigraphic context remained unknown until coring.
5. Abundant limestones related to elevated pCO_2 and localized basalt carbonization.
6. Best known for well-preserved fossil fishes but also contains a rich macroflora in microlaminated beds.
7. By current definition, the Durham and correlative assemblage, though post-ETE, is still latest Triassic and represents the oldest well-documented fauna of the Hartford Basin.

Discussion

Overview. This site, called the Durham locality, is in the lower Shuttle Meadow Formation and is perhaps the most famous fossil fish locality in the Hartford Basin (Fig. 42). The earliest reference appears in J.H. Redfield (1837), the same paper in which he named *Catopterus* (now *Redfieldius*) from Middlefield and Westfield. In that publication, Durham is casually cited as a fossil-fish site, implying it was already well known (also noted by Hitchcock in De La Beche, 1837). Mather (1843, p. 294) explicitly mentioned Durham and provided the only published stratigraphic section prior to the present study, shown as follows:

1. Drift and gravel beds.
2. Red sandstone.
3. Red and grey crumbling sandstone (very fissile).
4. Calcareous slate containing ichthyolites.
5. Sandstone and slate (fissile).
6. Shale.

Subsequently, the location was mentioned many times but not with any specifics about the stratigraphy.

In 1891, Samuel Ward Loper (Fig. 43) reported that he had collected fossil fishes for twenty years and recovered about 420 specimens from Durham and nearby areas (Davis and Loper, 1891); many were described by Newberry (1888). Loper conducted extensive excavations despite recurring flooding, and digging continued until at least 1900. His Durham collections, including numerous fish and plant fossils, are housed at Wesleyan University (McDonald, 1975), as well as Yale, the Smithsonian, and many other institutions.

Davis and Loper (1891) methodically sought additional fish-bearing outcrops using what would now be recognized as a hypothetico-deductive approach. They proposed that the fossiliferous units were more widespread than a single locality and used known black shale beds to construct testable predictions based on a structural model of the basin. From this model, they forecasted where equivalent horizons should surface in other fault blocks, assuming the fossil beds occupied the same stratigraphic position between lava flows. Loper then examined those predicted areas, where fossils had never been reported, making the fossil horizons a deductive test of the faulted-monocline hypothesis.

Their fieldwork followed these predictions rather than random prospecting, leading to multiple new discoveries. They even excavated pits where no outcrop was visible, successfully confirming their predictions. This represents a classic hypothetico-deductive confirmation: a structural hypothesis generates precise locational and faunal predictions, those predictions are tested empirically, and successful matches strongly support the hypothesis. This approach closely parallels our own method for tracing individual cycles across the basin, corroborated by units such as the Pompton Ashes or Westfield Turbidite.

Stratigraphy. McDonald (1975) was the first since Mather (1843) to compile a section at the Durham locality main fish-bearing unit (Fig. 19), the Bluff Head Bed, named for an outcrop on the northeast slope of Totoket Mountain near Bluff Head. Museum collections had already shown that there was a second, thinner fossiliferous horizon lower in the section—the "crinkle bed"—containing small fish and abundant clam shrimp (*Euestheria brodieana*) in microlaminated, crinkled shale. Prior to drilling the Silver Ridge B-1 core, the relationship between these beds was uncertain. Stratigraphic data from the core revealed that the "crinkle bed" represents the cycle immediately below the main fish-bearing unit (Fig. 44), whose deep-water facies is designated the Stagecoach Road Bed. About 190 m north-northwest along the base of Totoket Mountain, an intermittent stream exposes the Stagecoach Road Bed, overlain by blocks of the Bluff Head Bed, confirming consistent stratigraphy.

The absence of outcrop west of the crinkle bed/Stagecoach Road Bed precludes direct identification of the Southington Bed, which should be stratigraphically below (Fig. 44). However, highly altered, brecciated, and carbonated Talcott Basalt crops out about 500 m northeast along strike on Stagecoach Road. The basal contact of the Talcott and underlying New Haven Formation was briefly visible in that area during construction along Ericka Road. If the easternmost Talcott outcrops approximate the formation's upper surface and the dip is 8°, ~23 m of section should be present, enough to accommodate the Southington Bed. About 700 m southwest along strike from the base of the Stagecoach Road Bed lies the former Coe's Quarry (Simpson, 1969), now filled, which exposed a limestone tufa or possible travertine (Steinen et al., 1987). Percival (1842) described this

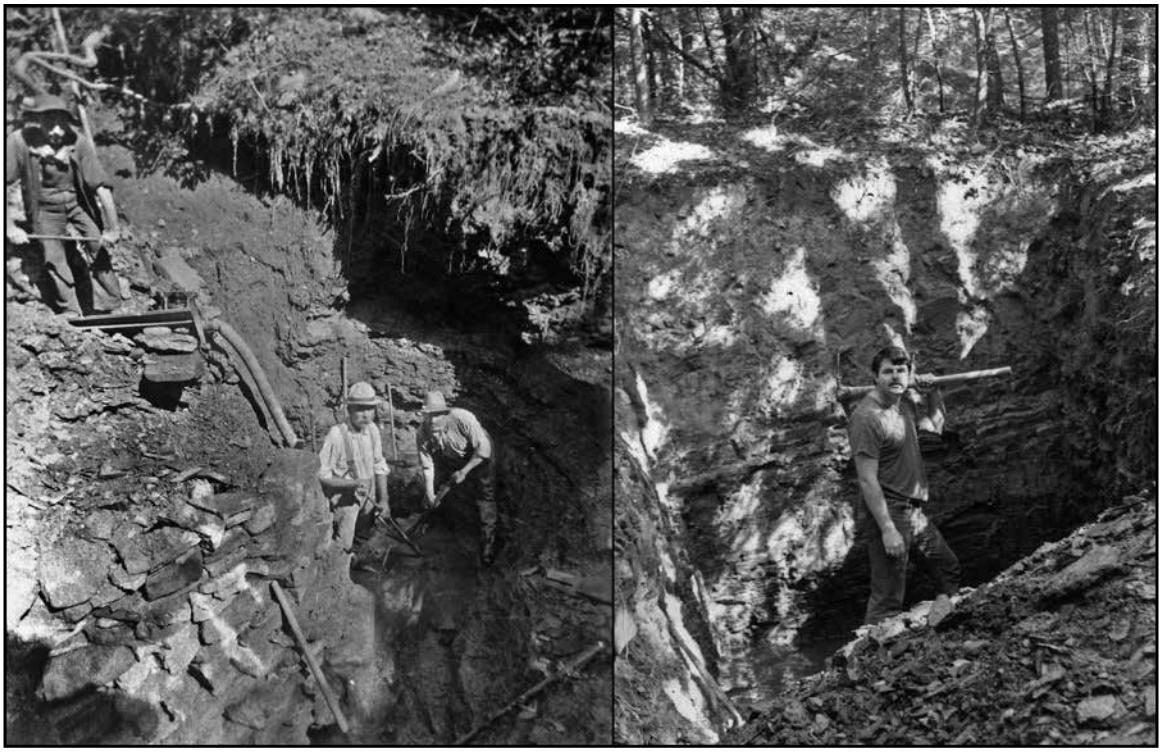

Figure 43. Excavations for fish and other fossils in the Bluff Head Bed, Shuttle Meadow Formation: Left—S. Ward Loper (nearest center) at the classic Durham Locality (Stop 4) in 1900 (photographer unknown); Right—N.G. McDonald at the Bluff Head locality ca. 1973.

limestone as resting on the anterior trap (Talcott Basalt). The Coe's Quarry limestone plausibly correlates with the Southington Bed, which is a limestone wherever recognized and supplied raw material for the Southington cement industry (Andrews, 1924; Olsen et al., 2024b).

The Coe's Quarry limestone was chiefly processed for agricultural lime, though some may have been used for cement (Simpson, 1969). It consists mainly of calcite and exhibits a porous texture with numerous voids, some infilled by cement. Several voids appear to be casts of conifer shoots. The limestone contains considerable organic matter and localized secondary silicification.

High* pCO_2 *and basalt carbonation. Steinen et al. (1987) proposed that the Coe's Quarry limestone represents a hot-spring travertine, but given the widespread extent of the Southington Bed, the carbonate at this level may not reflect a localized system. The lower lacustrine cycles of the Shuttle Meadow Formation are distinctly more limestone-rich than the middle and upper East Berlin Formation cycles observed at Stops 1–3, and even the Bluff Head Bed follows this pattern. We infer that the Coe's Quarry limestone represents a shoreline facies, a microbial or algal reef, of the shallow, rising or falling or even lowstand phase of the large, deep lake that deposited the Southington Bed microlaminated carbonate.

The underlying Talcott Basalt in this area is highly carbonated, in places so rich in carbonate that it has been mistaken for sedimentary limestone (Simpson, 1969) or even igneous carbonatite (pers. obs.). Steinen et al. (2017) suggest that this alteration and consequent friability explain the absence of Talcott exposures across an 8.3 km interval northward near Pistapaug Mountain. The analogy to current carbon-sequestration approaches using carbonation of mafic rocks to mitigate anthropogenic CO_2 is clear (e.g., Nisbet et al., 2024).

The prevalence of carbonates and the abundance of the fern *Clathropteris* characterize the Shuttle Meadow Formation, a pattern closely resembling that of homotaxial units in the Culpeper, Newark, Pomperaug, Fundy, and partly Moroccan basins. The recurrence of these sequences in the same stratigraphic position relative to the basalts suggests synchronous deposition across the basins (Olsen et al., 2024b). Paleosol carbonate proxy data indicate that CAMP volcanism doubled to tripled pCO_2 during each major eruptive phase (Schaller et al., 2011, 2012). The stratigraphic pattern in the Shuttle Meadow and equivalent units may reflect a facies syndrome linked to the ETE and CAMP, driven by weathering of large basaltic watersheds under alternating super-greenhouse and volcanic-winter conditions, producing Ca^{2+}- and HCO_3^--rich waters. Elevated pCO_2 may also have altered the Talcott Basalt where the Southington-Bed

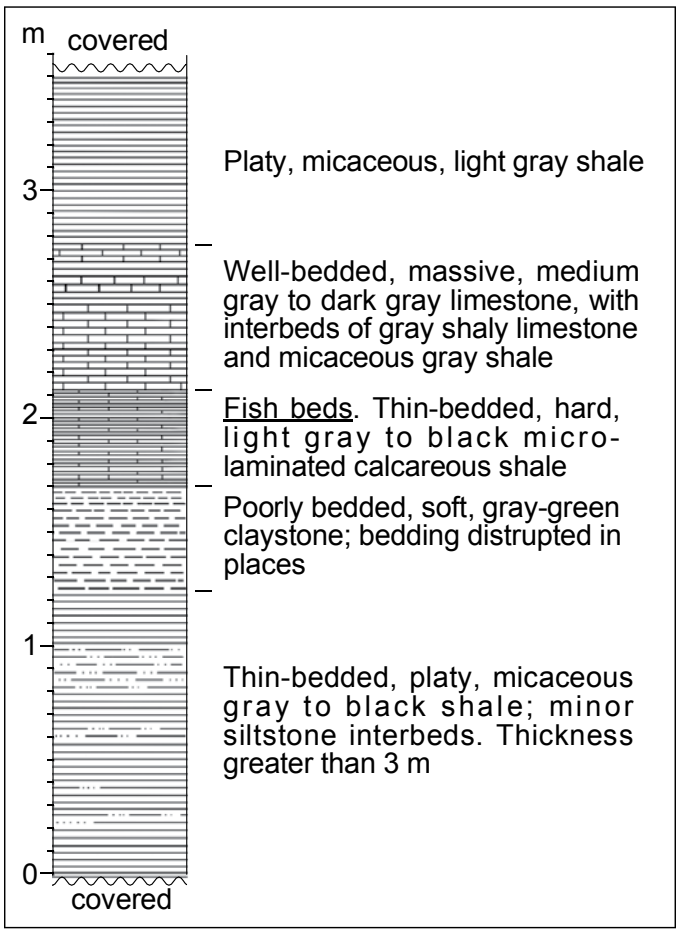

Figure 44. Stratigraphy at Stop 4, Durham locality, Bluff Head Bed of Shuttle Meadow Formation.

lake encroached upon it or where CO_2-enriched (not necessarily hydrothermal) springs entered the lake.

A smaller limestone sequence occurs in the basal East Berlin Formation above the Holyoke Basalt, which also supported a local cement industry (Everts et al., 1879; Starquist, 1943; Olsen et al., 2025b). This limestone formed in a much shallower, non-stratified lake lacking articulated fish but containing *Clathropteris*, rare elsewhere in the East Berlin Formation, otherwise absent from the rest of the East Berlin Formation (Olsen et al., 2025b).

Bluff Head Bed at Durham. The main feature of Stop 4 is the Bluff Head Bed (Figs. 19 and 44), a carbonate-rich, microlaminated unit characteristic of a stratified-lake setting. Outcrops here are ephemeral, and exposure of the bed is not guaranteed. However, nineteenth- and early twentieth-century quarrying has left abundant fragments in the intermittent streambed, and fossil fishes from this unit continue to appear in online forums and sales.

At this site, the bed is very dark-gray to black, closely matching the lithology of the Silver Ridge B-1 core. Fish taxa include *Semionotus* spp., *Redfieldius* spp., *Ptycholepis marshii*, and *Diplurus* cf. *D. longicaudatus* (Newberry, 1879, 1888; Schaeffer, 1948, 1952; Schaeffer et al., 1975; Schaeffer and McDonald, 1978). Numerous coprolites, attributed to the large coelacanth *Diplurus*, occur in these beds.

The Bluff Head Bed at Durham is notable for its abundance of macroscopic plants, including the conifers *Pagiophyllum simile* and *P. brevifolium*; the cycadeoids *Otozamites latior*, *O. brevifolius*, and *Cycadinocarpus chapini*; the leathery-leaved fern *Clathropteris (platyphylla) meniscoides*; the ginkgo *Baiera münsteriana*; the horsetail *Equisetites* sp.; and the indeterminate form *Loperia simplex*. This list updates Davis and Loper (1891), derived from Newberry (1888). Representative specimens are shown in Figure 45. Most were collected by Loper in the late nineteenth and early twentieth centuries, though new examples continue to appear online. The assemblage is unusual for its large specimens and relatively few conifers—though collecting bias cannot be ruled out. The near-unique occurrence of *Clathropteris meniscoides* in microlaminated sediments may represent a climatic signal.

Although putative theropod dinosaur teeth have been recovered from the Bluff Head and Westfield beds, the scale of excavations there is an order of magnitude smaller than at sites yielding articulated feathered dinosaurs and birds in China.

Age and significance of the lower Shuttle Meadow assemblage. The base of the Jurassic is formally defined at the Global Boundary Stratotype Section and Point (GSSP) by the first occurrence of the endemic ammonite *Psiloceras spelae tirolicum* (Hillebrandt et al., 2013) in the Austrian Alps, stratigraphically above the marine ETE horizon. Ash beds in coeval marine strata of Peru (Yager et al., 2017) indicate that the base of the Hettangian, and thus the Triassic–Jurassic boundary, is at 201.4 ± 0.2 Ma (Cohen et al., 2025), making it more than 100 kyr younger than the mass extinction at 201.564 ± 0.015 Ma (Blackburn et al., 2013). By this definition, the lower half of the Shuttle Meadow Formation, including strata at Stop 4 and the underlying Talcott Basalt, remains latest Triassic in age, even though it postdates the ETE (Fig. 13).

The Shuttle Meadow assemblages are significant because they formed near the peak of CAMP volcanism (Fig. 13). The climatic aftermath of CAMP, including prolonged volcanic winters and elevated pCO_2, plausibly persisted. The presence of the fern *Clathropteris* may represent an equatorward range expansion during this interval, and the abundant carbonate could reflect intense weathering of basaltic terrains. The obliquity-dominated orbital pacing of the Shuttle Meadow sequence is also distinctive and unexpected for equatorial latitudes, contrasting sharply with the precession-driven cycles of the middle and upper East Berlin Formation examined at Stops 1–3 (Fig. 13).

Return to vehicles. End of road log.

CONCLUSION

The Hartford Rift Basin's lake deposits illustrate key taphonomic processes and common sampling biases. Its outcrops, roadcuts, and cores enable scaling, from thin-section observations to basin-wide patterns linked to global and astronomical events.

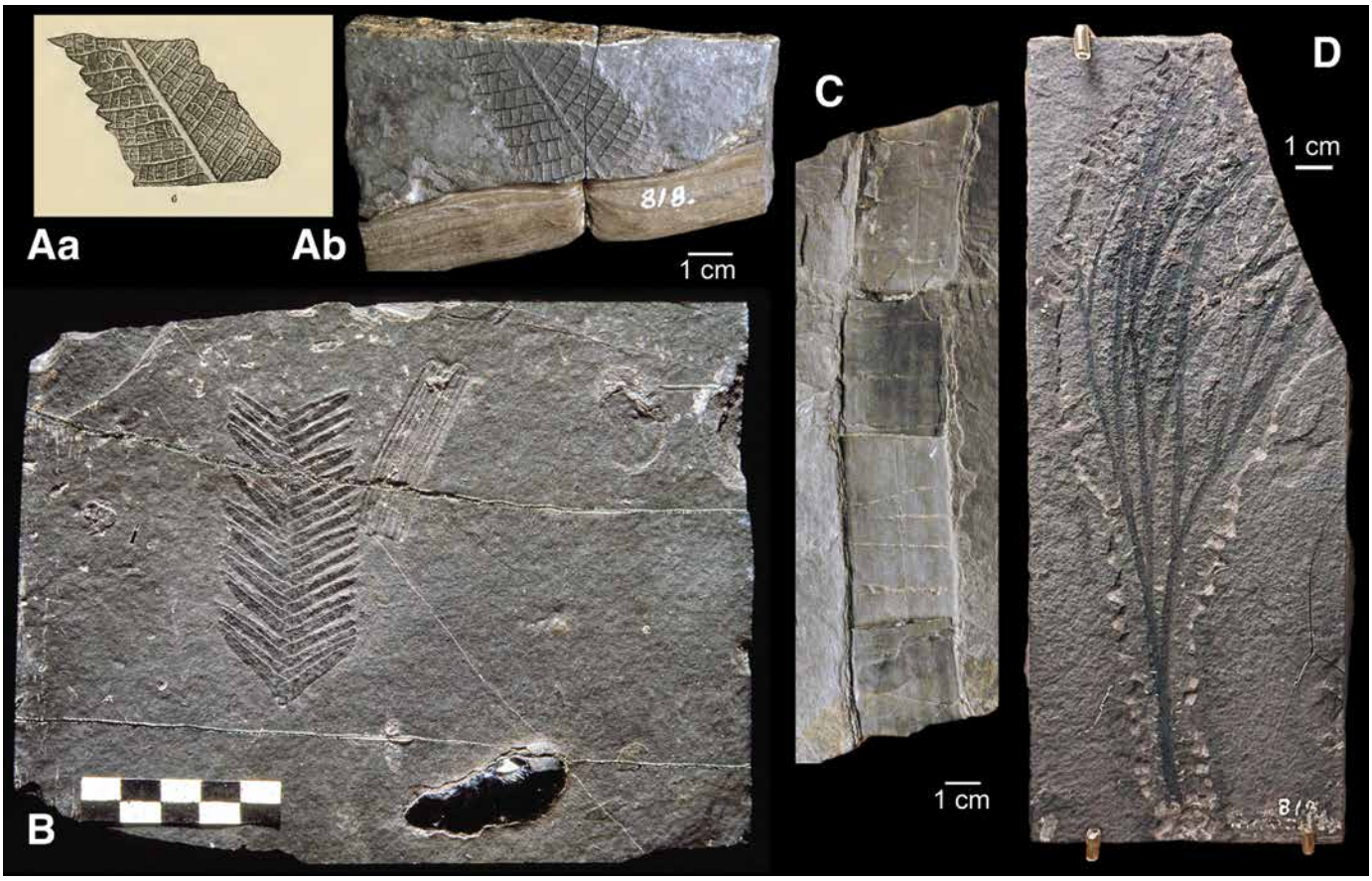

Figure 45. Plants from the Bluff Head Bed, classic Durham locality (Stop 4) collected by S.W. Loper. (A) The fern *Clathropteris meniscoides* (*C. platyphyllum* of Newberry, 1888); Aa—from Newberry (1888) referred to as coming from both Newark (Newberry 1888, p. 94) and Milford (Newberry 1888, caption for Pl. XII), New Jersey, in different parts of his text when it is in fact from Durham; Ab—specimen in the Joe Webb Peoples Museum at Wesleyan University (WUM 818); used with permission. (B) The cycadeoid *Otozamites* sp. with a coprolite and undermined plant impression in the Joe Webb Peoples Museum at Wesleyan University (WUM 1011); used with permission. (C) Referred specimen of *Loperia simplex*, an indeterminate stem or branch (YPM PB.011607: courtesy of the Peabody Museum of Natural History, Yale University). (D) The ginkgoalian *Baiera* sp. in the Joe Webb Peoples Museum at Wesleyan University (WUM 817), used with permission; specimen presently at Dinosaur State Park (Stop 1, Station 2) (see Fig. 15Dd); photo by Michael Ross, Dinosaur State Park.

They provide practical examples of applying modern analogs to ancient systems and testing hypotheses about deep time. The basin's deep-water *Lagerstätte* assemblages stand as benchmarks for the exceptional fossils that future discoveries may yield.

ACKNOWLEDGMENTS

We thank Tom Johnson and Lance Grande for reviewing the manuscript, and editor Peter Drzewiecki for many suggestions that greatly improved this paper. We also thank Dinosaur State Park and Mike Ross for access and photographs, the Connecticut Department of Transportation for access to Stop 2, and landowners for permission to visit Stop 3. Lance Grande, Jamie Kennedy, the National Park Service, and the Royal Tyrrell Museum kindly provided additional photographs. Research for this guidebook was supported by the Heising-Simons Foundation.

AI Tools

The lead author used Perplexity AI to check grammar and to suggest ways to shorten the text.

REFERENCES CITED

AECOM, 2015, Geotechnical Data Report: 5.1 Appendix B SHCST Contract No. 2015B-27 (Contract No. 2 GDR), South Hartford Conveyance and Storage Tunnel, Hartford, Connecticut, Contract No. 2015B-27, Hartford, Connecticut, Metropolitan District Commission (MDC), 1574 p.

Agassiz, J.L.R., 1833–1845, Recherches sur les poissons fossiles: Neuchâtel and Soleure, France, Petitpierre et Prince and H. Nicolet, 1420 p.

Agassiz, L., 1840, Études sur les glaciers: Neuchâtel, Switzerland, Chez l'auteur, 346 p.

Almond, M.J.R., and Hecky, R.E., 2002, Water Column Properties of Lake Bosumtwi, Ghana, 45th Annual Conference on Great Lakes Research; The Other Great Lakes: University of Manitoba, Winnipeg, Manitoba.

Anderson, R.Y., and Kirkland, D.W., 1960, Origin, varves, and cycles of Jurassic Todilto formation, New Mexico: American Association of Petroleum Geologists Bulletin, v. 44, no. 1, p. 37–52.

Anderson, R.Y., and Kirkland, D.W., 1969, Paleoecology of an Early Pleistocene Lake on the High Plains of Texas: Geological Society of America Memoir 113, 206 p., https://doi.org/10.1130/MEM113-p1.

Anderson, R.Y., Dean, W.E., Bradbury, J.P., and Love, D., 1985, Meromictic Lakes and Varved Lake Sediments in North America: U.S. Geological Survey Bulletin 1607, 19 p.

Andrews, F.D., 1924, History of the Discovery of Water-Limestone and Early Manufacture of Cement at Southington, Connecticut: Vineland, New Jersey, privately printed, 23 p.

Anselmetti, F., Ashwal, L., Ariztegui, D., Bohnhoff, M., Bomberg, M., Claeys, P., Eichelberger, J., Ellsworth, W.L., Goodenough, K., Heubeck, C., Kelemen, P., Koeberl, C., Kopf, A., Miller, K., Nordgulen, O., Noren, A., Onstott, T., Pease, V., P., Russell, J., Soreghan, G., Stein, M., Verschuren, D., and Yamada, Y., 2020, ICDP Science Plan: 2020–2030: Potsdam, International Continental Scientific Drilling Program, 36 p.

Bagalwa, M., Yalire, M., Balole, E., and Karume, K., 2014, A preliminary assessment of physico-chemical and bacteriological characteristics of Lake Edward and Majors Tributaries Rivers, Democratic Republic of Congo: Scholars Academic Journal of Biosciences, v. 2, no. 3, p. 236–245.

Beadle, L., 1966, Prolonged stratification and deoxygenation in tropical lakes. I. Crater Lake Nkugute, Uganda, compared with Lakes Bunyoni and Edward: Limnology and Oceanography, v. 11, no. 2, p. 152–163, https://doi.org/10.4319/lo.1966.11.2.0152.

Beadle, L.C., 1981, The Inland Waters of Tropical Africa: An Introduction to Tropical Limnology: London and New York, Longman, 475 p.

Benson, L.V., and Thompson, R.S., 1987, Lake-level variation in the Lahontan Basin for the past 50,000 years: Quaternary Research, v. 28, no. 1, p. 69–85, https://doi.org/10.1016/0033-5894(87)90034-2.

Benton, M.J., Zhonghe, Z., Orr, P.J., Fucheng, Z., and Kearns, S.L., 2008, The remarkable fossils from the Early Cretaceous Jehol Biota of China and how they have changed our knowledge of Mesozoic life: Presidential Address, delivered 2nd May 2008: Proceedings of the Geologists' Association, v. 119, no. 3–4, p. 209–228.

Blackburn, T.J., Olsen, P.E., Bowring, S.A., McLean, N.M., Kent, D.V., Puffer, J., McHone, G., Rasbury, E.T., and Et-Touhami, M., 2013, Zircon U-Pb geochronology links the end-Triassic extinction with the Central Atlantic Magmatic Province: Science, v. 340, no. 6135, p. 941–945, https://doi.org/10.1126/science.1234204.

Boehrer, B., and Schultze, M., 2008, Stratification of lakes: Reviews of Geophysics, v. 46, no. 2, https://doi.org/10.1029/2006RG000210.

Boehrer, B., Shatwell, T., Damoah, A., Aurich, P., Determann, M., Sanful, P., and von Tümpling, W., 2025, Gas accumulation in Lake Bosumtwi deep waters and its potential to contribute to fish kills: Environmental Science and Pollution Research International, v. 32, no. 9, p. 5371–5380, https://doi.org/10.1007/s11356-025-36032-z.

Bose, S., and Chafetz, H.S., 2009, Topographic control on distribution of modern microbially induced sedimentary structures (MISS): A case study from Texas coast: Sedimentary Geology, v. 213, no. 3–4, p. 136–149, https://doi.org/10.1016/j.sedgeo.2008.11.009.

Bouffard, D., Boegman, L., Ackerman, J.D., Valipour, R., and Rao, Y.R., 2014, Near-inertial wave driven dissolved oxygen transfer through the thermocline of a large lake: Journal of Great Lakes Research, v. 40, no. 2, p. 300–307, https://doi.org/10.1016/j.jglr.2014.03.014.

Boyer, B.W., 1982, Green River laminites: Does the playa-lake model really invalidate the stratified-lake model?: Geology, v. 10, no. 6, p. 321–324, https://doi.org/10.1130/0091-7613(1982)10<321:GRLDTP>2.0.CO;2.

Boyko, M., 1973, European Impact on the Vegetation around Crawford Lake in Southern Ontario [Master's thesis]: Toronto, University of Toronto, 115 p.

Bradley, W.C., 1929, The varves and climate of the Green River epoch: U.S. Geological Survey Professional Paper 158-E, p. 87–110.

Bradley, W.C., 1963, Paleolimnology, *in* Frey, D.G., ed., Limnology in North America: Madison, University of Wisconsin Press, p. 621–652.

Bradley, W.H., and Eugster, H.P., 1969, Geochemistry and paleolimnology of the trona deposits and associated authigenic minerals of the Green River Formation of Wyoming: U.S. Geological Survey Professional Paper 496-B, p. B1–B71, https://doi.org/10.3133/pp496B.

Bretschneider, C., 1951, Revised wave forecasting relationships: Coastal Engineering Proceedings, v. 1, no. 2, p. 1, https://doi.org/10.9753/icce.v2.1.

Brignon, A., 2017, The earliest discoveries of articulated fossil fishes (Actinopterygii) in the United States: A historical perspective: American Journal of Science, v. 317, no. 2, p. 216–250, https://doi.org/10.2475/02.2017.03.

Brinkman, D.L., and Hyatt, J.A., 2025, Archival Evidence of Strong, Longtime Ties between Yale Peabody Museum's Division of Vertebrate Paleontology and Connecticut's Dinosaur State Park: Bulletin - Peabody Museum of Natural History, v. 66, no. 1, p. 71–86, https://doi.org/10.3374/014.066.0104.

Brongniart, A., and Silliman, B., 1821, Miscellaneous observations relating to geology, mineralogy and some connected topics, in extracts of letters from Mr. Alex'r. Brongniart, member of the Royal Academy of Sciences, Engineer of Mines, &c. of Paris with the remarks to the editor to whom the letters were addressed: American Journal of Science and Arts, v. 3, no. 2, p. 216–227.

Buesseler, K., Livingston, H., Ivanov, L., and Romanov, A., 1994, Stability of the oxic-anoxic interface in the Black Sea: Deep Sea Research. Part I, Oceanographic Research Papers, v. 41, no. 2, p. 283–296, https://doi.org/10.1016/0967-0637(94)90004-3.

Buma, W.G., Lee, S.-I., and Seo, J.Y., 2018, Recent surface water extent of Lake Chad from multispectral sensors and GRACE: Sensors (Basel), v. 18, no. 7, 2082, https://doi.org/10.3390/s18072082.

Buntin, R.C.C., Moklestad, T., Matthews, N.A., Breithaupt, B., Murphy, P.C., Kapinos, I., and Noffke, N., 2025, A new theropod dinosaur lek in the Cretaceous Dakota Sandstone (Dinosaur Ridge, Colorado, USA): Cretaceous Research, v. 176, https://doi.org/10.1016/j.cretres.2025.106176.

Byrnes, J.B., 1972, The Bedrock Geology of Dinosaur State Park, Rocky Hill, Connecticut [M.Sc. thesis]: Storrs, University of Connecticut, 244 p.

Calderon, T., 1983, Relationship between blue color and radiation damage in calcite: Radiation Effects Letters, v. 76, no. 5, p. 187–191.

Chang, C.Y., 2024, Sediment Histories: Early Mesozoic Ice and North American Pleistocene–Holocene Deglaciation [Ph.D. dissertation]: New York, Columbia University, 310 p.

Chapman, R.W., 1965, Stratigraphy and petrology of the Hampden basalt in Central Connecticut: Geological and Natural History Survey of Connecticut Report Investigations, v. 3, p. 1–38.

Cleaveland, P., 1816, An Elementary Treatise on Mineralogy and Geology, Being an Introduction to the Study of These Sciences, and Designed for the Use of Pupils, for Persons, Attending Lectures on These Subjects, and as a Companion for Travellers in the United States of America: Boston, Cummings and Hilliard, 668 p.

Cohen, A.S., Talbot, M.R., Awramik, S.M., Dettman, D.L., and Abell, P., 1997, Lake level and paleoenvironmental history of Lake Tanganyika, Africa, as inferred from late Holocene and modern stromatolites: Geological Society of America Bulletin, v. 109, no. 4, p. 444–460, https://doi.org/10.1130/0016-7606(1997)109<0444:LLAPHO>2.3.CO;2.

Cohen, K., Harper, D., Gibbard, P., and Car, N., 2025, The ICS international chronostratigraphic chart this decade: International Union of Geological Sciences, v. 48, no. 1, p. 105–115, https://doi.org/10.18814/epiiugs/2025/025001.

Colbert, E.H., and Olsen, P.E., 2001, A new and unusual aquatic reptile from the Lockatong Formation of New Jersey (Late Triassic, Newark Supergroup): American Museum Novitates, v. 3334, p. 1–24, https://doi.org/10.1206/0003-0082(2001)334<0001:ANAUAR>2.0.CO;2.

Colton, R.B., and Hartshorn, J.H., 1966, Bedrock Geologic Map of the West Springfield Quadrangle, Massachusetts and Connecticut: U.S. Geological Survey Quadrangle Map GQ-537, scale 1:24,000.

Conti, A.A., 2016, Lacustrine Deposits of the Jurassic East Berlin Formation, Hartford Basin, Newark Supergroup: Balance-filled or Under-filled Lakes? [M.Sc. thesis]: Columbus, Ohio University, 185 p.

Coombs, W.P., Jr., 1980, Swimming ability of carnivorous dinosaurs: Science, v. 207, no. 4436, p. 1198–1200.

Davies, J.H.F.L., Marzoli, A., Bertrand, H., Youbi, N., Ernesto, M., and Schaltegger, U., 2017, End-Triassic mass extinction started by intrusive CAMP activity: Nature Communications, v. 8, https://doi.org/10.1038/ncomms15596.

Davies, J.H.F.L., Marzoli, A., Bertrand, H., Youbi, N., Ernesto, M., Greber, N.D., Ackerson, M., Simpson, G., Bouvier, A.-S., Baumgartner, L., Pettke, T., Farina, F., Ahrenstedt, H.V., and Schaltegger, U., 2021, Zircon petrochronology in large igneous provinces reveals upper crustal contamination processes: New U–Pb ages, Hf and O isotopes, and trace elements from the Central Atlantic magmatic province (CAMP): Contributions to Mineralogy and Petrology, v. 176, no. 1, https://doi.org/10.1007/s00410-020-01765-2.

Davis, W.M., and Loper, S.W., 1891, Two belts of fossiliferous black shale in the Triassic formation of Connecticut: Geological Society of America Bulletin, v. 2, p. 415–430, https://doi.org/10.1130/GSAB-2-415.

De La Beche, H.T., 1837, Researches in Theoretical Geology: New York, F.J. Huntington & Co., 342 p.

Dean, R.G., and Dalrymple, R.A., 1991, Water Wave Mechanics for Engineers and Scientists: Teaneck, New Jersey, World Scientific Publishing Company, 353 p.

Degens, E.T., Stoffers, P., Golubiić, S., and Dickman, M., 1978, Varve chronology: Estimated rates of sedimentation in the Black Sea deep basin: Initial Reports of the Deep Sea Drilling Project, v. 42, p. 499–508, https://doi.org/10.2973/dsdp.proc.42-2.114.1978.

Denny, P., 1972, Lakes of south-western Uganda: Freshwater Biology, v. 2, no. 2, p. 143–158, https://doi.org/10.1111/j.1365-2427.1972.tb00367.x.

Drzewiecki, P.A., and Hyatt, J.A., 2025, Distinguishing true tracks from undertracks and overtracks at Dinosaur State Park, Rocky Hill, Connecticut: Bulletin - Peabody Museum of Natural History, v. 66, no. 1, p. 141–174, https://doi.org/10.3374/014.066.0107.

Drzewiecki, P.A., Schroeder, T., Steinen, R.P., and Thomas, M.A., 2012, The Bedrock Geology of the Hartford South Quadrangle: With a Map and Cross Sections: State Geological and Natural History Survey of Connecticut, Department of Energy and Environmental Protection, Quadrangle Report, v. 40, scale 1:24,000.

Drzewiecki, P.A., Steinen, R., Bora, E., and Milardo, J.S., 2026, Constraining dinosaur behavior from paleoenvironmental interpretations: Early Jurassic East Berlin Formation at Dinosaur State Park, Rocky Hill, Connecticut, USA: Palaios, v. 41, no. 1, p. 1–23, https://doi.org/10.2110/palo.2025.026.

Dubey, S., and Roulin, A., 2014, Evolutionary and biomedical consequences of internal melanins: Pigment Cell & Melanoma Research, v. 27, no. 3, p. 327–338, https://doi.org/10.1111/pcmr.12231.

Dyer-Pietras, K.M., 2020, Insolation forcing of sub-lacustrine debris flows—Could monsoon intensification have played a role? Eocene lacustrine Green River Formation, Piceance Creek Basin, Colorado: Palaeogeography, Palaeoclimatology, Palaeoecology, v. 553, https://doi.org/10.1016/j.palaeo.2020.109738.

Eccles, D.H., 1974, An outline of the physical limnology of Lake Malawi (Lake Nyasa): Limnology and Oceanography, v. 19, no. 5, p. 730–742, https://doi.org/10.4319/lo.1974.19.5.0730.

Edmond, J.M., Stallard, R.F., Craig, H., Craig, V., Weiss, R.F., and Coulter, G.W., 1993, Nutrient chemistry of the water column of Lake Tanganyika: Limnology and Oceanography, v. 38, no. 4, p. 725–738, https://doi.org/10.4319/lo.1993.38.4.0725.

Eugster, H.P., and Surdam, R.C., 1973, Depositional environment of the Green River Formation of Wyoming: A preliminary report: Geological Society of America Bulletin, v. 84, no. 4, p. 1115–1120, https://doi.org/10.1130/0016-7606(1973)84<1115:DEOTGR>2.0.CO;2.

Everts, L.H., Co., and eds., 1879, History of the Connecticut Valley in Massachusetts, with Illustrations and Biographical Sketches of Some of Its Prominent Men and Pioneers: Philadelphia, Louis H. Everts, 1111 p.

Fagherazzi, S., and Wiberg, P.L., 2009, Importance of wind conditions, fetch, and water levels on wave-generated shear stresses in shallow intertidal basins: Journal of Geophysical Research: Earth Surface, v. 114, https://doi.org/10.1029/2008JF001139.

Farlow, J.O., and Galton, P.M., 2003, Dinosaur trackways of Dinosaur State Park, Rocky Hill, Connecticut, *in* LeTourneau, P.M., and Olsen, P.E., eds., The Great Rift Valleys of Pangea in Eastern North America, Volume T2: Sedimentology, Stratigraphy, and Paleontology: New York, Columbia University Press, p. 248–263.

Farlow, J.O., Brinkman, D.L., and Hyatt, J.A., 2025a, The Yale Peabody Museum dinosaur footprint block/slab from Dinosaur State Park, Rocky Hill, Connecticut: Bulletin - Peabody Museum of Natural History, v. 66, no. 1, p. 87–97, https://doi.org/10.3374/014.066.0105.

Farlow, J.O., Galton, P.M., Hyatt, J.A., Drzewiecki, P.A., Penrod, A., and Whitcraft, J., 2025b, Dinosaur footprints from the Lower Jurassic East Berlin Formation, Dinosaur State Park, Rocky Hill, Connecticut: Bulletin - Peabody Museum of Natural History, v. 66, no. 1, p. 175–259, https://doi.org/10.3374/014.066.0108.

Findenegg, I., 1935, Limnologische untersuchungen in Karntner seengebiete: Internationale Revue der Gesamten Hydrobiologie und Hydrographie, v. 32, p. 369–423.

Fisher, J.A., Waltham, D., Nichols, G.J., Krapf, C.B.E., and Lang, S.C., 2007, A quantitative model for deposition of thin fluvial sand sheets: Journal of the Geological Society, v. 164, no. 1, p. 67–71, https://doi.org/10.1144/0016-76492005-179.

Fox, B.R.S., Wartho, J., Wilson, G.S., Lee, D.E., Nelson, F.E., and Kaulfuss, U., 2015, Long-term evolution of an Oligocene/Miocene maar lake from Otago, New Zealand: Geochemistry, Geophysics, Geosystems, v. 16, no. 1, p. 59–76, https://doi.org/10.1002/2014GC005534.

Fraser, N.C., Grimaldi, D.A., Axsmith, B.J., Heckert, A.B., and Liutkus-Pierce, C., Smith, D., and Dooley, A.C., Jr., 2017, The Solite Quarry—A window into life by a Late Triassic lake margin, *in* Fraser, N.C., and Sues, H.-D., eds., Terrestrial Conservation Lagerstätten: Windows into the Evolution of Life on Land: Edinburgh, Scotland, Dunedin Academic Press, p. 105–129.

Galton, P.M., and Farlow, J.O., 2003, Dinosaur State Park, Connecticut, USA: History, footprints, trackways, exhibits: Zubia, v. 21, p. 129–173.

Ganz, K.J., Glines, M.R., and Rose, K.C., 2024, The distribution of depth, volume, and basin shape for lakes in the conterminous United States: Limnology and Oceanography, v. 69, no. 1, p. 22–36, https://doi.org/10.1002/lno.12475.

Gierlowski-Kordesch, E., and Rust, B.R., 1994, The Jurassic East Berlin Formation, Hartford Basin, Newark Supergroup (Connecticut and Massachusetts): A Saline Lake Playa Alluvial Plain System, *in* Renaut, R.W., and Last, W.M., eds., Sedimentology and Geochemistry of Modern and Ancient Saline Lakes: Tulsa, Oklahoma, Society for Economic Geology, p. 249–265, https://doi.org/10.2110/pec.94.50.0249.

Glenn, C.R., and Kelts, K., 1991, Sedimentary rhythms in lake deposits, *in* Einsele, G., Ricken, W., and Seilacher, A., eds., Cycles and Events in Stratigraphy: Berlin, Springer-Verlag, p. 188–221.

Grabau, A.W., 1923–1924, Stratigraphy of China, Part 1: Palaeozoic and Older: Peking, Geological Survey of China, 528 p.

Grabau, A.W., 1928, Stratigraphy of China, Part 2: Mesozoic: Bulletin of the Geological Survey of China, 771 p.

Grande, L., 1984, Paleontology of the Green River Formation, with a review of the fish fauna: Laramie, Wyoming, Geological Survey of Wyoming, 333 p.

Grande, L., 2010, An empirical synthetic pattern study of Gars (Lepisosteiform) and closely related species, based mostly on skeltal anatomy, The resurrection of the Holostei: Copeia, supplement, v. 10, no. 2a, p. 1–871.

Gray, N.H., 1982, Mesozoic volcanism in north-central Connecticut, *in* Joesten, R., and Quarrier, S.S., eds., Guidebook for Field Trips in Connecticut and South-Central Massachusetts, New England Intercollegiate Geological Conference, 74th Annual Meeting, State Geological and Natural History Survey of Connecticut, Guidebook No. 5, State Geological and Natural History Survey, Hartford, Connecticut, p. 173–193.

Gray, N.H., 1987, Mesozoic sedimentary and volcanic rocks in the Farmington River Gorge, Tariffville, Connecticut, *in* Roy, D.C., ed., Northeastern Section of the Geological Society of America: Boulder, Colorado, Geological Society of America, Geological Society of North America, Centennial Field Guide, v. 5, p. 165–168, https://doi.org/10.1130/0-8137-5405-4.165.

Green, M.O., and Coco, G., 2014, Review of wave-driven sediment resuspension and transport in estuaries: Reviews of Geophysics, v. 52, no. 1, p. 77–117, https://doi.org/10.1002/2013RG000437.

Gwynn, J.W., 1996, Commonly Asked Questions about Utah's Great Salt Lake and Ancient Lake Bonneville: Utah Geological Survey, Public Information Series, 23 p.

Håkanson, L., 1977, The influence of wind, fetch, and water depth on the distribution of sediments in Lake Vänern, Sweden: Canadian Journal of Earth Sciences, v. 14, p. 397–412, https://doi.org/10.1139/e77-040.

Halfman, J.D., and Johnson, T.C., 1988, High-resolution record of cyclic climatic change during the past 4 ka from Lake Turkana, Kenya: Geology, v. 16, no. 6, p. 496–500, https://doi.org/10.1130/0091-7613(1988)016<0496:HRROCC>2.3.CO;2.

Hanshaw, P.M., 1968, Bedrock Geologic Map of the Meriden Quadrangle, New Haven, Hartford, and Middlesex Counties, Connecticut: Geological Quadrangle Maps of the United States, v. GQ-738, p. 1–4, scale 1:24,000.

Hathaway, D.H., 2015, The Solar Cycle: Living Reviews in Solar Physics, v. 12, no. 4, p. 1–87.

Hay, O.P., 1902, Bibliography and Catalogue of the Fossil Vertebrates of North America: U.S. Geological Survey Bulletin 179, 868 p.

Hays, J.D., Imbrie, J., and Shackleton, N.J., 1976, Variations in the Earth's orbit: Pacemaker of the Ice Ages: Science, v. 194, no. 4270, p. 1121–1132, https://doi.org/10.1126/science.194.4270.1121.

Hellawell, J., and Orr, P.J., 2012, Deciphering taphonomic processes in the Eocene Green River Formation of Wyoming: Palaeobiodiversity and Palaeoenvironments, v. 92, no. 3, p. 353–365, https://doi.org/10.1007/s12549-012-0092-6.

Hethke, M., Fürsich, F.T., Jiang, B., and Klaus, R., 2013, Oxygen deficiency in Lake Sihetun; formation of the Lower Cretaceous Liaoning Fossillagerstätte (China): Journal of the Geological Society, v. 170, no. 5, p. 817–831, https://doi.org/10.1144/jgs2012-102.

Hillebrandt, A.V., Krystyn, L., Kürschner, W.M., Bonis, N.R., Ruhl, M., Richoz, S., Schobben, M.A.N., Urlichs, M., Bown, P.R., Kment, K., and McRoberts, C.A., 2013, The global stratotype sections and point (GSSP) for the base of the Jurassic System at Kuhjoch (Karwendel Mountains, Northern Calcareous Alps, Tyrol, Austria): Episodes, v. 36, no. 3, p. 162–198, https://doi.org/10.18814/epiiugs/2013/v36i3/001.

Hubert, J.F., Reed, A.A., and Carey, P.J., 1976, Paleogeography of the East Berlin Formation, Newark Group, Connecticut Valley: American Journal of Science, v. 276, no. 10, p. 1183–1207, https://doi.org/10.2475/ajs.276.10.1183.

Hubert, J.F., Reed, A.A., Dowdall, W.L., and Gilvhrist, J.M., 1978, Guide to the redbeds of central Connecticut: 1978 field trip, Eastern Section of SEPM: Amherst, Massachusetts, University of Massachusetts, Department of Geology and Geography, Contribution, 129 p.

Hutchinson, G.E., 1937, A contribution to the limnology of arid regions, primarily founded on observations made in the Lahontan Basin: Connecticut Academy of Arts and Sciences.

Hutchinson, G.E., 1957, A Treatise on Limnology. Vol. 1: Geography, Physics, and Chemistry: New York, John Wiley and Sons, 1015 p.

Huxley, T.H., 1868, On the animals which are most nearly intermediate between birds and reptiles: Annals & Magazine of Natural History, v. 2, p. 66–75.

Hyatt, J.A., Farlow, J.O., Galton, P.M., and Getty, P.R., 2025, Documenting footprints for tracksites at Dinosaur State Park, Rocky Hill, Connecticut: Bulletin - Peabody Museum of Natural History, v. 66, no. 1, p. 99–139, https://doi.org/10.3374/014.066.0106.

Hyodo, A., 2010, The Holocene Paleolimnology of Lake Superior [Ph.D. thesis]: London, Ontario, University of Western Ontario 353 p.

Imboden, D.M., and Wüest, A., 1995, Mixing mechanisms in lakes, *in* Lerman, A., Imboden, D.M., and Gat, J.R., eds., Physics and Chemistry of Lakes: Berlin, Springer, p. 83–138, https://doi.org/10.1007/978-3-642-85132-2_4.

Islek, F., Yuksel, Y., Sahin, C., and Guner, H.A.A., 2021, Long-term analysis of extreme wave characteristics based on the SWAN hindcasts over the Black Sea using two different wind fields: Dynamics of Atmospheres and Oceans, v. 94, https://doi.org/10.1016/j.dynatmoce.2020.101165.

Jelinowska, A., Tucholka, P., Guichard, F., Lefèvre, I., Badaut-Trauth, D., Chalié, F., Gasse, F., Tribovillard, N., and Desprairies, A., 1998, Mineral magnetic study of Late Quaternary South Caspian Sea sediments: Palaeoenvironmental implications: Geophysical Journal International, v. 133, no. 2, p. 499–509, https://doi.org/10.1046/j.1365-246X.1998.00536.x.

Jiang, B., Fürsich, F.T., Sha, J., Wang, B., and Niu, Y., 2011, Early Cretaceous volcanism and its impact on fossil preservation in Western Liaoning, NE China: Palaeogeography, Palaeoclimatology, Palaeoecology, v. 302, no. 3–4, p. 255–269, https://doi.org/10.1016/j.palaeo.2011.01.016.

Jiang, B., Harlow, G.E., Wohletz, K., Zhou, Z., and Meng, J., 2014, New evidence suggests pyroclastic flows are responsible for the remarkable preservation of the Jehol biota: Nature Communications, v. 5, no. 1, 3151, https://doi.org/10.1038/ncomms4151.

Johnson, T.C., 1980, Sediment redistribution by waves in lakes, reservoirs and embayments, *in* Stefan, H., ed., Proceedings of the Symposium on Surface Water Impoundments, 2–5 June 1980, Minneapolis, Minnesota: New York, American Society of Civil Engineers, p. 1307–1317.

Kent, D.V., and Olsen, P.E., 2008, Early Jurassic magnetostratigraphy and paleolatitudes from the Hartford continental rift basin (eastern North America): Testing for polarity bias and abrupt polar wander in association with the central Atlantic magmatic province: Journal of Geophysical Research, v. 113, https://doi.org/10.1029/2007JB005407.

Khazaei, B., Read, L.K., Casali, M., Sampson, K.M., and Yates, D.N., 2022, GLOBathy, the global lakes bathymetry dataset: Scientific Data, v. 9, no. 36, p. https://doi.org/10.1038/s41597-022-01132-9.

Klein, G.D., 1968, Trip C1: Sedimentology of Triassic Rocks in the lower Connecticut Valley, *in* Orville, P.M., ed., Guidebook for Fieldtrips in Connecticut, New England Intercollegiate Geological Conference, 60th Annual Meeting, Yale University, New Haven, Connecticut, October 25–27, 1968: Hartford, Connecticut, State Geological and Natural History Survey of Connecticut, Guidebook, p. C1–C19.

Komar, P.D., 1974, Oscillatory ripple marks and the evaluation of ancient wave conditions and environments: Journal of Sedimentary Research, v. 44, no. 1, p. 169–180.

Kominz, M.A., Beavan, J., Bond, G.C., and McManus, J., 1991, Are cyclic sediments periodic? Gamma analysis and spectral analysis of Newark Supergroup lacustrine strata: Kansas Geological Survey Bulletin, v. 233, p. 231–252.

Kranenburg, W., Tiessen, M., Veenstra, J., de Graaff, R., Uittenbogaard, R., Bouffard, D., Sakindi, G., Umutoni, A., Van de Walle, J., Thiery, W., and van Lipzig, N., 2020, 3D-modelling of Lake Kivu: Horizontal and vertical flow and temperature structure under spatially variable atmospheric forcing: Journal of Great Lakes Research, v. 46, no. 4, p. 947–960, https://doi.org/10.1016/j.jglr.2020.05.012.

Krynine, P.D., 1950, Petrology, stratigraphy, and origin of the Triassic sedimentary rocks of Connecticut: State of Connecticut, State Geological and Natural History Survey Bulletin, v. 73, 247 p.

Landwehrs, J.P., Feulner, G., Hofmann, M., and Petri, S., 2020, Climatic fluctuations modeled for carbon and sulfur emissions from end-Triassic volcanism: Earth and Planetary Science Letters, v. 537, https://doi.org/10.1016/j.epsl.2020.116174.

Lehmann, E.P., 1959, The bedrock geology of the Middletown quadrangle with map: State Geological and Natural History Survey of Connecticut Quadrangle Report, v. 8, p. 1–39, scale 1:24,000.

Leonard, E., 2013, The Taphonomy and Depositional Environment of Jurassic Lacustrine Fish Deposits, Westfield Bed, East Berlin Formation, Hartford Basin [senior honors thesis]: Middletown, Connecticut, Wesleyan University, 112 p.

LeTourneau, P.M., 1985, The Sedimentology and Stratigraphy of the Lower Jurassic Portland Formation, Central Connecticut [Master's thesis]: Middletown, Connecticut, Wesleyan University, 247 p.

LeTourneau, P.M., and McDonald, N.G., 1985, Trip B–7: The sedimentology, stratigraphy, and paleontology of the Lower Jurassic Portland Formation, Hartford Basin, central Connecticut, *in* Tracy, R.J., ed., Guidebook for Fieldtrips in Connecticut and adjacent areas of New York and Rhode Island, New England Intercollegiate Geological Conference, 77th Annual Meeting, Yale University, New Haven, Connecticut, p. 353–391.

LeTourneau, P.M., McDonald, N.G., Olsen, P.E., Ku, T.C., and Getty, P.R., 2015, Fossils and facies of the Connecticut Valley Lowland: Ecosystem structure and sedimentary dynamics along the footwall margin of an active rift, *in* Gilmore, M.S., and Resor, P.G., eds., Guidebook for Field Trips in Connecticut and Adjacent Regions: New England Intercollegiate Geological Conference, 107th Annual Meeting, Wesleyan University, Middletown, Connecticut, p. 107–151.

LeTourneau, P.M., McDonald, N.G. and, Ku, T.C., 2016, Taphonomic processes in Early Jurassic rift lakes of the Hartford Basin: Physical and biochemical controls on preservation of bony fishes: Geological Society of America Abstracts with Program, v. 48, no. 2, https://doi.org/10.1130/abs/2016NE-272281.

Lian, X.-N., Cai, C.-Y., and Huang, D.-Y., 2021, The early assemblage of Middle–Late Jurassic Yanliao biota: Checklist, bibliography and statistical analysis of described taxa from the Daohugou beds and coeval deposits: Palaeoentomology, v. 4, no. 2, p. 95–136, https://doi.org/10.11646/palaeoentomology.4.2.1.

Lindgren, J., Uvdal, P., Sjövall, P., Nilsson, D.E., Engdahl, A., Schultz, B.P., and Thiel, V., 2012, Molecular preservation of the pigment melanin in fossil melanosomes: Nature Communications, v. 3, no. 1, p. 824, https://doi.org/10.1038/ncomms1819.

Liutkus, C.M., Beard, J.S., Fraser, N.C., and Ragland, P.C., 2010, Use of fine-scale stratigraphy and chemostratigraphy to evaluate conditions of deposition and preservation of a Triassic Lagerstätte, south-central Virginia: Journal of Paleolimnology, v. 44, no. 2, p. 645–666, https://doi.org/10.1007/s10933-010-9445-1.

Llew-Williams, B.M., McCarthy, F.M.G., Krueger, A.M., Riddick, N.L., MacKinnon, M.D., Lafond, K.M., Patterson, R.T., Nasser, N.A., Head, M.J., Pisaric, M.F.J., Turner, K.W., Boyce, J.I., and Brand, U., 2024, Quantifying conditions required for varve formation in meromictic Crawford Lake, Ontario, Canada: Important process for delimiting the Anthropocene epoch: Journal of Paleolimnology, v. 71, no. 2, p. 101–124, https://doi.org/10.1007/s10933-023-00304-w.

Lyons, T.W., and Berner, R.A., 1992, Carbon-sulfur-iron systematics of the uppermost deep-water sediments of the Black Sea: Chemical Geology, v. 99, no. 1–3, p. 1–27, https://doi.org/10.1016/0009-2541(92)90028-4.

MacLennan, S., Sha, J., Kinney, S., Olsen, P., Chang, C., Fang, Y., Lui, J., Slibeck, B., Chen, E., and Schoene, B., 2024, Extremely rapid, yet noncatastrophic, preservation of the flattened-feathered and 3D dinosaurs of the Early

Cretaceous of China: Proceedings of the National Academy of Sciences of the United States of America, v. 121, no. 47, https://doi.org/10.1073/pnas.2322875121.
Manspeizer, W., and Olsen, P.E., 1981, Rift basins of the passive margin: Tectonics, organic-rich lacustrine sediments, basin analysis, *in* Hobbs, W., III, ed., Field Guide to the Geology of the Paleozoic, Mesozoic, and Tertiary Rocks of New Jersey and the Central Hudson Valley, New York: New York, Petroleum Exploration Society of New York, p. 25–105.
Mariotti, G., Pruss, S., Perron, J., and Bosak, T., 2014, Microbial shaping of sedimentary wrinkle structures: Nature Geoscience, v. 7, no. 10, p. 736–740, https://doi.org/10.1038/ngeo2229.
Marty, D., Strasser, A., and Meyer, C.A., 2009, Formation and taphonomy of human footprints in microbial mats of present-day tidal-flat environments: Implications for the study of fossil footprints: Ichnos, v. 16, no. 1–2, p. 127–142, https://doi.org/10.1080/10420940802471027.
Mather, W.W., 1843, Geology of New-York. Part I, Comprising the Geology of the First Geological District: Albany, New York, Carroll and Cook, Natural History of New York, Division IV: Geology 1, 653 p.
McCarthy, F.M., Patterson, R.T., Head, M.J., Riddick, N.L., Cumming, B.F., Hamilton, P.B., Pisaric, M.F., Gushulak, A.C., Leavitt, P.R., and Lafond, K.M., 2023, The varved succession of Crawford Lake, Milton, Ontario, Canada as a candidate Global boundary Stratotype Section and Point for the Anthropocene series: The Anthropocene Review, v. 10, no. 1, p. 146–176, https://doi.org/10.1177/20530196221149281.
McCune, A.R., 2004, 18: Diversity and speciation of semionotid fishes in Mesozoic rift lakes, *in* Dieckmann, U., Doebeli, M., Metz, J.A.J., and Tautz, D., eds., Adaptive Speciation: Cambridge, UK, Cambridge University Press, p. 362–379, https://doi.org/10.1017/CBO9781139342179.021.
McCune, A.R., Thomson, K.S., and Olsen, P.E., 1984, Semionotid fishes from the Mesozoic Great Lakes of North America, *in* Echelle, A.A., and Kornfield, I., eds., Evolution of Species Flocks: Orono, Maine, University of Maine at Orono Press, p. 27–44.
McDonald, N.G., 1975, Fossil Fishes from the Newark Group of the Connecticut Valley [M.A. thesis]: Middletown, Connecticut, Wesleyan University, 230 p.
McDonald, N.G., 1996, The Connecticut Valley in the Age of Dinosaurs: A Guide to the Geologic Literature, 1681–1995: Connecticut State Geological and Natural History Survey Bulletin, 242 p.
McDonald, N.G., 2010, Window into the Jurassic World. Dinosaur State Park, Rocky Hill, Connecticut: Rocky Hill, Connecticut, Friends of Dinosaur State Park and Arboretum, 105 p.
McDonald, N.G., and LeTourneau, P.M., 1989, Taphonomic phosphate loss in Early Jurassic lacustrine fishes, East Berlin Formation, Hartford Basin, New England, USA [abstract]: International Geological Congress, 28th Session, Washington, D.C., Abstracts, Volume 2: Washington, D.C., American Geophysical Union, p. 398.
McDonald, N.G., LeTourneau, P.M., Huber, P., and Olsen, P.E., 2025, Early Jurassic lake-shoreline environments of the Hartford Basin: Fossils, foodchains, and implications for the facies-linked distribution of dinosaur tracks and trackmakers: Bulletin - Peabody Museum of Natural History, v. 62, no. 2, p. 339–384.
McGee, D., Moreno-Chamarro, E., Marshall, J., and Galbraith, E., 2018, Western US lake expansions during Heinrich stadials linked to Pacific Hadley circulation: Science Advances, v. 4, no. 11, https://doi.org/10.1126/sciadv.aav0118.
Meacham, A., 2016, Selective Preservation of Fossil Ghost Fish: EGU General Assembly Conference Abstracts, v. 18, p. 10524.
Meacham, A.L., 2017, Unique Preservation of Fossil Ghost Fish in the Green River Formation [M.Sc. thesis]: Loma Linda University Electronic Theses, Dissertations & Projects: Loma Linda, California, Loma Linda University, 132 p.
Mondro, C.A., Fedo, C.M., Grotzinger, J.P., Lamb, M.P., Gupta, S., Dietrich, W.E., Banham, S., Weitz, C.M., Gasda, P., and Edgar, L.A., 2025, Wave ripples formed in ancient, ice-free lakes in Gale crater, Mars: Science Advances, v. 11, no. 3, https://doi.org/10.1126/sciadv.adr0010.
Morana, C., Sarmento, H., Descy, J.-P., Gasol, J.M., Borges, A.V., Bouillon, S., and Darchambeau, F., 2014, Production of dissolved organic matter by phytoplankton and its uptake by heterotrophic prokaryotes in large tropical lakes: Limnology and Oceanography, v. 59, no. 4, p. 1364–1375, https://doi.org/10.4319/lo.2014.59.4.1364.
Morrissey, A., and Scholz, C.A., 2014, Paleohydrology of Lake Turkana and its influence on the Nile River system: Palaeogeography, Palaeoclimatology, Palaeoecology, v. 403, p. 88–100, https://doi.org/10.1016/j.palaeo.2014.03.029.
Moumou, A., Youbi, N., El Hachimi, H., El Kadiri, K., Madeira, J., Mata, J., Amri, I., and Ait Baha, A., 2024, Morphology, Internal architecture, facies model, and emplacement mechanisms of lava flows from the Central Atlantic Magmatic Province (CAMP) of the Hartford and Deerfield Basins (USA): Geosciences, v. 14, no. 8, p. 204, https://doi.org/10.3390/geosciences14080204.
Musser, G., and Clarke, J.A., 2020, An exceptionally preserved specimen from the Green River Formation elucidates complex phenotypic evolution in Gruiformes and Charadriiformes: Frontiers in Ecology and Evolution, v. 8, https://doi.org/10.3389/fevo.2020.559929.
Mustoe, G.E., 2005, Diatomaceous origin of siliceous shale in Eocene lake beds of central British Columbia: Canadian Journal of Earth Sciences, v. 42, no. 2, p. 231–241, https://doi.org/10.1139/e04-099.
Newberry, J.S., 1879, Descriptions of New Fossil Fishes from the Trias: Annals of the New York Academy of Sciences, v. 1, no. 1, p. 127–128, https://doi.org/10.1111/j.1749-6632.1879.tb55116.x.
Newberry, J.S., 1888, Fossil Fishes and Fossil Plants of the Triassic Rocks of New Jersey and the Connecticut Valley: U.S. Geological Survey Monograph, v. 14, 152 p., https://doi.org/10.5962/bhl.title.36383.
Nisbet, H., Buscarnera, G., Carey, J.W., Chen, M.A., Detournay, E., Huang, H., Hyman, J.D., Kang, P.K., Kang, Q., Labuz, J.F., Li, W., Matter, J., Neil, C.W., Srinivasan, G., Sweeney, M.R., Voller, V.R., Yang, W., Yang, Y., and Viswanathan, H.S., 2024, Carbon mineralization in fractured mafic and ultramafic rocks: A review: Reviews of Geophysics, v. 62, no. 4, https://doi.org/10.1029/2023RG000815.
Noffke, N., 2021, Microbially induced sedimentary structures in clastic deposits: Implication for the prospection for fossil life on Mars: Astrobiology, v. 21, no. 7, p. 866–892, https://doi.org/10.1089/ast.2021.0011.
Noffke, N., Hagadorn, J., and Bartlett, S., 2019, Microbial structures and dinosaur trackways from a Cretaceous coastal environment (Dakota Group, Colorado, USA): Journal of Sedimentary Research, v. 89, no. 11, p. 1096–1108, https://doi.org/10.2110/jsr.2019.57.
Obiero, K., Wakjira, M., Gownaris, N., Malala, J., Keyombe, J.L., Ajode, M.Z., Smith, S., Lawrence, T., Ogello, E., Getahun, A., and Kolding, J., 2023, Lake Turkana: Status, challenges, and opportunities for collaborative research: Journal of Great Lakes Research, v. 49, no. 6, 102120, https://doi.org/10.1016/j.jglr.2022.10.007.
Odada, E.O., Oyebande, L., and Oguntola, A., 2006, Lake Chad: Experience and lessons learned brief: Lake Basin Management Initiative: Shiga, Japan, International Lake Environment Committee Foundation, https://ilec.or.jp/cms/wp-content/uploads/pub/06_Lake_Chad_27February2006.pdf (accessed February 2026).
Olsen, P.E., 1984, Comparative Paleolimnology of the Newark Supergroup: A Study of Ecosystem Evolution [Ph.D. thesis]: New Haven, Connecticut, Yale University, 724 p.
Olsen, P.E., 1985, Constraints on the formation of lacustrine microlaminated sediments: U.S. Geological Survey Circular, v. 946, p. 34–35.
Olsen, P.E., 1986, A 40-million-year lake record of early Mesozoic orbital climatic forcing: Science, v. 234, no. 4778, p. 842–848, https://doi.org/10.1126/science.234.4778.842.
Olsen, P.E., 1988, Continuity of strata in the Newark and Hartford Basins of the Newark Supergroup: U.S. Geological Survey Bulletin 1776, p. 6–18.
Olsen, P.E., 1990, Tectonic, climatic, and biotic modulation of lacustrine ecosystems: Examples from the Newark Supergroup of eastern North America, *in* Katz, B.J., ed., Lacustrine Basin Exploration: Case Studies and Modern Analogs: American Association of Petroleum Geologists Memoir 50, p. 209–224, https://doi.org/10.1306/M50523.
Olsen, P.E., 2010, Fossil great lakes of the Newark Supergroup—30 years later, *in* Benimoff, A.I., ed., Field Trip Guidebook, New York State Geological Association, 83nd Annual Meeting, College of Staten Island: New York, College of Staten Island, p. 101–162.
Olsen, P.E., 2017, Origins of Dinosaur Dominance in the Connecticut Valley Rift Basin: Middletown, Connecticut, Wesleyan University, A Field Trip Sponsored by the Keck Foundation & Hosted by Wesleyan University, Keck Geological Consortium, 39 p.
Olsen, P., 2023, Orbitally-paced latest Triassic-Early Jurassic meromictic lake deposits of Eastern North America—Their sunspot-modulated varves, turbidites, and supereruption ashes: Geological Society of America Abstracts with Programs, v. 55, no. 6, https://doi.org/10.1130/abs/2023AM-390385.
Olsen, P.E., and Douglas, A., 2022, Lacustrine Rift Basin Evolution and Orbital Pacing of Tropical Climate: A Comparison with the Quaternary Mediterranean

Sapropel Record—A Field Trip for the International Ocean Discovery Program (IODP) Forum Meeting, September 14–15, Palisades, New York, https://www.ldeo.columbia.edu/~polsen/nbcp/olsen+douglas_ct_iodp_ft_guidebook.pdf (accessed February 2026).

Olsen, P.E., and Kinney, S., 2016, Early post-depositional bedding-plane-parallel mélanges created by shear and liquefaction: A common but largely misinterpreted organic-rich mudrock facies: Geological Society of America Abstracts with Programs, v. 48, no. 7, https://doi.org/10.1130/abs/2016AM-287708.

Olsen, P.E., and McCune, A.R., 1991, Morphology of the *Semionotus elegans* species group from the Early Jurassic part of the Newark Supergroup of Eastern North America with comments on the family Semionotidae (Neopterygii): Journal of Vertebrate Paleontology, v. 11, no. 3, p. 269–292, https://doi.org/10.1080/02724634.1991.10011398.

Olsen, P.E., and McDonald, N.G., 2026, Environmental Context of Triassic-Jurassic Lagerstätten in Newark Supergroup Rift Basins, Eastern North America, with Special Reference to Footprint Assemblages: Bulletin of the Peabody Museum of Natural History, in press.

Olsen, P.E., Remington, C.L., Cornet, B., and Thomson, K.S., 1978, Cyclic change in Late Triassic lacustrine communities: Science, v. 201, no. 4357, p. 729–733, https://doi.org/10.1126/science.201.4357.729.

Olsen, P.E., Schlische, R.W., and Gore, P.J.W., 1989, Field guide to the tectonics, stratigraphy, sedimentology, and paleontology of the Newark Supergroup, eastern North America, *in* International Geological Congress, Guidebooks for Field Trips, v. 351, p. 1–174.

Olsen, P.E., Whiteside, J.H., and Huber, P., 2003, Causes and consequences of the Triassic-Jurassic mass extinction as seen from the Hartford basin, *in* Brady, J.B., and Cheney, J.T., eds., Guidebook for Field Trips in the Five College Region, 95th New England Intercollegiate Geological Conference, Department of Geology, Smith College, Northampton, Massachusetts: Northampton, Smith College, p. B5-1–B5-41.

Olsen, P.E., Whiteside, J.H., LeTourneau, P.M., and Huber, P., 2005, Trip A-4: Jurassic cyclostratigraphy and paleontology of the Hartford Basin, *in* McHone, N.W., and Peterson, M.J., eds., Guidebook for Field Trips in Connecticut, New England Intercollegiate Geological Conference, 97th Annual Meeting: New Haven, Connecticut,Yale University, p. 1–51.

Olsen, P.E., Philpotts, A.R., McDonald, N.G., Steinen, R.P., Kinney, S.T., Jaret, S.J., and Rasbury, E.T., 2016, Wild and wonderful implications of the 5 mm Pompton Ash of the Hartford and Newark basins (Early Jurassic, Eastern North America): Geological Society of America Abstracts with Programs, v. 48, no. 2, https://doi.org/10.1130/abs/2016NE-272509.

Olsen, P.E., Laskar, J., Kent, D.V., Kinney, S.T., Reynolds, D.J., Sha, J., and Whiteside, J.H., 2019, Mapping Solar System chaos with the Geological Orrery: Proceedings of the National Academy of Sciences of the United States of America, v. 116, no. 22, p. 10,664–10,673, https://doi.org/10.1073/pnas.1813901116.

Olsen, P.E., Sha, J., Fang, Y., Clara Chang, C., Kinney, S., Sues, H.D., Kent, D., Whiteside, J.H., Schaller, M., and Vajda, V., 2022, Arctic ice and the ecological rise of the dinosaurs: Science Advances, v. 8, https://doi.org/10.1126/sciadv.abo6342.

Olsen, P.E., McLean, N., Blackburn, T., Kinney, S., Tibbits, D., Chang, C., Schaller, M.F., Slibeck, B.B., Whiteside, J.H., Kent, D.V., Ramezani, J., and Et-Touhami, M., 2024a, Obliquity—not precession—dominated orbital pacing through the continental Triassic-Jurassic transition in the tropics, requiring recalibration of the CA-ID-TIMS-based age of the end-Triassic mass extinction (ETE): Abstract V22A-05 presented at AGU24, 9–13 December 2024, https://agu.confex.com/agu/agu24/meetingapp.cgi/Paper/1545539.

Olsen, P.E., Philpotts, A., Huber, P., Slibeck, B.B., and McDonald, N.G., 2024b, The Triassic–Jurassic Transition and the Dawn of the Modern World: Hadlyme, Connecticut, Geological Society of Connecticut, Guidebook, 120 p.

Olsen, P., Kinney, S., Tibbits, D., Fang, Y., Chang, C., Schaller, M., Slibeck, B., Whiteside, J., and Kent, D., 2025a, Obliquity pacing of tropical lacustrine cyclostratigraphy of the great end-Triassic hyperthermal and mass extinction: Competing radiative balance forcings induced by the Central Atlantic Magmatic Province (CAMP): EGU General Assembly 2025, Vienna, Austria, 27 April–2 May 2025, EGU25–10277, https://doi.org/10.5194/egusphere-egu25-10277.

Olsen, P.E., Slibeck, B.B., Kinney, S.T., and McDonald, N.G., 2025b, Field trip O: Paleoenvironmental and Paleobiological Perspectives on the Continental End-Triassic Mass Extinction: New England Intercollegiate Geological Conference, 108 p.

Olsen, P.E., Kent, D.V., Huber, P., and Kinney, S.T., 2026, Syndepositional faulting in the Hanging Hills and Watchungs, Hartford and Newark Basins, associated with the initial pulse of Central Atlantic Magmatic Province (CAMP): Geological Society of America, Abstracts with Programs, v. 58, no. 2, abstract 27-5.

Ostrom, J.H., 1967, Peabody paleontologists assist new dinosaur-track park: Discovery [Magazine of the Peabody Museum of Natural History, Yale University], v. 2, no. 2, p. 21–24.

Ostrom, J.H., 1972, Were some dinosaurs gregarious?: Palaeogeography, Palaeoclimatology, Palaeoecology, v. 11, p. 287–301, https://doi.org/10.1016/0031-0182(72)90049-1.

Ostrom, J.H., and Quarrier, S.S., 1968, The Rocky Hill dinosaurs; Trip C–3, *in* Orville, P.M., ed., Guidebook for Fieldtrips in Connecticut. New England Intercollegiate Geological Conference, 60th Annual Meeting: New Haven, Connecticut, Yale University, p. 1–12.

Peeters, F., Kipfer, R., Achermann, D., Hofer, M., Aeschbach-Hertig, W., Beyerle, U., Imboden, D.M., Rozanski, K., and Fröhlich, K., 2000, Analysis of deep-water exchange in the Caspian Sea based on environmental tracers: Deep Sea Research. Part I, Oceanographic Research Papers, v. 47, no. 4, p. 621–654, https://doi.org/10.1016/S0967-0637(99)00066-7.

Percival, J.G., 1842, Report on the Geology of the State of Connecticut: Osborn & Baldwin, printers, 495 p.

Peterffy, O., Calner, M., and Vajda, V., 2016, Early Jurassic microbial mats—A potential response to reduced biotic activity in the aftermath of the end-Triassic mass extinction event: Palaeogeography, Palaeoclimatology, Palaeoecology, v. 464, p. 76–85, https://doi.org/10.1016/j.palaeo.2015.12.024.

Pokorný, R., Nohra, R., Saad, P.A., and Vallon, L H., 2025, Death on "live broadcast"—fish mortichnia from the Upper Cretaceous plattenkalk of Lebanon: Paleobiology, v. 50, no. 4, p. 627–640.

Prado, G., Salvato, R.C., Becker-Kerber, B., Silva, E.P., Pinheiro, F.L., Osés, G.L., Galante, D., Rodrigues, F., Dias, J.J., and Carvalho, I.D.S., 2025, Fossil fish provide evidence of geomelanin preservation with implications on the visual accuracy of an extinct fish species: Lethaia, v. 58, no. 3, p. 1–17, https://doi.org/10.18261/let.58.3.7.

Puchniak, M.K., Awortwi, F.E., Sanful, P.O., Frempong, E., Hall, R.I., and Hecky, R.E., 2009, Effects of physical dynamics on the water column structure of Lake Bosomtwe/Bosumtwi, Ghana (West Africa): Internationale Vereinigung für theoretische und angewandte Limnologie: Verhandlungen, v. 30, no. 7, p. 1077–1081, https://doi.org/10.1080/03680770.2009.11902305.

Redfield, J.H., 1837, Fossil fishes of Connecticut and Massachusetts, with a notice of an undescribed genus: Annals of the Lyceum of Natural History of New York, v. 4, p. 35–40, https://doi.org/10.1111/j.1749-6632.1848.tb00259.x.

Renaut, R.W., and Owen, R.B., 2023, The Kenya Rift Lakes: Modern and Ancient: Limnology and Limnogeology of Tropical Lakes in a Continental Rift: Berlin, Springer, https://doi.org/10.1007/978-3-642-25055-2.

Roberts, D., Moreno-Casas, P., Bombardelli, F., Hook, S., Hargreaves, B., and Schladow, S., 2019, Predicting wave-induced sediment resuspension at the perimeter of lakes using a steady-state spectral wave model: Water Resources Research, v. 55, no. 2, p. 1279–1295, https://doi.org/10.1029/2018WR023742.

Rogers, J., 1985, Bedrock geological map of Connecticut: Connecticut Geologic and Natural History Survey: Natural Resource Atlas Map Series, v. 2, scale 1:125,000.

Ross, M.P., Knyff, C.F., Murphy, P.W., Rochette, E.M., and Burns, R.C., 2025, History of Dinosaur State Park, Registered National Natural Landmark, One of North America's Largest in Situ Dinosaur Trackways, Rocky Hill, Connecticut: Bulletin - Peabody Museum of Natural History, v. 66, no. 1, p. 51–69, https://doi.org/10.3374/014.066.0103.

Rossi, V., Unitt, R., McNamara, M., Zorzin, R., and Carnevale, G., 2022, Skin patterning and internal anatomy in a fossil moonfish from the Eocene Bolca Lagerstätte illuminate the ecology of ancient reef fish communities: Palaeontology, v. 65, no. 3, https://doi.org/10.1111/pala.12600.

Russell, J.M., and Johnson, T.C., 2005, A high-resolution geochemical record from Lake Edward, Uganda Congo and the timing and causes of tropical African drought during the late Holocene: Quaternary Science Reviews, v. 24, no. 12–13, p. 1375–1389, https://doi.org/10.1016/j.quascirev.2004.10.003.

Schaeffer, B., 1948, A study of *Diplurus longicaudatus*, with notes on the body form and locomotion of the Coelacanthini: American Museum Novitates, v. 1378, p. 1–32.

Schaeffer, B., 1952, The Triassic coelacanth fish *Diplurus*, with observations on the evolution of the Coelacanthini: Bulletin of the American Museum of Natural History, v. 99, no. 2, p. 27–78.

Schaeffer, B., Dunkle, D.H., and McDonald, N.G., 1975, *Ptycholepis marshi* Newberry, a Chondrostean fish from the Newark Group of Eastern North America: Fieldiana. Geology, v. 33, no. 12, p. 205–233.

Schaeffer, B., and McDonald, N.G., 1978, Redfieldiid fishes from the Triassic–Liassic Newark Supergroup of eastern North America: Bulletin of the American Museum of Natural History, v. 159, no. 4, p. 129–174.

Schaller, M.F., Wright, J.D., and Kent, D.V., 2011, Atmospheric pCO_2 perturbations associated with the Central Atlantic Magmatic Province: Science, v. 331, no. 6023, p. 1404–1409, https://doi.org/10.1126/science.1199011.

Schaller, M.F., Wright, J.D., Kent, D.V., and Olsen, P.E., 2012, Rapid emplacement of the Central Atlantic Magmatic Province as a net sink for CO_2: Earth and Planetary Science Letters, v. 323–324, p. 27–39, https://doi.org/10.1016/j.epsl.2011.12.028.

Schieber, J., 1999, Microbial mats in terrigenous clastics; the challenge of identification in the rock record: Palaios, v. 14, no. 1, p. 3–12, https://doi.org/10.2307/3515357.

Schieber, J., 2007, Benthic microbial mats as an oil shale component: Green River Formation (Eocene) of Wyoming and Utah, *in* Schieber, J., Bose, P.K., Eriksson, P.G., Banerjee, S., Sarkar, S., Altermann, W., and Catuneau, O., eds., Atlas of Microbial Mat Features Preserved within the Clastic Rock Record: Amsterdam, Elsevier, p. 225–232.

Schlische, R.W., 1993, Anatomy and evolution of the Triassic–Jurassic continental rift system, eastern North America: Tectonics, v. 12, p. 1026–1042, https://doi.org/10.1029/93TC01062.

Scholz, C.A., and Rosendahl, B.R., 1988, Low lake stands in Lakes Malawi and Tanganyika, East Africa, delineated with multifold seismic data: Science, v. 240, no. 4859, p. 1645–1648, https://doi.org/10.1126/science.240.4859.1645.

Scholz, C.A., Cohen, A.S., Johnson, T.C., King, J., Talbot, M.R., and Brown, E.T., 2011, Scientific drilling in the Great Rift Valley: The 2005 Lake Malawi Scientific Drilling Project—An overview of the past 145,000 years of climate variability in Southern Hemisphere East Africa: Palaeogeography, Palaeoclimatology, Palaeoecology, v. 303, no. 1-4, p. 3–19, https://doi.org/10.1016/j.palaeo.2010.10.030.

Schulz, R., Harms, F.J., and Felder, M., 2002, Die Forschungsbohrung Messel 2001: Ein Beitrag zur Entschlüsselung der Genese einer Ölschieferlagerstätte: Zeitschrift für Angewandte Geologie, v. 4, p. 9–17.

Seilacher, A., 1970, Begriff und Bedeutung der Fossil-Lagerstätten: Neues Jahrbuch für Geologie und Paläontologie. Abhandlungen, v. 1970, p. 34–39.

Seilacher, A., 2007, Trace Fossil Analysis: Berlin, Springer, 226 p.

Shanahan, T.M., Beck, J.W., Overpeck, J.T., McKay, N.P., Pigati, J.S., Peck, J.A., Scholz, C.A., Heil, C.W., and King, J., 2012, Late Quaternary sedimentological and climate changes at Lake Bosumtwi Ghana: New constraints from laminae analysis and radiocarbon age modeling: Palaeogeography, Palaeoclimatology, Palaeoecology, v. 361-362, p. 49–60, https://doi.org/10.1016/j.palaeo.2012.08.001.

Simpson, H., 1969, Preliminary Bedrock Geologic Map of Part of Durham Quadrangle, Connecticut: U.S. Geological Survey Open-File Report 69-257, 3 p. + map + cross sections, scale 1:24,000, https://doi.org/10.3133/ofr69257.

Simpson, H.E., 1966, Bedrock Geologic Map of the New Britain Quadrangle, Connecticut: U.S. Geological Survey Geologic Quadrangle 494, 1 map, scale 1:24,000, https://doi.org/10.3133/gq494.

Siver, P.A., and Velez, M.I., 2023, The oldest raphe-bearing diatoms: Evidence from the Upper Cretaceous of western and northern Canada: Cretaceous Research, v. 144, https://doi.org/10.1016/j.cretres.2022.105456.

Smith, I., and Sinclair, I., 1972, Deep water waves in lakes: Freshwater Biology, v. 2, no. 4, p. 387–389, https://doi.org/10.1111/j.1365-2427.1972.tb00378.x.

Specht, T.D., and Rosendahl, B.R., 1989, Architecture of the Lake Malawi rift, east Africa: Journal of African Earth Sciences (and the Middle East), v. 8, no. 2–4, p. 355–382, https://doi.org/10.1016/S0899-5362(89)80032-6.

St-Denis, C., and Fell, C., 1971, Diffusivity of oxygen in water: Canadian Journal of Chemical Engineering, v. 49, no. 6, p. 885, https://doi.org/10.1002/cjce.5450490632.

Starquist, V.L., 1943, The Stratigraphy and Structural Geology of the Central Portion of the Mount Tom and East Mountain ridges [M.A. thesis]: Northampton, Massachusetts, Smith College, 49 p.

Steinen, R., and Charney, A., 2020, The Bedrock Geology of the Wallingford Quadrangle, New Haven County, Connecticut, with a Map and Cross-section (text): State Geological and Natural History Survey of Connecticut: Quadrangle Report, v. 42, 192 p.

Steinen, R.P., Gray, N.H., and Mooney, J., 1987, A Mesozoic carbonate hot-spring deposit in the Hartford Basin of Connecticut: Journal of Sedimentary Research, v. 57, no. 2, p. 319–326.

Steinen, R.P., Martin, L.G., Conti, A.A., Jorgensen, C.T., and Gierlowski-Kordesch, E.H., 2015, Stratigraphic observations on cored boreholes in the Mesozoic Hartford Basin, Hartford, Connecticut: Geological Society of America Abstracts with Programs, v. 47, no. 3, p. 54.

Steinen, R.P., Bogart, J., Charney, A., VanderLeest, R., and Glairon, S., 2017, A hypothesis for the disappearance of the Talcott Basalt in the vicinity of Wallingford, CT: Geological Society of America Abstracts with Programs, v. 49, no. 2, abstract 56-1, https://doi.org/10.1130/abs/2017NE-290397

Stüeken, E.E., Martinez, A., Love, G., Olsen, P.E., Bates, S., and Lyons, T.W., 2019, Effects of pH on redox proxies in a Jurassic rift lake: Implications for interpreting environmental records in deep time: Geochimica et Cosmochimica Acta, v. 252, p. 240–267, https://doi.org/10.1016/j.gca.2019.03.014.

Sturm, M., and Matter, A., 1978, Turbidites and varves in Lake Brienz (Switzerland): Deposition of clastic detritus by density currents, *in* Matter, A., and Tucker, M.E., eds., Modern and Ancient Lake Sediments: Hoboken, New Jersey, Wiley, p. 147–168, https://doi.org/10.1002/9781444303698.ch8.

Takeda, I., 1992, Estimation of water depth from wave ripple marks: Journal of the Sedimentological Society of Japan, v. 37, no. 37, p. 31–42.

Thorpe, M.R., 1936, A fossil fish in the Connecticut red sandstone: American Journal of Science, ser. 5–32, no. 191, p. 319–321, https://doi.org/10.2475/ajs.s5-32.191.319.

Törő, B., and Pratt, B.R., 2015, Eocene paleoseismic record of the Green River Formation, Fossil Basin, Wyoming, U.S.A.: Implications of synsedimentary deformation structures in lacustrine carbonate mudstones: Journal of Sedimentary Research, v. 85, no. 8, p. 855–884, https://doi.org/10.2110/jsr.2015.56.

Tu, C., Chen, Z.Q., Retallack, G.J., Huang, Y., and Fang, Y., 2016, Proliferation of MISS-related microbial mats following the end-Permian mass extinction in terrestrial ecosystems: Evidence from the Lower Triassic of the Yiyang area, Henan Province, North China: Sedimentary Geology, v. 333, p. 50–69, https://doi.org/10.1016/j.sedgeo.2015.12.006.

Uhen, M.D., Allen, B., Behboudi, N., Clapham, M.E., Dunne, E., Hendy, A., Holroyd, P.A., Hopkins, M., Mannion, P., and Novack-Gottshall, P., 2023, Paleobiology database user guide version 1.0: PaleoBios, v. 40, no. 11, p. 1–56, https://doi.org/10.5070/P9401160531.

VanHouten, F.B., 1962, Cyclic sedimentation and the origin of analcime-rich Upper Triassic Lockatong Formation, west-central New Jersey and adjacent Pennsylvania: American Journal of Science, v. 260, no. 8, p. 561–576, https://doi.org/10.2475/ajs.260.8.561.

Van Houten, F.B., 1964, Cyclic lacustrine sedimentation, upper Triassic Lockatong Formation, central New Jersey and adjacent Pennsylvania, *in* Merriam, D.F., ed., Symposium on Cyclic Sedimentation: Kansas Geological Survey Bulletin 169, p. 497–531.

Van Houten, F.B., 1969, Late Triassic Newark Group, north central New Jersey and adjacent Pennsylvania and New York, *in* Subitzkey, S., ed., Geology of Selected Areas in New Jersey and Eastern Pennsylvania and Guidebook of Excursions: New Brunswick, New Jersey, Rutgers University Press, p. 314–347.

Vastano, J.A., 2025, The Upper Triassic "Solite Deposit" of Virginia and North Carolina: Description of New Insect Taxa and Reexamination of Paleoenvironmental Conditions [Ph.D. thesis]: New Brunswick, New Jersey, Rutgers, The State University of New Jersey, 392 p.

Verburg, I., Kakogozo, B., Kihakwi, A., Kotilainen, P., Makasa, L., and Peltonen, A., 1997, Hydrodynamics of Lake Tanganyika and meteorological results. FAO, Lake Tanganyika Research (LTR) Project, GCP/RAF/271/FIN-TD/59: Bujumbura, Burundi, Food and Agriculture Organization of the United Nations, 54 p.

Wang, S., Hethke, M., Wang, B., Tian, Q., Yang, Z., and Jiang, B., 2019, High-resolution taphonomic and palaeoecological analyses of the Jurassic Yanliao Biota of the Daohugou area, northeastern China: Palaeogeography, Palaeoclimatology, Palaeoecology, v. 530, p. 200–216, https://doi.org/10.1016/j.palaeo.2019.05.028.

Wetzel, R.G., 2001, Limnology: Lake and River Ecosystems: San Diego, California, Academic Press, 1006 p.

Whiteside, J.H., Olsen, P.E., Eglinton, T.I., Cornet, B., McDonald, N.G., and Huber, P., 2011, Pangean great lake paleoecology on the cusp of the end-Triassic extinction: Palaeogeography, Palaeoclimatology, Palaeoecology, v. 301, no. 1–4, p. 1–17, https://doi.org/10.1016/j.palaeo.2010.11.025.

Wiley, C.N., 1933, Early cement manufacture in Connecticut: Connecticut Society for Civil Engineering Annual Report, v. 49, p. 129–145.

Wise, D.U., 1988, Mesozoic stress history of the upper Connecticut Valley at Turners Falls, Massachusetts, *in* Proceedings, New England Intercollegiate Geological Conference, 74th Annual Meeting (Keene, NH): Fieldtrip Guidebook 1988, p. 351–372.

Wood, D.A., and Scholz, C.A., 2017, Stratigraphic framework and lake level history of Lake Kivu, East African Rift: Journal of African Earth Sciences, v. 134, p. 904–916, https://doi.org/10.1016/j.jafrearsci.2016.06.014.

Wotzlaw, J.F., Guex, J., Bartolini, A., Gallet, Y., Krystyn, L., McRoberts, C.A., Taylor, D., Schoene, B., and Schaltegger, U., 2014, Towards accurate numerical calibration of the Late Triassic: High-precision U-Pb geochronology constraints on the duration of the Rhaetian: Geology, v. 42, no. 7, p. 571–574, https://doi.org/10.1130/G35612.1.

Yager, J.A., West, A.J., Corsetti, F.A., Berelson, W.M., Rollins, N.E., Rosas, S., and Bottjer, D.J., 2017, Duration of and decoupling between carbon isotope excursions during the end-Triassic mass extinction and Central Atlantic Magmatic Province emplacement: Earth and Planetary Science Letters, v. 473, p. 227–236, https://doi.org/10.1016/j.epsl.2017.05.031.

Yang, Z., Wang, S., Tian, Q., Wang, B., Hethke, M., McNamara, M.E., Benton, M.J., Xu, X., and Jiang, B., 2019, Palaeoenvironmental reconstruction and biostratinomic analysis of the Jurassic Yanliao Lagerstätte in northeastern China: Palaeogeography, Palaeoclimatology, Palaeoecology, v. 514, p. 739–753, https://doi.org/10.1016/j.palaeo.2018.09.030.

Zangler, B., 1969, The Triassic rocks of Dinosaur State Park, Rocky Hill, Connecticut: Dinosaur State Park, Connecticut Geological and Natural History Survey, p. 1–50.

Zhong, Y., Huyskens, M.H., Yin, Q.-Z., Wang, Y., Ma, Q., and Xu, Y.-G., 2021, High-precision geochronological constraints on the duration of 'Dinosaur Pompeii' and the Yixian Formation: National Science Review, v. 8, https://doi.org/10.1093/nsr/nwab063.

Zolitschka, B., Francus, P., Ojala, A.E., and Schimmelmann, A., 2015, Varves in lake sediments—A review: Quaternary Science Reviews, v. 117, p. 1–41, https://doi.org/10.1016/j.quascirev.2015.03.019.

Manuscript Accepted by the Society 31 January 2026

Printed in the USA